

UNIVERSITÉ DU QUÉBEC À TROIS-RIVIÈRES

GESTION DÉCENTRALISÉE EN TEMPS RÉEL D'UN SYSTÈME PILE À  
COMBUSTIBLE MODULAIRE

THÈSE PRÉSENTÉE  
COMME EXIGENCE PARTIELLE DU  
DOCTORAT EN GÉNIE ÉLECTRIQUE

PAR  
ARASH KHALATBARISOLTANI

FÉVRIER 2022

UNIVERSITÉ DU QUÉBEC À TROIS-RIVIÈRES

REAL-TIME DECENTRALIZED MANAGEMENT OF A MODULAR FUEL CELL  
SYSTEM

A THESIS PRESENTED  
IN PARTIAL FULFILLMENT OF  
THE REQUIREMENTS FOR THE DEGREE

DOCTOR OF PHILOSOPHY IN ELECTRICAL ENGINEERING

BY  
ARASH KHALATBARISOLTANI

FEBRUARY 2022

Université du Québec à Trois-Rivières

Service de la bibliothèque

Avertissement

L'auteur de ce mémoire ou de cette thèse a autorisé l'Université du Québec à Trois-Rivières à diffuser, à des fins non lucratives, une copie de son mémoire ou de sa thèse.

Cette diffusion n'entraîne pas une renonciation de la part de l'auteur à ses droits de propriété intellectuelle, incluant le droit d'auteur, sur ce mémoire ou cette thèse. Notamment, la reproduction ou la publication de la totalité ou d'une partie importante de ce mémoire ou de cette thèse requiert son autorisation.

**UNIVERSITÉ DU QUÉBEC À TROIS-RIVIÈRES**

**DOCTORAT EN GÉNIE ÉLECTRIQUE (Ph. D.)**

**Direction de recherche :**

---

Loïc Boulon directeur de recherche

---

Xiaosong Hu codirecteur de recherche

**Jury d'évaluation :**

---

Loïc Boulon Directeur de recherche

---

Xiaosong Hu Codirecteur de recherche

---

Messaoud Ouameur Président

---

Antoine Lesage-Landry Évaluateur externe

---

Javier Solano Évaluateur externe

Thèse soutenue le 10 février 2022



## **Abstract**

Fuel cell vehicles (FCVs) have been broadly considered substitutes for traditional internal combustion engine (ICE) vehicles. It is crucial to efficiently and healthily use hydrogen-powered power sources to diminish FCVs' operating costs. It can be fulfilled through well-designed energy management strategies (EMSs), which organize the energy sources to generate the requested power. The hardware modularity has already been investigated in the multi-stack FCVs (MFCS), while the software modularity has escaped the attention. The hardware modularity aspect of the MFCSs is related to having flexibility and reconfiguration in different electrical and fluidic structures. Literature consideration shows that most of the existing power splitting approaches are centralized. Moreover, some issues regarding efficiency, availability, modularity, flexibility (plug & play), robustness, durability, and cost need to be addressed. In this respect, a new direction called decentralized power allocation strategy has come under close consideration in this Ph.D. thesis to overcome the limitations and increase the decision-making scheme's reliability and scalability. Unlike the typical centralized power management approaches, a decentralized control scheme comprises light-connected control units instead of a big centralized one to augment reliability and scalability. Several decentralized EMSs are established to provide a robust and modular powertrain system. The thesis's main contributions are outlined: First, a decentralized power-splitting strategy based on the auxiliary problem principle (APP) decomposition method

is developed to prove the concept stage. Next, a comprehensive comparison between the consensus alternating direction method of multipliers (C-ADMM) and the Proximal Jacobian alternating direction method of multipliers (PJ-ADMM) is conducted to demonstrate the main characteristics of the decentralized optimization algorithms in the EMS field. Finally, decentralized model predictive control (MPC) is introduced for real-time decision-making because it can handle time-varying constrained systems and is suited for the integration of driving predictive information. Additionally, a learning-based tuning method is integrated to seek the optimal hyperparameters of the suggested EMS.

# Contents

Abstract.....	i
Contents .....	iii
List of Tables .....	vii
List of Figures.....	viii
List of Symbols.....	xi
Chapitre 1 - Introduction.....	1
1.1 Introduction .....	1
1.2 Different applications of the modular energy system .....	4
1.2.1 Rail application.....	4
1.2.2 Road transport.....	5
1.2.3 Maritime application.....	6
1.2.4 Submarines application.....	8
1.2.5 Air transportation.....	8
1.3 Possible prospects of modular-based powertrain systems .....	9
1.4 Different energy management strategies for modular fuel cell vehicles	
11	
1.4.1 Centralized-based control structure .....	11
1.4.2 Distributed-based control structure.....	12

1.4.3	Decentralized-based control structure .....	13
1.4.4	Comparison between centralized, distributed & decentralized control strategies .....	14
1.5	Decentralized convex-based optimization (DCO) approaches .....	15
1.6	Problem statement .....	21
1.7	Aims and objectives .....	22
1.8	Methodology .....	22
1.9	Thesis structure .....	23
<b>Chapitre 2 - Power Allocation Strategy Based on Decentralized Convex Optimization in Modular Fuel Cell Systems for Vehicular Applications ...25</b>		
2.1	Introduction .....	25
2.2	Methodology .....	25
2.3	Synopsis of the analyses of the results .....	28
2.4	Outcomes .....	30
2.1	Conclusion .....	31
<b>Chapitre 3 - A Comparison of Decentralized ADMM Optimization Algorithms for Power Allocation in Modular Fuel Cell Vehicles..... 41</b>		
3.1	Introduction .....	41
3.2	Methodology .....	41
3.3	Synopsis of the analyses of the results .....	43

3.4 Outcomes.....	45
3.1 Conclusion.....	45
<b>Chapitre 4 - Look-Ahead Decentralized Safe-Learning Control for a Modular</b>	
<b>Powertrain Using Convex Optimization and Federated Reinforcement</b>	
<b>Learning.....</b>	<b>61</b>
4.1 Introduction.....	61
4.2 Methodology.....	61
4.3 Synopsis of the analyses of the results.....	66
4.4 Outcomes.....	68
4.5 Conclusion.....	69
4.5.1 Abstract.....	70
4.5.2 Introduction.....	71
4.5.3 FCV powertrain configuration and modeling.....	76
4.5.4 The general optimization problem formulation of the look-ahead PAS.....	81
4.5.5 Reformulation of Cen-MPC via C-ADMM.....	83
4.5.6 General description of the hyper-parameters tuning algorithm based on Federated reinforcement learning.....	87
4.5.7 Results and Discussions on Numerical case studies.....	90
4.5.8 Experimental implementation.....	95

4.5.9 Conclusion .....	97
4.5.10 References.....	98
Chapitre 5 - Conclusion and Future Directions .....	100
5.1 Outline of the Research Achievements .....	100
5.2 Outlook and Future Research Trends for Decentralized EMS.....	101
5.2.1 Integrating Advanced Modeling Methods .....	102
5.2.2 Including Fault Diagnosis and Fault-Tolerant Control.....	103
5.2.3 Co-optimization and integration of different objectives.....	103
5.2.4 Improving the implementation capabilities of the proposed decentralized method .....	106
References.....	108
Publication and conference papers.....	116
Appendix A – Résumé .....	119

## List of Tables

Table 1-I A detailed comparison between the advantages and disadvantages of the modular energy system.....	4
Table 1-II Comparison between centralized, distributed & decentralized control strategies.....	15
Table 1-III A comparison of different types of communication.....	18
Table 1-IV Comparison between the Lagrangian-based and Consensus-based DCOs.....	19
Table 1-V Summarization of Lagrangian-based methods.....	20
Table 1-VI Summarization of Consensus-based Algorithm.....	21
Table 4-I The detailed comparison of computational complexity and final price.....	67
Table 4-II The approximated battery unit parameters.....	80
Table 4-III The detailed comparison of computational complexity and final price.....	94

## List of Figures

Figure 1-1 Efficiency curves comparison. (a) Single high-power source, and (b) Modular energy system composed of four parallel low-power sources. ....	2
Figure 1-2 Powertrain configuration of the developed modular tramway [15]. ..	5
Figure 1-3 Powertrain of the hybrid modular source city bus [18]. ....	6
Figure 1-4 Configuration of the modular hybrid-electric boat [21]. ....	7
Figure 1-5 Powertrain configuration of the uncrewed aerial vehicle [24]. ....	9
Figure 1-6 Scheme of the selected modular FCV powertrain architecture. ....	10
Figure 1-7 Different forms of developing control strategy unit for a module FCV: a) centralized, b) distributed, and c) decentralized. ....	11
Figure 1-8 Popular communication and sharing information topologies for the decentralized optimization algorithms. ....	18
Figure 1-9 Classified the DCOs based on the decomposition methods. ....	18
Figure 1-10 The decentralized methods according to the type of the pooled information. ....	19
Figure 2-1 The developed modular test bench. ....	26
Figure 2-2 The configuration of the D-APP PAS [57]. ....	27
Figure 2-3 The general systematic flowchart of the D-APP strategy. ....	28
Figure 2-4 The APP results under real driving profile: (a) power profiles, (b) the modules ( $M1, M2$ ) split powers, (c) the SoC of battery. ....	29
Figure 3-1 The parallel communication procedure of the decentralized PJ-ADMM. ....	43
Figure 3-2 The information flow between the FC modules via the C-ADMM. ....	43
Figure 3-3 Optimal PASs results: (a) the profiles based on C-ADMM, (b) the profiles based on PJ-ADMM, and (c) the SoC evaluations. ....	44
Figure 4-1 The adaptive look-ahead Dec-MPC framework and the modular powertrain system sequence operation. ....	62



Figure 4-2 The systematic flowchart of the Dec-MPC algorithm .....	63
Figure 4-3 Visual representation of the module-to-module FRL algorithm and the learning steps .....	65
Figure 4-4 Optimized results of the MPC-based approaches: (a) the powers based on Dec-MPC, (b) the powers based on adaptive Dec-MPC, (c) the comparison between the total output modules powers of the FC modules, and (d) the comparison between SoC levels. ...	66
Figure 4-5 Optimal final cost and computational complexity of Cen-MPC, Dec-MPC, and adjustable Dec-MPC as functions of optimization window size .....	68
Figure 4-6 Diagram of the communications topologies and the underlying powertrain for Cen-PAS and Dec-PAS with four FC modules ( $FC_m, m = 1, \dots, 4$ ) and one battery pack (Bat). a) Cen-PAS with four local control units ( $M_m, m = 1, \dots, 4$ ) and one centralized unit (c), b) Dec-PAS without a centralized controller. ....	73
Figure 4-7 The schematic of the established small-scale modular test bench. ...	77
Figure 4-8 The characteristic curves of the two actual FCS modules: (a) polarization curves, (b) power curves, and (c) hydrogen curves. ....	78
Figure 4-9 The adaptive look-ahead Dec-MPC framework and the modular powertrain system sequence operation .....	81
Figure 4-10 The employed decomposition technique .....	84
Figure 4-11 Visual representation of the multi-step MPC-based PAS .....	85
Figure 4-12 The step-by-step flowchart of the Dec-MPC algorithm .....	87
Figure 4-13 The general operation of the FRL-based approach to seeking the optimal hyperparameter based on the current powertrain states ( $P_{avg}$ and $SoC$ ) in two sequence optimization steps. ....	88
Figure 4-14 Visual representation of the module-to-module FRL algorithm and the learning steps .....	89
Figure 4-15 The real profile characteristics: (a) power, (b) velocity, (c) acceleration, (d) power distribution, (e) velocity distribution, and (f) acceleration distribution .....	90

- Figure 4-16 Optimized results of the MPC-based approaches: (a) the powers based on Dec-MPC, (b) the powers based on adaptive Dec-MPC, (c) the comparison between the total output modules powers of the FC modules, and (d) the comparison between SoC levels. ...91
- Figure 4-17 (a) The computational complexity of the developed MPC-based approaches, (b) the number of iterations based on the DCO-based MPCs, (c) the moving horizon trajectories, and (d) the distribution of the lookahead horizon decided by the FRL control policy. ....93
- Figure 4-18 Optimal final cost and computational complexity of Cen-MPC, Dec-MPC, and adjustable Dec-MPC as functions of optimization window size. ....95
- Figure 4-19 The experimental results of the suggested Dec-MPC: (a) the output power profiles, (b) the FC modules' power profiles, and (c) the SoC level fluctuations. ....96
- Figure 4-20 The experimental results of the learning-enabled Dec-MPC approach: (a) the power profile of *FC1*, (b) the distribution of *FC1*, (c) the power profile of *FC2*, and (d) the distribution of *FC2*. ....97

## List of Symbols

EVs	Electric Vehicles
FCVs	Fuel Cell Vehicles
HEVs	Hybrid Electric Vehicles
PHEVs	Plug-in Hybrid Electric Vehicles
PJ-ADMM	Proximal Jacobian Alternating Direction Method of Multipliers
ADMM	Alternating Direction Method of Multipliers
ATC	Analytical Target Cascading
APP	Auxiliary Problem Principle
C-ADMM	Consensus Alternating Direction Method of Multipliers
DCO	Decentralized Convex Optimization
DP	Dynamic Programming
EMSs	Energy Management Strategies
FC	Fuel Cell
FCS	Fuel Cell Systems

FCVs	Fuel Cell Vehicles
ICE	Internal Combustion Engine
MPC	Model Predictive Control
MESs	Modular Energy Systems
OPF	Optimal Power Flow
OCD	Optimality Condition Decomposition
PHM	Prognostics and Health Management Approach
UC	Unit Commitment

# Chapitre 1 - Introduction

## 1.1 Introduction

An introduction to the Ph.D. thesis is presented in this chapter. Firstly, the research gap in existing studies is specified. Then, the corresponding solutions, specifically modular energy systems (MESs) and decentralized optimization algorithms, are discussed accordingly to highlight the main contributions of this thesis. Single-stack fuel cell systems (FCSs) face several challenges, such as efficiency, availability, durability, and cost. In the FCS, each cell needs appropriate distribution of humidification, hydrogen, water, and temperature. In malfunctioning cell/cells, uneven heating and variations in cell voltages can happen, and, as a result, continuing operation under this condition may be non-appropriate.

Furthermore, the traction power of buses, trucks, trailers, trains, and ships can reach high-level capacity, so it is necessary to shift to big-size FCS, generating higher power. However, stacking more cells declines the reliability of the powertrain systems. A modular energy system (MES) is introduced in the literature to address these deficiencies and imperfections. In [1], Marx *et al.* provided a survey of multi-stack FCSs with different architectures. It has been concluded that a more reliable system is obtained by utilizing a parallel configuration by enabling the degraded mode of operation. Garnier *et al.* [2] analyzed a multi-stack FCS with a power converter architecture for transportation applications. Candusso *et al.* [3] investigated the electrical operation equipped with an anti-parallel diode under malfunctioning conditions. A survey of variant power conditioning topologies is provided in

[4]. Thounthong *et al.* [5] reviewed different methods regarding the power-conditioning systems for the single-stack and multi-stack FCSs. Palma and Enjeti [6] suggested a modular multi-stack FCS powered by a modular power conditioning system. There are several advantages for the MES compared to the single-stack ones. One of the main advantages of multiple FCSs is the accessibility to several maximum efficiency operating points, as shown in Figure 1-1 [1].

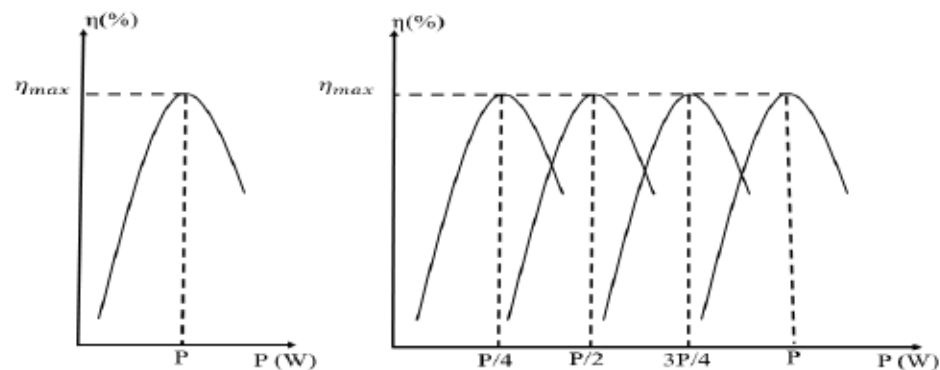


Figure 1-1 Efficiency curves comparison. (a) Single high-power source, and (b) Modular energy system composed of four parallel low-power sources.

Additionally, a MES can increase availability and durability by providing a redundancy function to the system [7, 8]. A MES can operate in a degraded mode if one or more modules break down due to malfunction [7, 9, 10]. A simple reconfiguration and replacing of the components without changing the entire system or pausing the operation can revert the power system to continue in its normal state [11]. The flexible configuration of these systems provides modularity as well as function partitioning. The modularity rules out the probability of cascading failure occurrence in the system and assures a nonstop operation of the system in various operating modes [11]. If only one or few FC modules are used in low power requirements, the unused FC modules do not degrade. This way of operation prolongs the lifetime of the system [12]. A flexible architectural arrangement is another strength of MESs.



Adjusting the position of the center of gravity can be done through various architectural configurations of powertrain components and their subsystems, which impact the mass distribution of the vehicle [13].

Another fundamental advantage of utilizing the MESs is reaching the economy of scale and large-scale production volumes in the intended power source. By acting on the number of modules, the MESs make the same elementary module possible for a wide range of applications in terms of power demand. This characteristic is because several similar modules manufactured by one production line can meet the power demand. In this way, the average costs start reducing as the output, the customers' needs for the particular manufactured product, escalates. This is when the economies of scale and series production happen. From another perspective, the required initial price of designing and implementing a MES is higher than a single-source system. However, in the long term, the modularity could compensate for this cost since the price of replacing one low-power component is much less than a high-power one. It is worth mentioning that the economy of scale is valid for a niche market and small series vehicles. Till the production reaches a high number of units/year of a given car, the design and the production of a reliable single source will probably be more attractive from an economic perspective. The modularity of the developed method is connected to the fact that mass manufacture of a modular energy system will reduce FCV final cost. It will be more cost-effective to have a modular energy module adaptable to various vehicle applications, from light-duty to heavy-duty. Thus, combining several modules may handle a broad range of transportation applications.

Contrary to the benefits mentioned above, the modular system encounters various drawbacks. First, because of several connected power units, the initial expense of a MES is higher than

a centralized energy system. Additionally, the maintenance cost to keep the system functional increases because of its multi-structure. Another point to mention is that it is more difficult to use several power sources effectively. Thus, management and designing an effective control strategy for such a system are challenging. Additionally, compared to the centralized energy system, the configuration and sizing methods will be more complex in the modular system design. The advantages and disadvantages of the MESs are summarized in Table 1-I.

Table 1-I A detailed comparison between the advantages and disadvantages of the modular energy system.

Advantages	Disadvantages
Efficiency improvement	High initial ancillary cost
The economy of scale, series production, and overall cost decline	High maintenance expense
Flexible architecture (mass distribution)	More challenging to deploy and design (architecture and dimensioning)
Availability and durability	Coordination and control problem

## 1.2 Different applications of the modular energy system

Based on the aforementioned benefits and drawbacks, it is clear that the modular system may be effective in various applications. Thus, MESs are required for transportation other than rail, road, sea, and air. The following sections show some of the most essential applications for each group.

### 1.2.1 Rail application

The enhancement of MES technologies has paved the way for applying these configurations in rail transportation applications [14]. In [15], different energy management methods are proposed to control the power flow among the powertrain



components in a low-floor light rail vehicle (LF-LRV) tramway. This tramway's powertrain, shown in Figure 1-2, comprises two PEMFCs, two battery packs, two supercapacitors, four bidirectional DC/DC converters, two unidirectional DC/DC converters, an auxiliary service module, and a braking resistor. The battery packs are connected in parallel by a converter. In this way, the output voltage of each battery pack is isolated, which leads to more flexibility in the inverter input voltage, the topology of each package, and operation management. Since the utilized FCs are arranged in a parallel configuration, the isolation and reconnection procedure can be conducted with minimum stress on the other components. This configuration is also more beneficial in degraded mode operation and reduces the average degradation per cycle than series one.

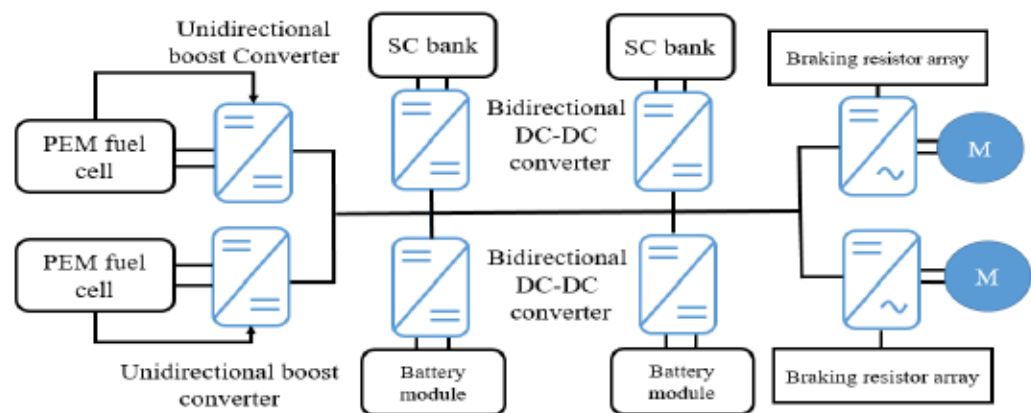


Figure 1-2 Powertrain configuration of the developed modular tramway [15].

### 1.2.2 Road transport

Several examples of utilizing modular FCS and batteries for road vehicles can be found in the literature. The German multinational automotive corporation, Daimler, has announced the emergence of a FC hybrid bus in Hamburg with the capability of 250 kilometers operating range and almost 50 percent less hydrogen consumption than the

last generation. The powertrain of this bus is practically maintenance-free with a long operating life thanks to the provided modularity by its FCS configuration in which two FCSs are connected to the DC bus [16]. In [17], to increase power, availability, and durability, two PEMFCs are connected in series, and the connection with the batteries is parallel to control a heavy-duty vehicle. The most significant advantages of this configuration are simplicity and low cost. The DC-bus of the car is directly connected to a pack of lead-acid batteries. The batteries act as an electrical source buffer coupled to the DC converter in a parallel configuration in the explained vehicle. In [18], two 40-kW FCS stacks are connected in a parallel configuration. The whole drive train is controlled through an adaptive supervisory control strategy. The power train configuration of this bus is presented in Figure 1-3.

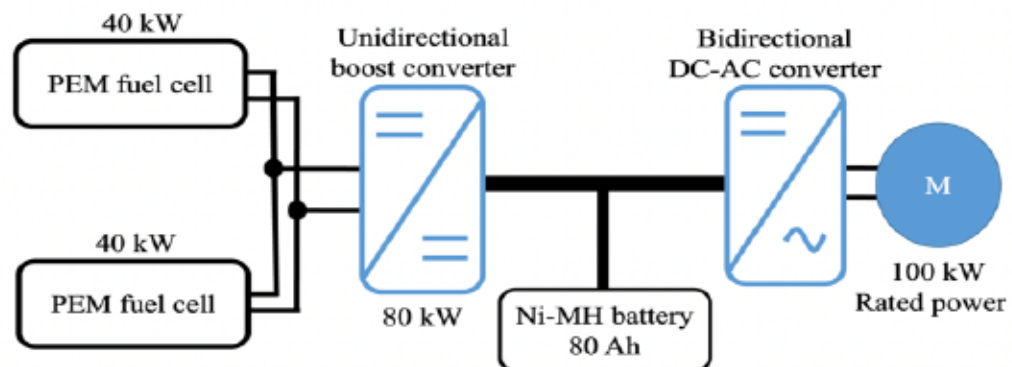


Figure 1-3 Powertrain of the hybrid modular source city bus [18].

### 1.2.3 Maritime application

Numerous examples of modular FCS and batteries for navigational purposes can be found in the scientific literature. For instance, a 92-meter-long vessel, with the help of several gas-electric propulsion systems (Gensets) next to FCS and battery systems, brings about

a safer level, lower noise and vibrations, and lower cost maintenance necessities [19]. Because of the parallel arrangement of the MES, the FCS system has prevented from being degradation after one year. In [20], several alternative powertrains based on different configurations of FCSs and batteries for an electric ship are studied. The power for the electric boat was provided by 12 packs of batteries (650 kW) and a 250 kW Genset. The research stated that the FCSs powertrain is more beneficial than others. Five Ballard HD6 FCS modules have been used in a parallel structure to satisfy the required high power current with a fixed voltage to implement this powertrain. Figure 1-4 demonstrates a hydrogen-powered vessel. The consumed hydrogen of two 30-kW FCSs is produced by electrolyzing seawater [21]. The primary feature of this vessel is that the hydrogen storage is ten times lighter than the storage by a battery pack, and it can be stored for a long time without any drop. Additionally, this forward-looking concept offers low hydrogen consumption, zero emission, zero noise, efficient energy storage, and backup power [21].

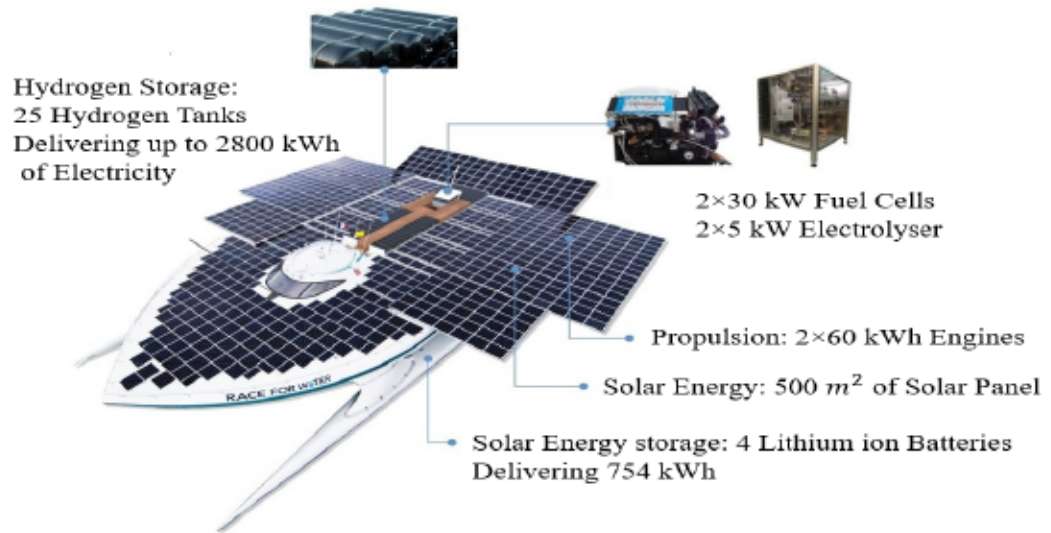


Figure 1-4 Configuration of the modular hybrid-electric boat [21].

#### *1.2.4 Submarines application*

Immersion autonomy and discretion (heat and sound) must be fulfilled in military submarines. The submarines with batteries have a very low immersion autonomy since they need to come back up to the water's surface to use the diesel engines to recharge the batteries. Integrating FCSs with batteries leads to a drastic increase in immersion performance. Moreover, noise and heat generation is much less in this way. For instance, the Class 212 submarine designed by Siemens is equipped with nine modules of 30 kW FCSs, in which one FCS is used as a backup. A lead-acid battery has been added to improve the total performance [22].

#### *1.2.5 Air transportation*

In [23], research in an uncrewed aerial vehicle (UAV) application stated that modular-stack configuration performs way better than single stack in terms of efficiency and availability. In [24], a hydrogen-powered four-seater passenger aircraft is introduced. This aircraft produces no local air pollution and has shown good prospects to make future transport more sustainable. The powertrain comprises four low-temperature FCSs ( $T < 70$  °C) placed in the center capsule, as shown in Figure 1-5. This aircraft can cruise up to 750 kilometers. By using liquid hydrogen, this range can be doubled at the cost of more complicated infrastructure [24].

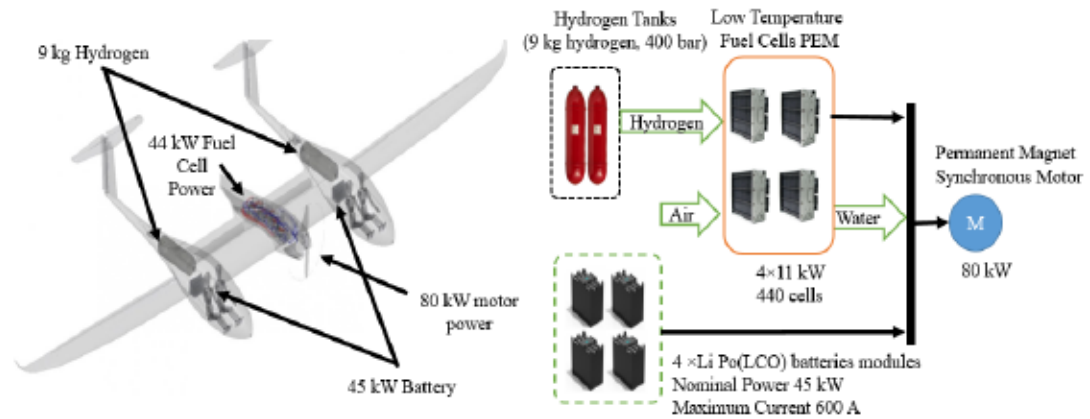


Figure 1-5 Powertrain configuration of the uncrewed aerial vehicle [24]

### 1.3 Possible prospects of modular-based powertrain systems

Concerning the discussed MES concept in the thesis, different possible research areas can be pointed out as worthy of attention. One of the essential research directions would be to create an advanced EMS for the modular system. A suitable and well-design EMS can make most of the previously discussed advantages of MESs viable. Another direction is to design an appropriate architecture and sizing of powertrain components for such a modular architecture. In this Ph.D. thesis, due to the importance of power decision-making strategy, the primary focus is designing and developing forward-thinking EMS control methods. In this regard, to investigate the design of the EMS part, a FCV architecture composed of two FC modules and one battery pack is selected, as shown in Figure 1-6. As can be observed, the two open-cathode PEMFCs are paralleled and connected to a DC bus to supply the requested power. The battery pack is placed to tackle the FCS's slow response characteristic, and the purpose of the regenerative braking is to improve FCV efficiency. In this regard, a modular test bench based on an electric vehicle is established [25]. The developed small-scale test bench comprises two modules, a



battery pack, a programmable DC electronic load, and a multi-range programmable DC power supply for simulating the requested load profile. The critical components of each module are a 500-W open-cathode PEMFCS (H-500), a smoothing inductor, and an adjustable unidirectional boost DC-DC converter. Six series 12-V 18-Ah battery packs give the voltage of the DC bus. Each module has its autonomous Dec-MPC inside of a National Instrument CompactRIO. The optimal reference of each module is calculated at every control instant with an interval of 10 Hz.

To achieve this thesis's primary goal, which is to apply a decentralized power allocation strategy, the presented figure makes it easier for the readers to understand the main powertrain configuration. The complete structure includes the local fuel cell system and powers electronic components. It is common to use such a presentation in different articles [18, 26, 27]. In the thesis, regenerative braking is not considered. The vehicle is equipped with a typical braking system, in which surplus kinetic energy is converted to wasted heat because of friction in the brakes.

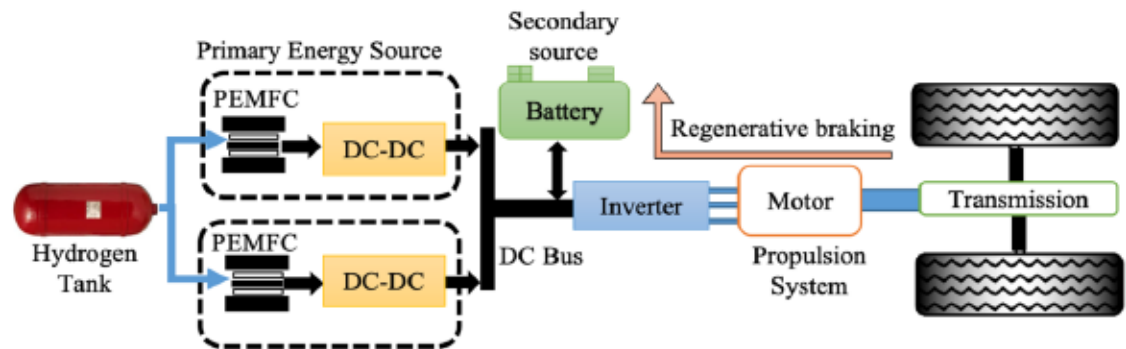


Figure 1-6 Scheme of the selected modular FCV powertrain architecture.

## 1.4 Different energy management strategies for modular fuel cell vehicles

Developing a promising energy management strategy (EMS) to coordinate multiple power sources is of great importance to efficiently use the FCV with a modular powertrain. The possible control and management strategy configurations for a modular FCV can be categorized into three primary forms: centralized, distributed, and decentralized, as demonstrated in Figure 1-7.

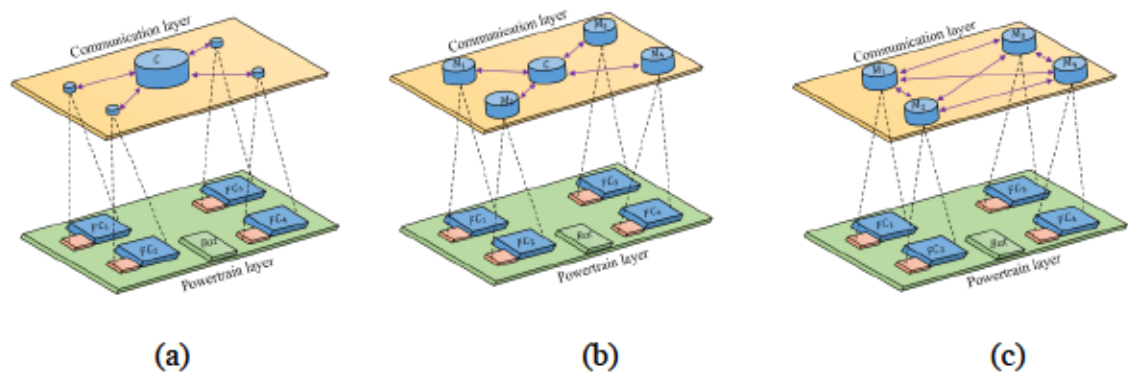


Figure 1-7 Different forms of developing control strategy unit for a module FCV: a) centralized, b) distributed, and c) decentralized.

### 1.4.1 Centralized-based control structure

All power modules are linked to a central control unit in this type of controller. The management unit collects detailed information about the modular system and provides control signals. This centralized decision-making structure is easy to set up and can be developed quickly. Somaiah and Agarwal [28] recommended implementing power point tracking in a multi-stack FCS using a power conditioning unit for each FCS. In [27], efficiency optimization and an instantaneous optimization-based EMS are suggested by Han et al. for a dual-stack FCS. Ramadan *et al.* [29] provided a thermal management strategy to reduce startup duration, heating/cooling, and cycling problems. Each FCS is activated based

on the demanded power and temperature. The multi-stack FCS useful life is influenced by each FCS useful life, operating conditions, and schedule in this work. Herr *et al.* [30] proposed a EMS based on the MILP method to prolong the powertrain systems' useful life through a prognostics and health management approach (PHM). Marx *et al.* [31] investigated the impact of components sizing of a multi-stack FCS. The obtained results demonstrated an improvement in hydrogen consumption and degradation rate in a high hybridization rate. Fernandez *et al.* [32] introduced a EMS based on an adaptive state machine to improve hydrogen consumption and lifespan. The suggested approach is integrated with a Kalman filter identification method to determine each FCS's maximum power and efficiency. To enhance the multi-stack FCS parameters estimation accuracy, Wang *et al.* [33] put forward a EMS based on a forgetting factor recursive least square online identification algorithm. In another study, Yan *et al.* [34] suggested a hierarchical control method based on an equivalent fitting circle strategy. Zhang *et al.* [35] proposed a hysteresis-based EMS to make activation time evenly distributed and decrease the number of switching over three-stack FCS. It is important to mention that all the existed EMSs for the multi-stack FCS are based on the centralized configuration. These centralized managements are not fault tolerant and do not provide the modularity from the software perspective.

#### *1.4.2 Distributed-based control structure*

As its name implies, the distributed structure does not require a central management unit. Instead, this configuration uses several coordinators, each managing a part of the power system's modules. Each power module only exchanges information with the coordinator units that operate each energy module independently. When one or more units fail, the other collaborating units can continue their operations and provide control signals to the functional



modules. Concerning overall powertrain system uptime, this distributed-based control system significantly improves over a centralized one. Furthermore, while their fault tolerance is higher than the centralized one, this comes at a maintaining price in a distributed-based control system.

#### *1.4.3 Decentralized-based control structure*

A decentralized strategy is similar to a distributed one in that it does not require a central control unit. However, going a step further in modularity eliminates the need to have multi coordinator units. Each control unit of the power modules directly exchanges data with its neighbor control units. The control units (software part) are allocated between the power modules (hardware part), improving the control strategy's performance. This decentralized-based scheme enables the modular controllers to share their control management responsibilities. Such a control system is safer than the centralized and distributed structures from the independent failure of power system components (hardware and software perspectives), improving its effective uptime considerably. Furthermore, the decentralized control structure is more scalable and flexible (plug-and-play) concerning changes in the modular power system [36, 37]. Another point to mention is that due to the ability to offer parallel processing and calculations, the decentralized-based EMS can reduce computational complexity more than the previous control structures, forming the solution speed and the maximum size perspectives.

While the decentralized-based strategy can bring several unique advantages for modular powertrain applications, there are also several disadvantages to this type of control strategy. In the modular powertrain system, a control strategy needs to be working toward the predefined common goals. Since the power decision-making strategy is delegated in a

decentralized control layer, ensuring that all control units consistently pursue the main powertrain objectives is more challenging. In this regard, addressing the coordination problems effectively requires receiving considerable attention. In addition, since several similar parallel control decisions need to be made simultaneously, the decentralized and modular structure is more susceptible to duplicating efforts, which results in inefficiency and extra costs.

Additionally, each module's control strategy may be tempted to modify its operation in an incongruity effort to maximize efficiency selfishly. Putting local goals above global goals is essential to make sure that one module's policy and control management does not interfere with or disrupt the work of other modules. Furthermore, external factors and unknown disturbances might make it impossible to benefit from the decentralization concept.

#### *1.4.4 Comparison between centralized, distributed & decentralized control strategies*

As mentioned above, there are several benefits and downsides to every control strategy configuration. To sum up all the discussions regarding different management structures, a thorough comparison among these control strategies is presented in Table 1-II. As can be obviously observed from Table 1-II, with less prone to malfunction and offering flexibility (plug-and-play), the decentralized decision-making structure has important characteristics compared to others. In addition, the reconfiguration and adaptive capabilities of the decentralized-based control will assist in declining its deployment and maintenance costs in the future. In this regard, the decentralized control configuration will likely prove an inspired direction in the years to come for the modular powertrain. Based on the provided discussion, the decentralized power splitting strategy is chosen to control the selected modular FCV powertrain configuration.

Table 1-II Comparison between centralized, distributed & decentralized control strategies

Methods	Pros	Cons
Centralized	Simple management algorithm Fast developed process Reasonable maintenance cost	Likely to malfunctions High computational time Expensive and extremely reliable processor unit
Distributed	Less likely to fail than a centralized control unit Better performance Allows for a more flexible control strategy	More expensive maintenance costs than a centralized one Irregular performance when not well optimized
Decentralized	Parallelizable and needs low computational efforts Best performance Fault-tolerant Higher level of security Highly plug-and-play and scalable Several cheap possessor units	More challenging to coordinate and design the control units Higher maintenance costs

### 1.5 Decentralized convex-based optimization (DCO) approaches

Based on the previous explanation, in this subsection, a comprehensive literature review of the decentralized methods is given to select the most suitable approach. As mentioned earlier, the multi-stack powertrains bring about modularity and reliability from electrical and fluidic perspectives. They do not guarantee these aspects in their management and control units. Therefore, there has been a growing trend in the literature to shift from centralized power allocation strategies (Cen-PASs) to decentralized power allocation strategies (Dec-PASs). For instance, in [38, 39], two Dec-PASs based on game theory are proposed. However, the main drawback of these strategies is that the players are selfish and may not converge to their optimal results.

Furthermore, these Dec-PASs cannot entirely satisfy the nonlinearities in the behavior and the constraints of different sources. Another significant problem with these strategies is that they need a lot of data exchange, which is not feasible for the onboard applications. In [40], a droop-based Dec-PAS is proposed for seeking optimal power-sharing. However, this approach cannot perform well in a wide range of operations and does not consider the powertrain system's lifespan. To evade the problems mentioned above in other domains with multi-source systems, such as smart grids [41, 42], special attention has been given to decentralized convex optimization (DCO) algorithms [43]. In the DCO methods, the central complex optimization problem is decomposed and then reformulated for each small subproblem regarding shared information and newly defined constraints. One of the most famous classical decomposition methods is introduced in [44] based on Lagrangian Relaxation with slow convergence. Several other ways, such as auxiliary problem principle (APP) [45], consensus-based algorithm [46], Karush-Kuhn-Tucker (KKT) conditions [47], and alternating direction method of multipliers (ADMM) [48, 49], have been proposed to enhance the convergence rate. ADMM has attracted much attention since it can guarantee global convergence and does not require a significant amount of data exchange despite other algorithms. This method amalgamates dual decomposition with the multipliers technique and the augmented Lagrangian approach. ADMM decomposition-based method can be categorized into Gauss-Seidel ADMM (GS-ADMM), Variable Splitting ADMM (VS-ADMM), and Jacobian ADMM (J-ADMM) [50]. GS-ADMM cannot be straightforwardly applied to an optimization problem with more than three subproblems and hence cannot guarantee the convergence in this case [50]. VS-ADMM is also not practical for large-size optimization problems, and J-ADMM may diverge for various problems although its updating procedure is parallel. In this regard, J-ADMM and GS-ADMM have been advanced



to Proximal Jacobian ADMM (PJ-ADMM) and Consensus ADMM (C-ADMM), respectively, to be more practical for the distributed optimization problems. The update processes of PJ-ADMM and C-ADMM are parallel, and convergence performance can be guaranteed simultaneously [51]. These two DCO-based algorithms offer several advantages compared to centralized ones. Firstly, parallel execution feature enables them to solve complex optimization problems with less computational effort. Secondly, they can autonomously adapt to new changes, which provides robustness in any subsystem failure. In a modular energy system, robustness may be defined as a system's ability to withstand a sudden failure and continue operating normally in the case of an electrical fault. In [52, 53], two classic ADMM algorithms are suggested for solving Cen-PASs in hybrid electric vehicles. However, their central control units do not offer modularity, plug & play aspects, and robustness in terms of software. [42] summarizes different notable applications of the DCOs, such as direct current optimal power flow (DC-OPF), alternative current optimal power flow (AC-OPF), and unit commitment (UC), in the literature. Different connection topologies for the DCOs to share information among the subproblems are shown in Figure 1-8. The results in [54] showed that the star-connection would lead to a faster convergence rate than the ring-connection strategy. Similar research in [55] investigated the advantages of the ring-connection topology as compared to the star-connection topology, including (1) the reduced amount of data to be communicated, (2) higher level of security, (3) more robustness, and (4) privacy protection of individual agents since the data are not shared in a central controller. The complete connection offers the fastest convergence rate between all types of connection forms compared to the other configurations. From a contradictory perspective, a high range of data exchange among the adjacent modules is needed in this

topology. To do so, a ring configuration is employed to form the shared information between the modules. A comparison of different types of communication is presented in Table 1-III.

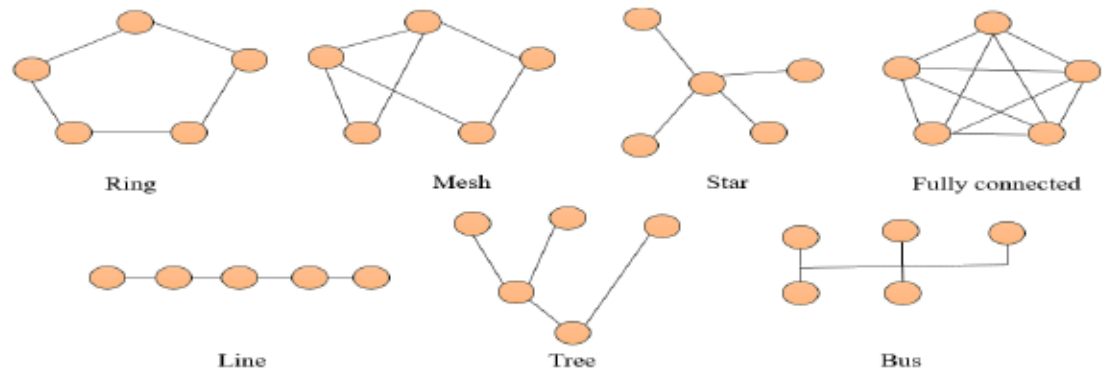


Figure 1-8 Popular communication and sharing information topologies for the decentralized optimization algorithms.

Table 1-III A comparison of different types of communication

Type	Convergence speed	Data	Security	Privacy	Robustness
Star	Medium	Medium	Medium	Medium	Medium
Ring	Low	Low	High	High	Higher
Full	High	High	Medium	Medium	Medium

Depending on the decomposition techniques and shared information, the DCOs can be classified into two main categories, as shown in Figure 1-9 and Figure 1-10. Table 1-IV is compared the five most important characteristics of the Lagrangian-based and consensus-based DCOs.

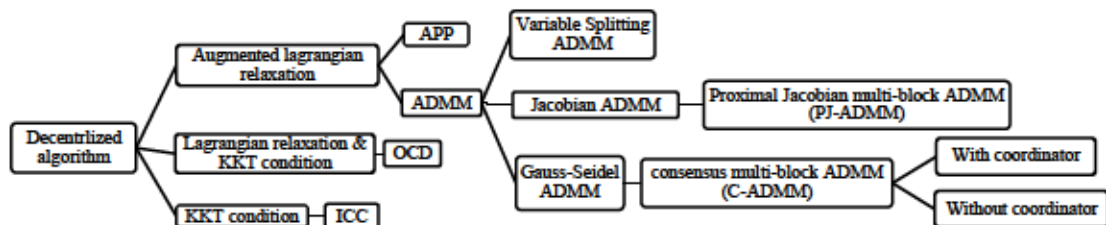


Figure 1-9 Classified the DCOs based on the decomposition methods.

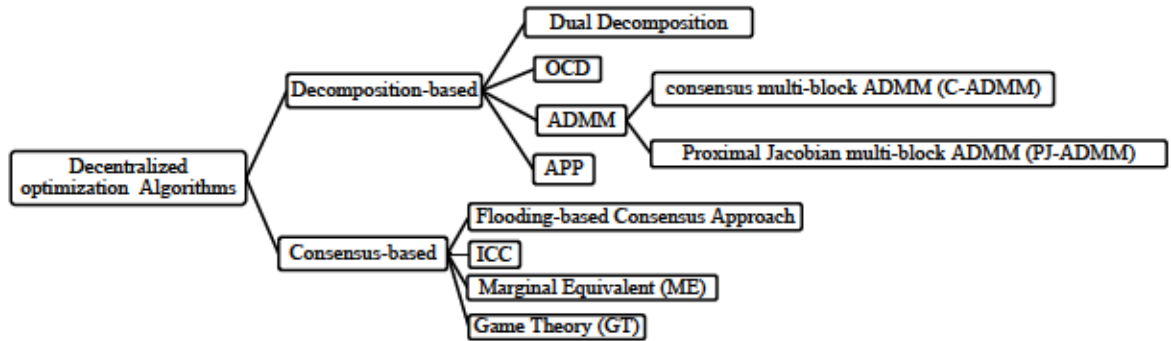


Figure 1-10 The decentralized methods according to the type of the pooled information

Table 1-IV Comparison between the Lagrangian-based and Consensus-based DCOs.

Algorithm	Method	Type of information	Data	Iteration	Computational effort
Lagrangian-based	Leaving each entity with an optimization problem to solve	Physical variables of the boundary system	High	Low	High
Consensus-based	Solves a set of a linear combination of gradient terms per iteration	Cost of subproblem	Low	High	Low

To investigate in detail, Table 1-V and Table 1-VI summarize the features of Lagrangian and consensus-based methods.

Considering the discussed DCOs in the previous studies, it is reasonable to select the Lagrangian-based schemes to tackle the real-time decentralized EMS application of the thesis. A real-time system can generate accurate outputs from the computations based on the logical results and the physical time when those results are generated [56]. When a controller responds to a request, its response time typically falls into a variation interval, also known as latency jitter. A powertrain system can only allow a certain amount of latency without damage or failure. The latency of a control unit should be at least five times smaller than the latency of the process the controller is meant to control to provide a reliable automation

solution. For appropriate hardware selection, requirements should include handling processor interrupts in real-time and providing a development and runtime software environment that can handle the required elapsed time and latency jitter. These methods are more robust than the other approaches, and they are more accessible for implementation, giving them more practical capabilities.

Table 1-V Summarization of Lagrangian-based methods.

Algorithm	Dual decomposition	ADMM	APP	OCD
Advantages		Scalable/ fine-grained Nodal-based	Robust Area-based	
Speed	Slow	Fast	Fast	Fast
Disadvantages	Difficulty in convergence	Dependent on the tuning parameters	Dependent on tuning parameters	Relies on how the system is partitioned- Differentiable Cost functions
Data exchange	High	Medium	Low	High
Computational	High	Medium	Low	Low
Iteration	High	Low	Low	High
Convergence	Strict convexity finiteness of all local functions	Convex function	Convex Differentiable function	No proof

Nevertheless, special consideration should be paid to the choice of tuning parameters to obtain satisfactory results in terms of the initialization and customization of the algorithm. Furthermore, these methods are preferable to consensus-based schemes since their convergence to the global answer can be proven, and they easily enable each modular system to achieve optimal results even in the case of a halt or malfunction in one of them. In this regard, APP, C-ADMM, and PJ-ADMM are singled out among the Lagrangian-based approaches due to their parallel structures and fast convergence, which seem like feasible solutions in our case study.



Table 1-VI Summarization of Consensus-based Algorithm.

Algorithm	ICC	GT	RL
Advantages	<ul style="list-style-type: none"> <li>Fully decentralized</li> </ul>	<ul style="list-style-type: none"> <li>Robust</li> <li>Adaptive</li> <li>Scalable</li> <li>Fully decentralized</li> </ul>	<ul style="list-style-type: none"> <li>Model-free</li> </ul>
Disadvantages	<ul style="list-style-type: none"> <li>Sensitive to hyperparameters</li> <li>Problem with addressing the constraints</li> <li>Cannot reach a good outcome for nonlinear cost functions</li> <li>The amount of data exchange between neighbor modules is high.</li> </ul>	<ul style="list-style-type: none"> <li>System-level security constraints may not be effectively handled</li> <li>Significant information exchange</li> <li>Self-optimizing manner</li> <li>Converge if general Nash equilibrium exists for the problem</li> </ul>	<ul style="list-style-type: none"> <li>Optimality cannot be guaranteed</li> <li>High training rate</li> </ul>

### 1.6 Problem statement

The fuel cell system encounters reliability and durability shortcomings compared to the internal combustion engine. In the literature, the multi-stack fuel cell system is introduced, and many studies are conducted to improve further this kind of system. The main weakness regarding the current multi-stack system is that even these systems provide flexibility and plug-and-play from the hardware point of view. At the same time, they do not offer such characteristics from the software perspective. The control unit of an interconnected multi-stack system with a centralized control strategy is susceptible to malfunction and would not be plug-and-play. For instance, in case of an electrical fault in the control unit, the fuel cell system will stop its regular operation. Furthermore, a multi-stack system with a centralized control unit would not be reconfigurable to the new powertrain changes.

### **1.7 Aims and objectives**

To correctly solve the preceding section's problem, three primary goals are identified, and the thesis's significant steps are detailed in connection to these objectives. The main goal is to illustrate the completely decentralized technique in a multiple-stack powertrain system. The second goal is to examine the capability of establishing a decentralized strategy from various perspectives. The third goal is to enhance the previous phase, based on a one-step optimization technique, by including knowledge about future driving profiles. After studying the excited decentralized controllers, the Lagrangian-based decomposition approach was chosen to meet the significant purpose of this research. The overall optimization issue is then subdivided into two subproblems. To accomplish the second objective, two well-known decomposition strategies are carefully contrasted. Two critical aspects of robustness and cost sensitivity are thoroughly examined. To accomplish this thesis's final objective, a machine-learning technique is used to address the limitations of incorporating this information and the dynamic reactions of the components as computing complexity increases.

### **1.8 Methodology**

Based on the explanations mentioned above, due to the shortcomings in the multi-stack FCSs from the software perspective, it is essential to shift toward decentralized energy management schemes. Such a system is robust against faults and brings flexibility and plug-and-play. Based on the developed bases, after presenting the literature review of the multi-stack fuel cell system, in Chapter 2, a proof of concept of the modular system with a single-step decentralized control strategy is proposed for a two-stack system. In this regard, the optimization problem is formulated. Subsequently, a detailed comparison shows how this approach is close to the centralized method concerning the final hydrogen consumption and

degradation costs and the computational time complexity. After presenting this step, Chapter 3 presents two powerful decentralized optimization algorithms to more specifically concentrate on the fault robustness of the proposed strategies. Different critical aspects such as hyperparameter tuning and cost sensitivity are presented in this chapter. For the last step of this thesis, in Chapter 4, to improve the proposed method's performance, the decentralized optimization method is shifted from the one-step form into the multi-step optimization one by adding the model predictive concept to the studied optimization problem.

Additionally, a decentralized learning-based algorithm is added to the decentralized look-ahead scheme to have an adjustable optimization horizon. The decentralized strategy's learning mechanism is based on three standard driving cycles. There is only one real driving profile for the electric car under study. Furthermore, just three available standard driving profiles are well-suited to the selected light-duty electric vehicle. Indeed, to obtain a trustworthy outcome, it is critical to train the learning process using a database of real-world driving patterns. The result reported in this chapter is the first proof of the central concept. Integrating the new driving profiles is the first step to making the suggested method even better. Ultimately, based on the conducted research, a conclusion summarizes all of the core results in this thesis. Then, several future possible directions and perspectives are given.

## **1.9 Thesis structure**

The remainder of this thesis is structured as follows. Chapter 2 presents the proof of concept of the decentralized EMS in an article entitled “Power Allocation Strategy Based on Decentralized Convex Optimization in Modular Fuel Cell Systems for Vehicular Applications”. Chapter 3 describes the main characteristics of such decentralized optimization algorithms by presenting an article entitled “A Comparison of Decentralized

ADMM Optimization Algorithms for Power Allocation in Modular Fuel Cell Vehicles”. Chapter 4 explains the integration of the decentralized optimization approach with the model predictive control technique by presenting an article entitled “Look-Ahead Decentralized Safe-Learning Control for a Modular Powertrain Using Convex Optimization and Federated Reinforcement Learning”. Finally, the conclusion is presented in Chapter 5 with a detailed description of the future steps concerning the further improvement of this thesis.

# **Chapitre 2 - Power Allocation Strategy Based on Decentralized Convex Optimization in Modular Fuel Cell Systems for Vehicular Applications**

## **2.1 Introduction**

Although the design of a centralized EMS for FCVs is a familiar issue and has been carefully investigated in many studies by researcher groups, the aim of exploring a decentralized and modular control method has been disregarded. In this light, exploring and evaluating the benefits of a decentralized architecture for power splitting management as a dissertation's first step might be novel. Thus, the first investigation began with a proof of concept for a decentralized approach to power management. This technique uses decentralized control to create a resilient and adaptable (plug and play) system that does not require a centralized control unit to serve as the central coordinator. Decentralization: This architecture is defined by a systematic module-level management strategy that can allocate power in a way that meets the multi-objective cost function and other constraints.

## **2.2 Methodology**

This paper presents a decentralized convex optimization (DCO) framework based on the auxiliary problem principle (APP) to solve a multi-objective power allocation strategy (PAS) problem in a modular fuel cell vehicle (MFCV). In this regard, the operational principle of the suggested D-APP for the PAS problem is elaborated. Moreover, a small-scale test bench based on an electric vehicle is developed, as shown in Figure 2-1. Several simulations and



experimental validations are performed to verify the advantages of the proposed strategy compared to the existing centralized ones.

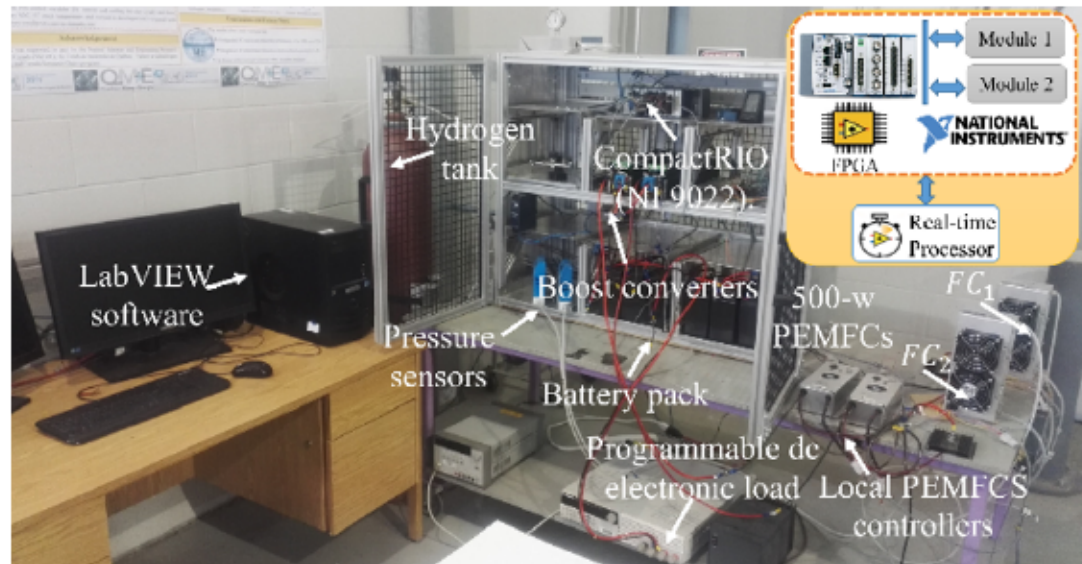


Figure 2-1 The developed modular test bench

A detailed framework to clarify the decentralized solution to the optimization problem is presented. The PAS problem is decomposed into two individual subproblems where the output power of each FC module is the coupling variable, and each of the subproblems is associated with one of the two FC modules, as shown in Figure 2-2. Then, the output power of each FC is duplicated into two new terms, real and virtual variables, to mimic the rest of the powertrain system. The virtual variables are linked to each of the two subproblems. The local PAS subproblems are defined and formulated for each module. An iterative procedure based on the decentralized APP approach is carried out to coordinate between subproblems and seek the optimal operating point of the original modular powertrain system, as shown in Figure 2-3. At the end of each iteration, the local optimization algorithms based on the defined cost functions and constraints are used to calculate the real power of the local FC modules and the virtual power of the neighboring FC modules. These values are then sent to



the neighboring FC modules. As for each of the real and virtual variables, it is essential to have the same values once the APP approach has converged, equality constraints are used by the two local PASs, thus restricting the error of the shared powers to be zero. If the calculated errors by the PAS modules and their duplicated ones are less than a predetermined level, convergence is obtained. If not, a set of penalty multipliers ( $\lambda$ ) are calculated, and then the local PASs are solved via the new variables. This algorithm is run repeatedly until it converges. Since the convergence speed of the algorithm is faster than the system dynamics, the virtual variables get very close to the real values. It is worth noting that although the number of shared variables increases the size of the matrixes, the decentralized forms are solved in a parallel manner which reduces the computational time.

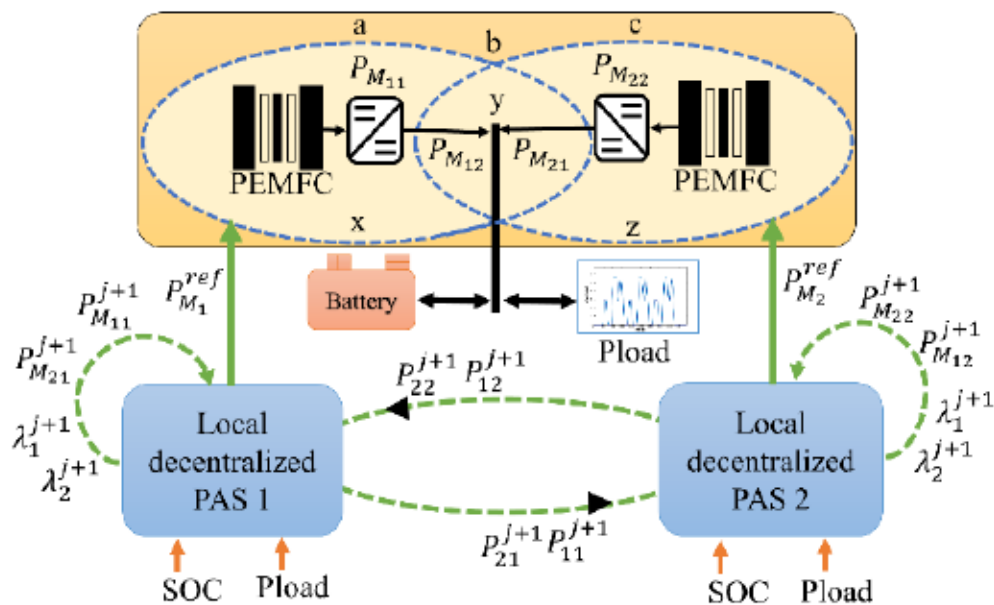


Figure 2-2 The configuration of the D-APP PAS [57].

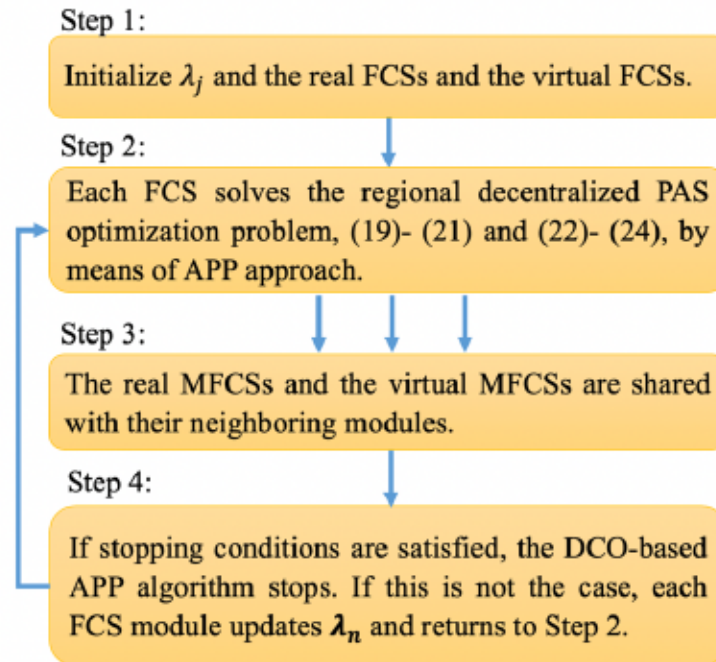


Figure 2-3 The general systematic flowchart of the D-APP strategy.

The decentralized characteristic of the control management unit is achieved through a single-step auxiliary problem principle (APP) algorithm that can ultimately decompose the underlying centralized EMS optimization problem. Moreover, dynamic programming (DP) as the benchmark optimization method has been developed for evaluation purposes. Finally, the proposed method is investigated on a modular powertrain that executes the decision-making algorithm through a modular-to-modular network without a centralized coordinator. As a result, the proposed modular EMS offers distinctive characteristics compared to the centralized one.

### 2.3 Synopsis of the analyses of the results

The power-split strategy based on DCO between the modules and the battery unit is shown in Figure 2-4, where Pload is the requested power, FC is the power provided by the modules, and Battery is the battery unit power. From Figure 2-4 (b), the modules primarily

operate in the high-efficiency region to avoid the degradation price, which leads to a lower cost of degradation with the aid of a battery pack.

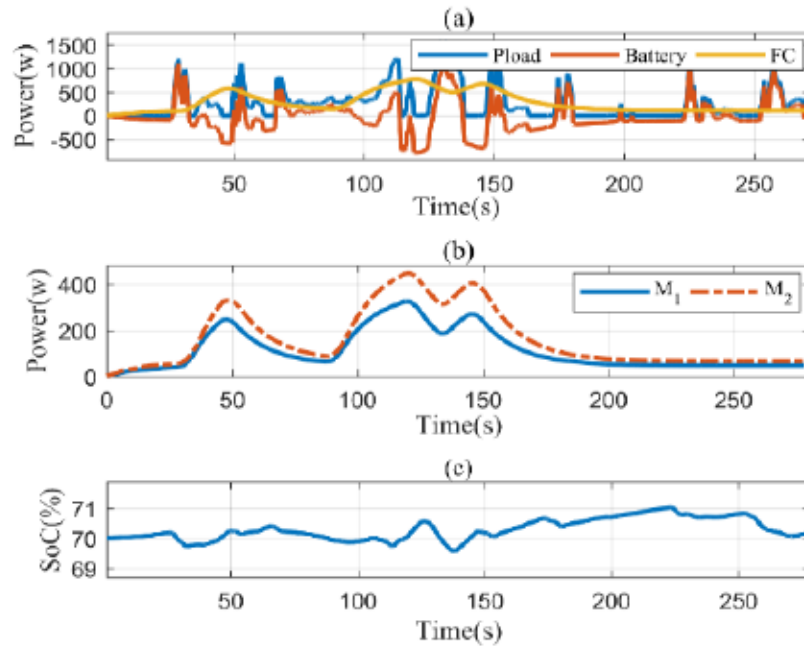


Figure 2-4 The APP results under real driving profile: (a) power profiles, (b) the modules ( $M_1, M_2$ ) split powers, (c) the SoC of battery.

The cost of each optimization approach is determined using a single evaluation function to ensure that they may be compared fairly. The assessment is made using the hydrogen consumption and degradation rates of the battery and PEMFC modules. The D-APP has achieved a near end-user price to DP (with a 12% difference) while the computational burden is less. The final end-user cost is approximately \$0.2134, to which the total hydrogen price of \$0.1033 contributes the most (48.41% of the end-user expense). Between these two  $M_1$  with about \$0.0641 (30.04% of the end-user cost) contributes more compared to  $M_2$  with about \$0.0392 (18.37% of the final cost). The second highest cost is the modules degradation cost which is precisely \$0.0330 (15.46% of the end-user cost). The battery degradation cost is around \$0.0077 (3.61% of the final cost). It is the lowest cost compared to the ones related

to the modules. The penalty term to recharge the battery pack is approximately \$0.0694 (32.52% of the final cost).

## 2.4 Outcomes

The investigation of a single-step decentralized EMS to increase modularity and resilience has resulted in discovering new pieces of knowledge about a module-level power allocation control technique. To be more explicit, these comprehensions were developed by analyzing the decentralized-based power splitting technique employing a variety of numerical studies in its unique context, as indicated below.

- Real-time accuracy and capability of the convex powertrain models: The developed EMS powertrain modeling has been assessed as one of the significant phases in the control process. The effectiveness of the modeling step can be found by comparing the results of the optimization method to the results on the test bench.
- Communication layer and information flow: The communication process has been elucidated and presented with detailed data management by the control modules.
- Resulting optimization performance: The extensive comparison of decentralized solutions to the EMS problem demonstrated that the suggested algorithm, with its specific decentralized characteristic, may be recognized as a beneficial power management approach and is worthy of future exploration.

The subsequent research study displays the results of the proposed power allocation through comprehensive analysis.

**Article 1:** Power Allocation Strategy based on Decentralized Convex Optimization in Modular Fuel Cell Systems for Vehicular Applications

**Authors:** Arash Khalatbarisoltani, Mohsen Kandidayeni, Loïc Boulon, and Xiaosong Hu

**Journal:** IEEE Transactions on Vehicular Technology (published)

**Publication date:** 1/ October / 2020 (DOI: 10.1109/TVT.2020.3028089)

## 2.1 Conclusion

The chapter put forward a DCO algorithm for MFCVs to address a multi-objective PAS optimization problem. Firstly, a novel distributed normalized cost function, including hydrogen consumption and health-conscious constraints of the FC modules and the battery pack, is minimized via a fully D-APP algorithm. Secondly, the effectiveness of the D-APP algorithm is validated via several numerical studies, namely the effect of parameter tuning and driving behavior. Finally, the performance of the algorithm is compared with the DP strategy and SQP. This comparison shows that D-APP can achieve an end-user price near DP (7.69% difference) while using a real-time method.

Moreover, compared to SQP, the decentralized method leads to less computational time and less sensitivity when having complex functions with several constraints. Finally, experimental validation is performed on a developed test bench that illustrates the proposed D-APP's effectiveness. The focus of this chapter has been mainly on the proof of concept of the decentralized optimization algorithm. However, the outcomes seem to be very interesting in modular applications. The robustness and the modularity points of view have not been discussed. Therefore, the next chapter will perform a comprehensive study regarding the raised matters for two advanced decentralized optimization algorithms.



# Power Allocation Strategy Based on Decentralized Convex Optimization in Modular Fuel Cell Systems for Vehicular Applications

Arash Khalatbarisoltani<sup>1</sup>, Member, IEEE, Mohsen Kandidayeni<sup>2</sup>, Member, IEEE,  
Loïc Boulon, Senior Member, IEEE, and Xiaosong Hu<sup>3</sup>, Senior Member, IEEE

**Abstract**—Recently, modular powertrains have come under attentions in fuel cell vehicles to increase the reliability and efficiency of the system. However, modularity consists of hardware and software, and the existing powertrains only deal with the hardware side. To benefit from the full potential of modularity, the software side, which is related to the design of a suitable decentralized power allocation strategy (PAS), also needs to be taken into consideration. In the present study, a novel decentralized convex optimization (DCO) framework based on auxiliary problem principle (APP) is suggested to solve a multi-objective PAS problem in a modular fuel cell vehicle (MFCV). The suggested decentralized APP (D-APP) is leveraged for accelerating the computational time of solving the complex problem. Moreover, it enhances the durability and the robustness of the modular powertrain system as it can deal with the malfunction of the power sources. Herein, the operational principle of the suggested D-APP for the PAS problem is elaborated. Moreover, a small-scale test bench based on a light-duty electric vehicle is developed and several simulations and experimental validations are performed to verify the advantages of the proposed strategy compared to the existing centralized ones.

**Index Terms**—Fuel cell system, distributed optimization, fuel cell hybrid vehicle, energy management, multi-agent system.

## I. INTRODUCTION

FUEL cell vehicles (FCVs) have become a propitious substitute for internal combustion engines (ICEs) to mitigate the greenhouse gas (GHG) emissions in transportation sector

Manuscript received April 24, 2020; revised July 31, 2020; accepted September 22, 2020. Date of publication October 1, 2020; date of current version January 22, 2021. This work was supported in part by the Natural Sciences and Engineering Research Council of Canada (NSERC) and in part by the Canada Research Chairs program. The work of X. Hu was supported by the Chongqing Natural Science Foundation for Distinguished Young Scholars under Grant cstc2019jcyj0010, Chongqing Science and Technology Bureau, China. The review of this article was coordinated by Dr. Theo Hofman. (Corresponding authors: Loïc Boulon and Xiaosong Hu.)

Arash Khalatbarisoltani and Loïc Boulon are with the Hydrogen Research Institute, Department of Electrical and Computer Engineering, Université du Québec à Trois-Rivières, Trois-Rivières, QC G8Z 4M3, Canada (e-mail: arash.khalatbarisoltani@uqtr.ca; loic.boulon@uqtr.ca).

Mohsen Kandidayeni is with the e-TESS lab, Department of Electrical and Computer Engineering, Université de Sherbrooke, Sherbrooke, QC J1K 2R1, Canada, and also with the Hydrogen Research Institute of Université du Québec à Trois-Rivières, Trois-Rivières, QC G8Z 4M3, Canada (e-mail: mohsen.kandidayeni@usherbrooke.ca).

Xiaosong Hu is with the State Key Laboratory for Mechanical Transmission, Department of Automotive Engineering, Chongqing University, Chongqing 400044, China, and also with the Advanced Vehicle Engineering Centre, Cranfield University, MK43 0AL Cranfield, U.K. (e-mail: xiaosonghu@iecc.org).

Digital Object Identifier 10.1109/TVT.2020.3028089

[1], [2]. Among several types of fuel cell (FC), proton exchange membrane fuel cell (PEMFC) has been adopted broadly in green mobility thanks to its appropriate characteristics [3]. However, the use of a sole FC system (FCS) cannot satisfy all the requirements in vehicular applications as its performance is drastically declined in the presence of dynamic load profiles. Moreover, it is not able to capture the energy from regenerative braking owing to its energy storage incapability. Hence, hybridization of the FCS with other power sources, such as battery (B) or supercapacitor (SC), has been abundantly practiced in the literature to compensate for the mentioned weaknesses [4], [5].

In FCVs, the end-user cost is defined based on several factors, such as hydrogen consumption, FCS degradation, and battery unit degradation. To minimize this cost, it is required to define a well-developed multi-objective power allocation strategy (PAS). A variety of PASs, such as rule-based [6]–[8], equivalent consumption minimization [9], [10], model predictive control [11], adaptive [12], [13], dual-mode [14], and heuristic [15], [16], have been suggested in the past few decades for the FCVs. Some of these papers have also highlighted the possibility of integrating the prognostic and health management techniques into the design of PASs [17]. These techniques can be categorized into two main groups of model-based [18], [19], and data-driven [20], [21]. They are utilized to estimate the state of health (SOH) and remaining useful life (RUL) and then this estimation can be included as an input in the strategy to distribute the power. For the sake of combining the advantages of model-based and data-driven methods, a hybrid prognostic framework is introduced in [22]. The suggested method provides an uncertain characterization of RUL probability distribution. This method can be integrated into the existing PASs as a guiding principle for making appropriate sequential decisions to prolong the powertrain system lifetime. However, all the discussed strategies have been developed for single FCSs. Hence, they are very sensitive to the malfunction of the power sources, which is likely to happen in such a powertrain configuration.

In this respect, a new direction called modular energy systems (MESS) has come under attentions to overcome the limitations of a single FCS and increase reliability as well as the scalability of the FCVs [23]. Unlike the typical FCVs, a modular FCV (MFCV) is composed of a battery pack and a set of low-power FC modules, instead of a high-power one, to augment the reliability and the scalability characteristics. Several PASs have



been suggested for such modular systems, such as rule-based [24], hysteresis strategy [25], and droop control [26], [27]. In [28], Marx *et al.* have reported a comparative review of different concepts for these modular topologies in multi-stack FCs from a hardware point of view. They have concluded that the robustness is improved in parallel-connected configuration compared to other topologies. In [29], a PAS based on forgetting factor recursive least square is proposed for a MES composed of two 300-W PEMFC stacks with a parallel configuration. The strategy shows lower hydrogen consumption compared to average power and daisy chain algorithms. In [24], an adaptive state machine strategy is proposed for a MES composed of four 500-W PEMFCs and a battery pack. This strategy has improved the hydrogen economy compared to Daisy Chain and Equal distribution strategies while keeping the PEMFCs with the same health states.

Therefore, the hardware modularity has been already investigated in the MFCs while the software modularity has escaped the attentions. Literature consideration shows that most of the existing PASs, regardless of having a modular or normal powertrain topology, are centralized. Therefore, they are very sensitive to a precipitous single point of failure through their powertrains from a software point of view. Moreover, the additional degrees of freedom in the MESs make the centralized algorithms substantially complicated and time-consuming to be solved. In this respect, some papers have focused on the distributed optimization algorithms to solve the PAS optimization problems [30]–[34]. In [30], a projected interior point method is proposed under the framework of model predictive control (MPC) to solve the power allocation problem and concluded that this strategy is faster than CVX tool, which is a general-purpose convex optimization software. In [31], CVX tool is utilized to solve a formulated convex optimization problem for a plug-in FCV, and it is shown that the proposed approach can effectively distribute the power between the power sources and also find the optimal sizes of each source. In [32], the slew rate of the PEMFC current and the battery state of charge (SoC) are considered to formulate the PAS in the form of quadratic programming (QP). Subsequently, a solver is utilized to solve the QP problem based on the alternating direction method of multipliers (ADMM). It is concluded that this approach is much faster than interior point or active set methods. In [33], a PAS for a hybrid electric vehicle is proposed based on ADMM and concluded that this strategy can achieve up to 90% of fuel saving obtained by dynamic programming (DP) while it is 3000 times faster than DP. In [34], a distributed optimization approach is put forward to solve the PAS of a hybrid vehicle. The comparison of this distributed algorithm with a centralized convex optimization problem shows that the proposed algorithm can result in the same fuel economy as the centralized method while its computational time is declined up to 1825 times. Although the discussed papers in [30]–[34] have improved the PAS formulation to a further step regarding the accuracy and computational time reduction, they are not still fully decentralized, and are sensitive to the occurrence of malfunction in their systems. In [35], [36], a decentralized approach based on non-cooperative game theory is proposed to formulate the PAS in a multi-source hybrid vehicle.

The method in these papers shows a comparable performance to that of the centralized strategies. Moreover, the potential of this approach for dealing with the sudden reconfigurations in the system is also demonstrated in [35]. However, this decentralized method is not able to deal with the constraints with a high amount of nonlinearity which are inevitable in FCVs.

In the light of the discussed papers, it can be stated that the design of MESs for a FCV application has gained considerable attentions. However, most of the existing works only deal with one side of modularity, either hardware or software. The hardware is related to the configuration of the powertrain (for instance a parallel multi-stack PEMFC system coupled with a battery pack), and the software is related to the development of a suitable PAS (like a decentralized algorithm). Furthermore, most of the papers which have focused on the software side are for hybrid electric vehicles with an ICE and not a FCV.

In this regard, this paper puts forward a decentralized convex optimization (DCO) methodology based on auxiliary problem principle (APP) [37]–[39] to solve a constrained convex approximation power distribution problem in a MFCV. This MFCV is composed of two PEMFCs, which are connected in parallel, and a battery pack. To the best of the authors' prior knowledge, this is one of the first attempts, if any, to formulate an accelerated decentralized PAS for a MFCV to benefit from the full modularity potential considering hardware and software viewpoints. To this end, a multi-objective cost function, including the hydrogen consumption, battery SOC variation, PEMFC health state, and battery health state, is defined and minimized by the proposed decentralized APP (D-APP). To verify the performance of the suggested D-APP, it is compared with dynamic programming, which is an offline strategy, and an online centralized PAS based on sequential quadratic programming (SQP). Moreover, the performance of the D-APP has been justified by an experimental modular FC (MFC) test bench developed for the purpose of this work.

The rest of this paper is organized as follows. The powertrain and the modeling are detailed in Section II. Section III formulates the convex PAS for a MFCV. The application of the D-APP is explained in Section IV. Several numerical studies are given in section V. A real-time implementation via the developed small-scale MFC test bench is performed to confirm the effectiveness of the DCO in Section VI. Finally, conclusion and future directions are presented in Section VII.

## II. MFCV POWERTRAIN CONFIGURATION AND MODELING

### A. Powertrain Structure and Modeling

For the purpose of this study, a small-scale MFC test bench has been developed based on a low-speed vehicle called Nemo [40]. This test bench is presented in Fig. 1 and used for evaluating the performance of the proposed decentralized PAS. The MFC test bench is composed of two FC modules, a battery pack, a power supply, and a programmable load to emulate the propulsion system. The main device in each module is a 500-W FCS, a smoothing inductor, and a unidirectional DC-DC converter to

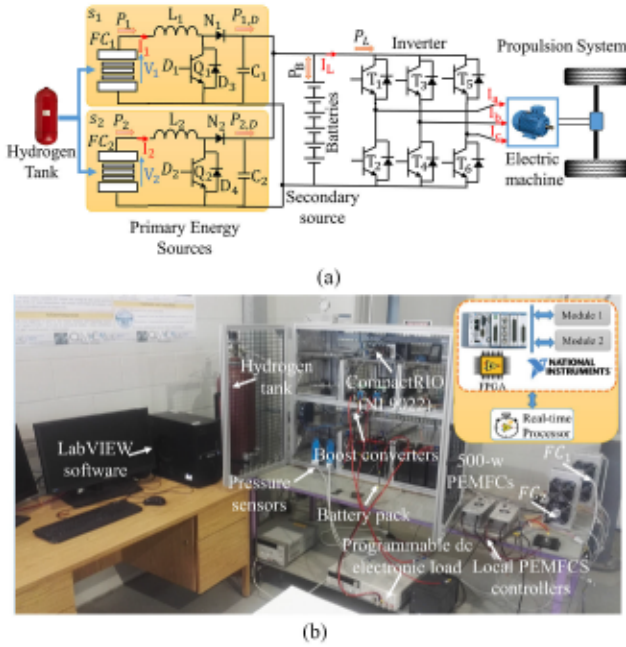


Fig. 1. A MFC powertrain: a) schematic of powertrain, b) developed test bench.

control the current of the FCS. The powertrain is formulated as:

$$\sum_{m=1}^M P_m[k] D_m[k] + P_B[k] = P_L[k], \quad (1)$$

where  $P_m[k]$  is the power of each FCS while  $M = \{1, 2\}$  is the index of each FC module,  $D_m$  is the duty cycle defined by each DCO-based control unit controller,  $P_B[k]$  is the power of the battery,  $P_L[k]$  is the requested power from the propulsion system, and  $k$  is the index of time period.

### B. MFCS Modeling and Constraints

The FCSs are modeled as a voltage source by means of their static polarization curves which are validated by experimental tests, as shown in Fig. 2. The polarization curves of the employed FCSs are illustrated in Fig. 2(a). Moreover, the power and hydrogen consumption curves of each utilized FCS are presented in Fig. 2(b) and Fig. 2(c), respectively. Each FC has two fans which consume approximately 12 W. It is worth mentioning that the FCSs do not have the same performance as they have different ageing milestones.

To avoid FC degradation owing to the start-stop cycles and operation at open circuit voltage (OCV) within very low-power region, the requested power from the FCSs is supplied under some limitations. Equations (2.a) and (2.b) apply the FCSs' power and slew rate limits, respectively.

$$P_{m,\min} \leq P_m[k] \leq P_{m,\max}, \quad (2a)$$

$$R_{d,m} \Delta t \leq P_m[k] - P_m[k-1] \leq R_{u,m} \Delta t, \quad (2b)$$

where  $P_{m,\min}$  and  $P_{m,\max}$  are the minimum and the maximum power of the FCSs,  $R_{d,m}$  and  $R_{u,m}$  are the minimum and the

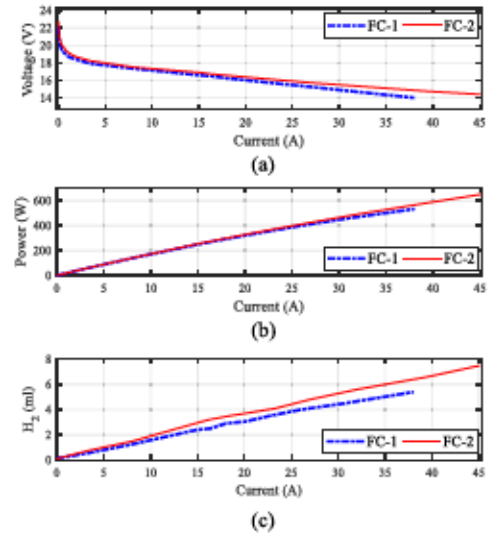


Fig. 2. The characteristics of the utilized 500-W FCSs, a) polarization curves, b) power curves, and c) hydrogen consumption curves.

TABLE I  
THE BATTERY PACK PARAMETERS

Variable	Symbol	Value	Unit
Series resistance	$R_s$	0.0141	$\Omega$
Capacity	$Q_B$	18.2	Ah
Parallel capacitor	$C_c$	1792	F
Parallel resistance	$R_c$	0.0177	$\Omega$

maximum slew rates, and  $\Delta t$  is the time step duration. It should be noted that when the FCs go under degradation (which is a slow process), their rated power decreases. In this regard, the considered constraints regarding the minimum and maximum power of the PEMFC should be updated from time to time to keep the operation of the FCs within the safe and allowed zone [41].

### C. Battery Modeling and Constraints

The battery pack which is passively linked to the DC bus is modeled by:

$$I_B[k] = \frac{V_0[k] - R_s I_B[k] - V_B[k]}{R_c} + C_c \frac{d}{dt} (V_0[k] - R_s I_B[k] - V_B[k]), \quad (3)$$

where  $V_B$  and  $I_B$  are the voltage and the current of the battery unit, and  $V_0$  is the battery OCV. Technical description of the battery system is given in Table I.

Equation (4.a) and (4.b) impose the power and the slew rate boundaries of the battery.

$$P_{B,\min} \leq P_B[k] \leq P_{B,\max}, \quad (4a)$$

$$R_{d,B} \Delta t \leq P_B[k] - P_B[k-1] \leq R_{u,B} \Delta t, \quad (4b)$$

where  $P_{B,\min}$  is the minimum battery power,  $P_{B,\max}$  is the battery maximum power,  $R_{d,B}$  is the falling slew rate, and  $R_{u,B}$  is



TABLE II  
CHARACTERISTICS OF THE TWO BOOST CONVERTERS

Variable	Symbol	Value
Inductor inductance	$L_m$	1.2 mH
Inductor resistance	$r_{Lm}$	23.7 mΩ
Average efficiency	$\eta_{h,m}$	95.7%

the rising slew rate. Equation (5.a) presents the SoC limitations.

$$SoC_{\min} \leq SoC[k] \leq SoC_{\max}, \quad (5a)$$

$$SoC[k+1] = SoC[k] - \frac{P_B[k] \Delta t}{Q_B V_B[k] 3600}, \quad (5b)$$

$$SoC[0] = SoC_0, \quad (5c)$$

where  $SoC_{\min}$  and  $SoC_{\max}$  are the minimum and the maximum limits of the SoC, and (5.b) denotes the SoC equation starting from  $SoC_0$  which is determined by (5.c). The service life of battery unit is affected by the depth of discharge [42]. According to the manufacturer's datasheet, when adopting the depth of discharge of 30%, the battery lifetime ( $n_B$ ) is equal to the 80% of capacity fade. The battery's state of health ( $SoH_B$ ) is calculated by (6).

$$SoH_B[k+1] = SoH_B[k] - \frac{|P_B[k]| \Delta t}{2n_B Q_B V_B[k] 3600}, \quad (6a)$$

$$SoH_B[0] = SoH_{B,0}, \quad (6b)$$

$$SoH_{B,\min} \leq SoH_B[k], \quad (6c)$$

where  $SoH_{B,\min}$  and  $SoH_{B,0}$  denote the minimum and the initial SoH values, respectively.

#### D. Boost Converter Modeling and Characteristics

The DC-DC converters' equations are as follows:

$$\begin{cases} L_m \frac{d}{dt} I_m[k] = V_m[k] - u_{h,m}[k] - r_{Lm} I_m[k], \\ \begin{cases} u_{h,m}[k] = m_{h,m} V_B[k] \\ I_{h,m}[k] = m_{h,m} I_m[k] \eta_{h,m}^z \end{cases} \end{cases} \quad z = \begin{cases} 1 & \text{if } P_m[k] > 0 \\ -1 & \text{if } P_m[k] < 0 \end{cases} \quad (7)$$

where  $m_{h,m}$  is the modulation ration,  $I_m$  is the FCS's current,  $V_m$  is the FCS's voltage, and  $V_B$  is the battery pack voltage. The technical parameters of the utilized DC-DC converters are given in Table II.

### III. FORMULATION OF THE GENERAL PROBLEM

The multi-objective PAS problem for the considered MFCV is formulated as (8)–(12). Beside hydrogen consumption, the health limitations are normalized and added into the proposed cost function to extend the lifetime of the FCSs and the battery pack. The cost function ( $s[k]$ ) takes into account four items and is calculated by:

$$s[k] = s_{h,m}[k] + s_{d,m}[k] + s_B[k] + s_{SoC}[k], \quad (8)$$

where  $s_{h,m}[k]$  is the normalized hydrogen consumption cost shaping function for each FCS, obtained by:

$$s_{h,m}[k] = \frac{h_m[k] - h_{m,\min}}{h_{m,\max} - h_{m,\min}}, \quad (9)$$

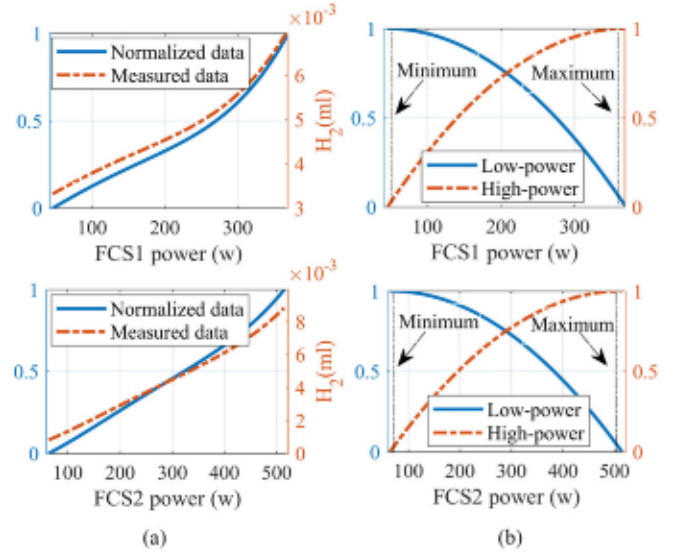


Fig. 3. a) The measured and normalized hydrogen consumption curves, b) the low-power and the high-power cost shaping functions.

where  $h_m[k]$  is the hydrogen consumption,  $h_{m,\min}$  is the minimum and  $h_{m,\max}$  is the maximum hydrogen consumption of each FCS, as shown in Fig. 2(c). The normalized FC degradation term ( $s_{d,FCm}[k]$ ) is defined by:

$$s_{d,FCm}[k] = \alpha_l s_{d,m}^l[k] + \alpha_h s_{d,m}^h[k], \quad (10a)$$

where  $s_{d,m}^l[k]$  is the normalized degradation cost shaping term related to low power operation, given by:

$$s_{d,m}^l[k] = 1 - \frac{[P_m[k] - P_{m,\min}]^2}{[P_{m,\max} - P_{m,\min}]^2}, \quad (10b)$$

$s_{d,m}^h[k]$  is the normalized degradation cost shaping term related to high power operation as:

$$s_{d,m}^h[k] = 1 - \frac{[P_m[k] - P_{m,\max}]^2}{[P_{m,\max} - P_{m,\min}]^2}, \quad (10c)$$

$\alpha_l$  and  $\alpha_h$  are the constant coefficients which are defined by:

$$\alpha_l = \frac{\varepsilon_l}{\varepsilon_l + \varepsilon_h}, \quad (10d)$$

$$\alpha_h = \frac{\varepsilon_h}{\varepsilon_l + \varepsilon_h}, \quad (10e)$$

where  $\varepsilon_l = 8.662 \mu V/h$  and  $\varepsilon_h = 10 \mu V/h$  are the low-power and the high-power cell degradation rates [43], [44]. Fig. 3 illustrates the measured and the normalized data of the hydrogen consumption beside the low-power and the high-power cost shaping functions. The normalized battery pack degradation function ( $s_B[k]$ ) is calculated by:

$$s_B[k] = \frac{P_B[k]}{P_{L,\max}}, \quad (11)$$

where  $P_{L,\max}$  is the maximum requested power.

$s_{SoC}[k]$  is a punishment term to try to maintain the SoC level similar or near to its initial value ( $SoC_0$ ).

$$s_{SoC}[k] = \beta[SoC[k] - SoC_0], \quad (12)$$

where  $\beta$  is a big positive coefficient. The equality and inequality constraints are based on (1)–(2) and (4)–(6).

#### IV. DECENTRALIZED APP CONVEX ALGORITHM

In this section, a detailed framework is presented to clarify the relaxation approach and the decentralized solution of the aforementioned optimization problem. In this algorithm, the PAS problem is decomposed into two individual subproblems where the output power of each FC module is the coupling variable and each of subproblems is assigned into one of the two FC modules. Then, the output power of each FC is duplicated into two new terms, real variable and virtual variable to mimic the rest of the powertrain system. The virtual variables are linked to each of the two subproblems. The local PAS subproblems are defined and formulated for each module, and an iterative procedure based on the decentralized APP approach is carried out to coordinate between subproblems and seek the optimal operating point of the original modular powertrain system. At the end of each iteration, the local optimization algorithms based on the defined cost functions and constraints are used to calculate the real power of the local FC modules and the virtual power of the neighboring FC modules. These values are then sent to the neighboring FC modules. As each of the real and virtual variables are essential to have the same values once the APP approach is converged, equal constraints are used by the two local PASs restricting the error of the shared powers to be zero. If the calculated errors by the PAS modules and their duplicated ones are less than a predetermined level, the convergence is obtained. If not, a set of penalty multipliers ( $\lambda$ ) are calculated and then the local PASs are solved again via the new variables. This algorithm is run repeatedly until it converges. Since the convergence speed of the algorithm is faster than the system dynamic, the virtual variables get very close to the real values, and this makes the final results be very close to the DP. It is worth noting that although the number of sharing variables increases the size of the matrixes, the decentralized forms are solved in a parallel manner which reduces the computational time. As shown in Fig. 4, in the developed DCO-based algorithm, the general optimization problem with coupling constrains is decomposed into two sub-problems of  $M_1$  and  $M_2$ . The battery pack is assumed to be located in the shared area as a storage device and all of the FC modules are needed to be informed about the estimated SoC level. The equality constraints for  $M_1$  can be formulated in terms of  $F_{M_1}(a, b) = 0$  and for  $M_2$  by means of  $F_{M_2}(b, c) = 0$ .

In a similar way, the inequality constraints for  $M_1$  and  $M_2$  are represented in the form of  $G_1(a, b) \leq 0$  and  $G_2(b, c) \leq 0$ , respectively. By defining the two sets:  $A = \{(a, b) : F_{M_1}(a, b) = 0, G_{M_1}(a, b) \leq 0\}$  for  $M_1$  and  $B = \{(b, c) : F_{M_2}(b, c) = 0, G_{M_2}(b, c) \leq 0\}$  for  $M_2$ , the feasible response is a point  $(a, b, c)$  that satisfies  $(a, b) \in A$  and  $(b, c) \in B$ . Moreover,  $M_1$  and  $M_2$  have a vector  $(X, Y)$  with regard to the

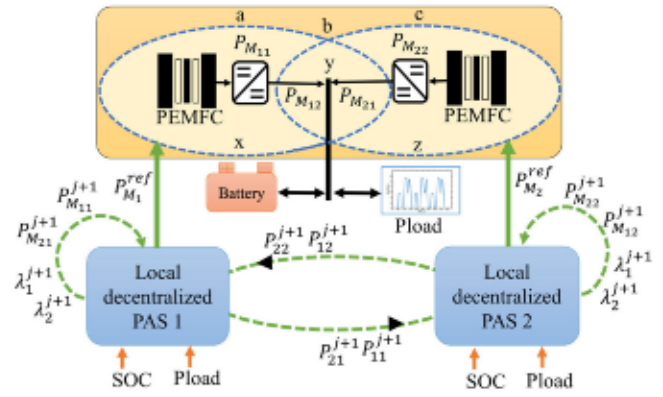


Fig. 4. The configuration of the D-APP PAS [45].

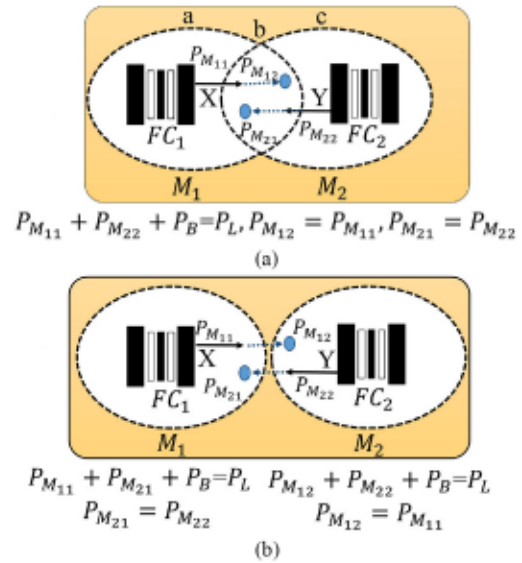


Fig. 5. The APP steps. a) defining the virtual modules, b) duplicating the virtual modules.

data which need to be shared with the neighboring FC module, as shown in Fig. 5. The vector  $X$  has the real FC module power ( $P_{M_{11}}$ ), and the virtual FC module power ( $P_{M_{21}}$ ), which is the  $M_2$  power in point of  $M_1$ . The vector  $Y$  has the real FC module power ( $P_{M_{22}}$ ) and the virtual FC module power ( $P_{M_{12}}$ ), which is the  $M_1$  power in point of  $M_2$ .

By taking (8)–(12) into account, the cost of  $M_1$  and  $M_2$  ( $C_M[k]$ ) and the battery pack cost ( $C_B[k]$ ) are separately defined as:

$$C_M[k] = s_{h,m}[k] + s_{d,m}[k], \quad (13a)$$

$$C_B[k] = s_B[k] + s_{SoC}[k], \quad (13b)$$

Based on (13), the centralized optimization is reformulated by:

$$\min \{C_{M_{11}}\{P_{M_{11}}[k]\} + C_{M_{22}}\{P_{M_{22}}[k]\} + C_B\{P_B[k]\}\}, \\ \{P_{M_{11}}[k], P_{M_{12}}[k]\} \in A \{P_{M_{12}}[k], P_{M_{22}}[k]\} \in B, \quad (14)$$

In order to solve the modified sub-problems, a regional decomposition framework based on APP approach is suggested



in [37]. For the sake of relaxing the coupling between  $M_1$  and  $M_2$ ,  $P_{M_{dd}} - P_{M_{df}} = 0$ ,  $d, f = 1, 2$   $d \neq f$ , and instead of applying standard Lagrangian technique, linearized augmented Lagrangian technique is applied to (14) to aid the convergence speed [38].

$$\begin{aligned} & \{P_{M_{11}}[k], P_{M_{21}}[k], P_{M_{12}}[k], P_{M_{22}}[k]\} \\ & = \min \{C_{M_{11}} \{P_{M_{11}}[k]\} + C_{M_{22}} \{P_{M_{22}}[k]\} + C_B \{P_B[k]\} \\ & \quad + \frac{\beta}{2} \|P_{M_{11}}[k] - P_{M_{12}}[k]\|^2 \\ & \quad + \frac{\beta}{2} \|P_{M_{22}}[k] - P_{M_{21}}[k]\|^2 : P_{M_{11}}[k] - P_{M_{12}}[k] \\ & = 0, P_{M_{22}}[k] - P_{M_{21}}[k] = 0\}, \{P_{M_{11}}[k], P_{M_{21}}[k]\} \in A, \\ & \quad \{P_{M_{12}}[k], P_{M_{22}}[k]\} \in B, \end{aligned} \quad (15)$$

The new quadratic function does not change the optimal result although the decomposition of the coupled C-PAS considerably improves the convergence speed [39].

#### A. Centralized APP

After applying the APP decomposition [37], (15) is solved by means of a sequence process. The suggested algorithm based on APP is formulated as follows:

$$\begin{aligned} & \{P_{M_{11}}^{j+1}[k], P_{M_{21}}^{j+1}[k], P_{M_{12}}^{j+1}[k], P_{M_{22}}^{j+1}[k]\} \\ & = \min \{C_{M_1} \{P_{M_{11}}[k]\} + C_{M_2} \{P_{M_{22}}[k]\} \\ & \quad + C_B \{P_B[k]\} + \frac{\beta}{2} \{P_{M_{11}}[k] - P_{M_{12}}^j[k]\}^2 \\ & \quad + \frac{\beta}{2} \{P_{M_{21}}[k] - P_{M_{22}}^j[k]\}^2 \\ & \quad + \frac{\beta}{2} \{P_{M_{12}}[k] - P_{M_{12}}^j[k]\}^2 + \frac{\beta}{2} \{P_{M_{22}}[k] - P_{M_{22}}^j[k]\}^2 \\ & \quad + \rho \{P_{M_{11}}[k] - P_{M_{12}}[k]\} \{P_{M_{11}}^j[k] - P_{M_{12}}^j[k]\} \\ & \quad + \rho \{P_{M_{22}}[k] - P_{M_{21}}[k]\} \{P_{M_{22}}^j[k] - P_{M_{21}}^j[k]\} \\ & \quad + \lambda_1^j \{P_{M_{11}}[k] - P_{M_{12}}[k]\} + \lambda_2^j \{P_{M_{22}}[k] - P_{M_{21}}[k]\}, \end{aligned} \quad (16)$$

$$\lambda_1^{j+1} = \lambda_1^j + \alpha \{P_{M_{11}}^{j+1}[k] - P_{M_{12}}^{j+1}[k]\}, \quad (17)$$

$$\lambda_2^{j+1} = \lambda_2^j + \alpha \{P_{M_{22}}^{j+1}[k] - P_{M_{21}}^{j+1}[k]\}, \quad (18)$$

where  $j$  is the index of optimization iteration, and  $\alpha, \beta$ , and  $\rho$  are predefined positive values. The starting points  $P_{M_{11}}, P_{M_{21}}, P_{M_{12}}, P_{M_{22}}$ , and  $\lambda$  can be set as the prior answer or zero (cold start).  $\lambda_{1,2}^j$ , as the Lagrange multipliers, are the estimated virtual FC module costs to keep the equality coupling constraints on the shared area at iteration  $j$ . The centralized APP utilizes the power values and the Lagrange parameters obtained from the previous step. It then alternates the achieved solutions of regional FC modules and updates the Lagrange multipliers. This

iterative process will be completed if the stopping requirements are fulfilled.

#### B. Decentralized APP

With the aim of reducing the computational time and improving the fault-tolerant and the modularity features, (16)–(18) is divided into smaller subproblems for each autonomous FC module. The D-APP for the  $M_1$  is formulated by:

$$\begin{aligned} & \{P_{M_{11}}^{j+1}[k], P_{M_{21}}^{j+1}[k]\} \\ & = \min \{C_{M_{11}} \{P_{M_{11}}[k]\} + C_B \{P_B[k]\} \\ & \quad + \frac{\beta}{2} \{P_{M_{11}}[k] - P_{M_{11}}^j[k]\}^2 \\ & \quad + \frac{\beta}{2} \{P_{M_{21}}[k] - P_{M_{21}}^j[k]\}^2 \\ & \quad + \rho P_{M_{11}}[k] \{P_{M_{11}}^j[k] - P_{M_{12}}^j[k]\} \\ & \quad - \rho P_{(M_21)}[k] \{P_{(M_22)}^j[k] - P_{(M_21)}^j[k]\} \\ & \quad + \lambda_1^j P_{(M_11)}[k] - \lambda_2^j P_{(M_21)}[k]\}, \end{aligned} \quad (19)$$

$$\lambda_1^{j+1} = \lambda_1^j + \alpha \{P_{M_{11}}^{j+1}[k] - P_{M_{12}}^{j+1}[k]\}, \quad (20)$$

$$\lambda_2^{j+1} = \lambda_2^j + \alpha \{P_{M_{21}}^{j+1}[k] - P_{M_{22}}^{j+1}[k]\}, \quad (21)$$

The D-APP for the  $M_2$  is given by:

$$\begin{aligned} & \{P_{M_{12}}^{j+1}[k], P_{M_{22}}^{j+1}[k]\} \\ & = \min \{C_{M_{22}} \{P_{M_{22}}[k]\} + C_B \{P_B[k]\} \\ & \quad + \frac{\beta}{2} \{P_{M_{22}}[k] - P_{M_{22}}^j[k]\}^2 \\ & \quad + \frac{\beta}{2} \{P_{M_{12}}[k] - P_{M_{12}}^j[k]\}^2 \\ & \quad + \rho P_{M_{22}}[k] \{P_{M_{22}}^j[k] - P_{M_{21}}^j[k]\} \\ & \quad - \rho P_{M_{12}}[k] \{P_{M_{11}}^j[k] - P_{M_{12}}^j[k]\} \\ & \quad - \lambda_1^j P_{M_{12}}[k] + \lambda_2^j P_{M_{11}}[k]\}, \end{aligned} \quad (22)$$

$$\lambda_1^{j+1} = \lambda_1^j + \alpha \{P_{M_{12}}^{j+1}[k] - P_{M_{11}}^{j+1}[k]\}, \quad (23)$$

$$\lambda_2^{j+1} = \lambda_2^j + \alpha \{P_{M_{22}}^{j+1}[k] - P_{M_{21}}^{j+1}[k]\}, \quad (24)$$

These new modifications (19)–(21) and (22)–(24) basically lead to two D-APPs as a decentralized control layer, as shown in Fig. 4. In [37], the APP parameters are defined based on:

$$\alpha = \frac{1}{2} \beta = \rho, \quad (25)$$

It is worth mentioning that this parallel process will be stopped if the stopping conditions are satisfied. To better clarify the

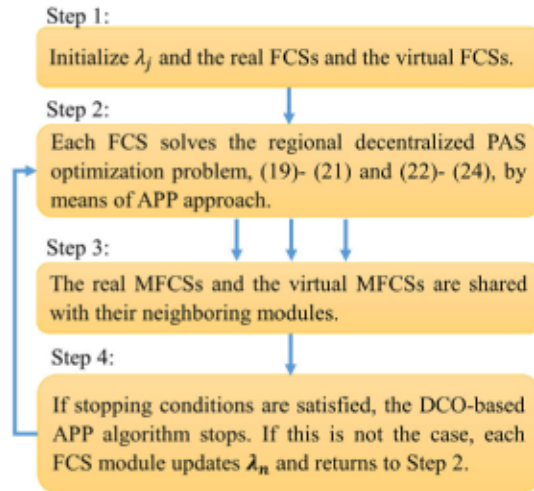


Fig. 6. The general step-by-step flowchart of the D-APP strategy.

performance of the discussed method, a diagrammatic representation of the developed decentralized PAS layer is presented in Fig. 6.

## V. COMPARISON AND RESULTS OF NUMERICAL CASE STUDIES

In this section, to have a comprehensive discussion, a number of important items are considered to elucidate the DCO-based PAS. An optimal PAS based on DP has been developed to serve as a baseline. Moreover, SQP, as a well-known centralized approach, is used to evaluate the performance of the proposed decentralized method.

The numerical studies have been tested via MATLAB. The calculation time depends on the utilized PC hardware (Processor = Core i5, 2.30 GHz, RAM = 4.00 GB). The total end-user cost,  $S_T$ , in USD, which includes five items is calculated by:

$$S_T = S_{SoC} + \sum_k \sum_m S_{H,m} [k] + S_{d,m} [k] + S_B [k], \quad (26)$$

The hydrogen cost ( $S_{H,m}[k]$ ), in USD, is computed by:

$$S_{H,m} [k] = H_m [k] C_{H_2} \Delta t, \quad (27)$$

where  $H_m[k]$  is the hydrogen consumption (per gram) and  $C_{H_2}$  is the hydrogen price. The modules' degradation cost ( $S_{d,m}[k]$ ), in USD, is calculated by:

$$S_{d,m} [k] = S_{d,m}^l [k] + S_{d,m}^h [k], \quad (28a)$$

where  $S_{d,m}^l [k]$  is the cost of low-power degradation and  $S_{d,m}^h [k]$  is the cost of high-power degradation, given by:

$$S_{d,m}^l [k] = \frac{n_m \varepsilon_l C_m \Delta t \mu_{l,m}}{3600 V_{n,m}}, \quad (28b)$$

$$S_{d,m}^h [k] = \frac{n_m \varepsilon_h C_m \Delta t \mu_{h,m}}{3600 V_{n,m}}, \quad (28c)$$

where  $n_m$  is the cell numbers,  $\varepsilon_l$  is the low power cell-level degradation,  $\varepsilon_h$  is the high power cell-level degradation, and

 TABLE III  
THE REFERENCE PRICE OF HYDROGEN, BATTERY, AND FCS

Cost	Symbol	Value
Hydrogen	$C_{H_2}$	3.9254 \$/Kg [46]
FCS	$C_m$	35 \$/kW [47]
Battery unit	$C_B$	189 \$/kWh [48]

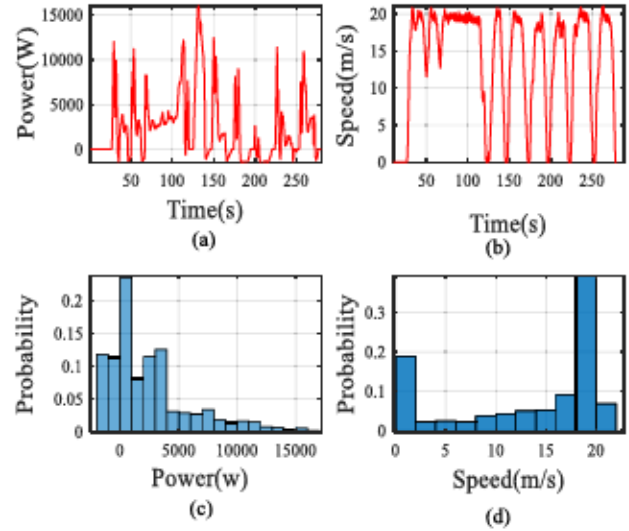


Fig. 7. Six different analyses of the real cycle (a) the power, (b) the speed, (c) the power histogram, (d) the speed histogram.

$C_{FC,m}$  is the FCS cost.  $\mu_l$  and  $\mu_h$  are determined by:

$$\mu_{l,m} = \begin{cases} 1, & \text{If } P_{\min,m} \leq P_m \leq 0.2P_{nom,m} \\ 0, & \text{otherwise} \end{cases} \quad (28e)$$

$$\mu_{h,m} = \begin{cases} 1, & \text{If } 0.8P_{nom,m} \leq P_m \leq P_{\max,m} \\ 0, & \text{otherwise} \end{cases} \quad (28f)$$

where  $V_{n,m}$  is the 10% voltage drop of the nominal voltage of each module and  $P_{nom,m}$  is the output power recommended by the FCS manufacturing company for a nominal use of FCS [44]. The cost of the battery unit degradation ( $S_B[k]$ ), in USD, is determined by:

$$S_B [k] = C_B \{SoH_B [k] - SoH_B [0]\}, \quad (29)$$

where  $C_B$  is the battery pack price. The punishment term for the battery pack ( $S_{SoC}$ ) in USD is calculated based on the price of the hydrogen to recharge the battery unit at the end of the driving profile to reach the same level as the initial SoC. The battery pack is recharged by utilizing the FC stacks at their maximum efficiency points. This cost is added to the final end-user price. The reference price of the hydrogen, the FCS, and the battery pack are listed in Table III.

### A. Optimal Power Distribution Under Real Driving Pattern

As shown in Fig. 7, a real profile is herein considered. The power split based on DP, SQP, and DCO between the modules and the battery unit are shown in Fig. 8, Fig. 9, and Fig. 10, respectively, where  $P_{load}$  is the requested power, FC is the



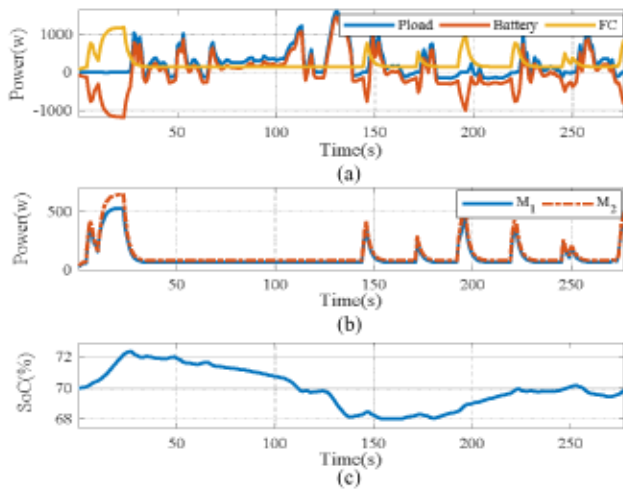


Fig. 8. The DP results under real driving profile: (a) power profiles, (b) the modules ( $M_1, M_2$ ) split powers, (c) the SoC.

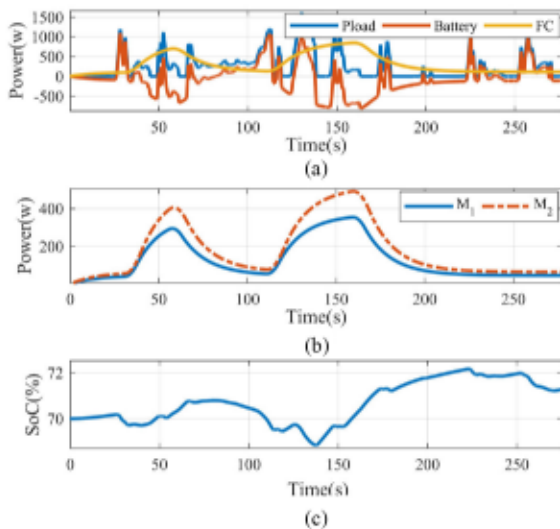


Fig. 9. The SQP results under real driving profile: (a) power profiles, (b) the modules ( $M_1, M_2$ ) split powers, (c) the SoC.

power provided by the modules, and Battery is the battery unit power. Fig. 8 demonstrates the performance of DP regarding the distribution of power and battery SoC. From this figure, it is seen that in the very beginning (0 to 25 s), the FC modules recharge the battery. Then, from 25 s to almost 140 s, the FC modules operate in low power and battery SoC level decreases. From 140 s on, the modules slightly recharge the battery to reach the same level of SoC as the initial one. In fact, knowing the driving cycle in advance makes DP have such a good performance. Fig. 9 illustrates the SQP strategy performance.

According to Fig. 9c, during the first 50s, this strategy tries to sustain the SoC level very close to 70%. Afterwards, it fluctuates between charging and discharging and finishes almost with 71% of SoC. Fig. 10 presents the power distribution obtained by the proposed decentralized strategy. From Fig. 10(b), the modules largely operate at the efficient region to mitigate the degradation price, which leads to lower cost of degradation with the aid of

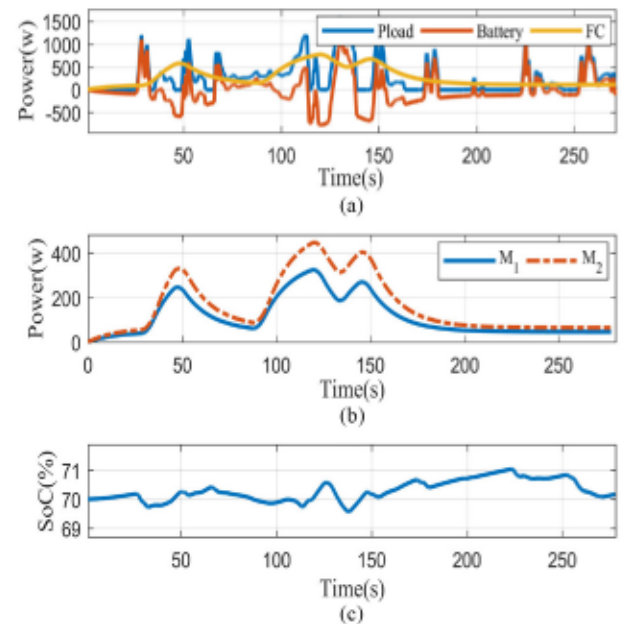


Fig. 10. The APP results under real driving profile: (a) power profiles, (b) the modules ( $M_1, M_2$ ) split powers, (c) the SoC.

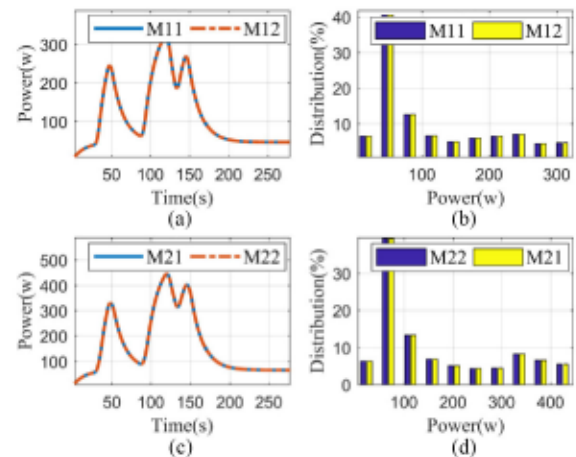


Fig. 11. The profile and the distribution of the modules' optimal powers (a) the power profile of the  $M_1$  ( $M_{11}$ : the real,  $M_{12}$ : the virtual), (b) the distribution of the  $M_1$ , (c) the power profile of the  $M_2$  ( $M_{22}$ : the real,  $M_{21}$ : the virtual), (d) the distribution of the  $M_2$ .

battery power differences. Fig. 10(c) depicts the SoC level of the battery. The SoC fluctuates between 68.9% and 71.1%, less than approximately 2.2% variation. This strategy also manages to reach a very close SoC level to the initial one, as shown in Fig. 10(c). The time series and the distribution of the real and the virtual FCs' power based on DCO are presented in Fig. 11. It is evident that in both of the modules, the real and the virtual power are well-matched, and are almost located in the efficient region.

To evaluate the developed DCO-based method, the performance of the obtained results is compared with DP as an off-line optimization method and SQP as a centralized optimization algorithm. According to Table IV, the D-APP has achieved a near end-user price to DP (with 12% difference) while the

TABLE IV  
THE FINAL PRICE AND THE COMPUTING PERFORMANCES

	DP		SQP		D-APP	
	M <sub>1</sub>	M <sub>2</sub>	M <sub>1</sub>	M <sub>2</sub>	M <sub>1</sub>	M <sub>2</sub>
Computation time (s)	1040.3211		52.7360		15.325	15.130
Number of iterations	-		6057		1892	1868
Hydrogen consumption (\$)	M <sub>1</sub>	M <sub>2</sub>	M <sub>1</sub>	M <sub>2</sub>	0.0051	0.0026
FC degradation (\$)	0.004	0.002	0.005	0.003	0.0014	0.0010
Battery degradation (\$)	5	7	6	1	0.0005	0.0005
$S_{SoC}$	0	0	0	0	0.0010	0.0005
Total Cost (\$)	0.0100		0.01550		0.0112	

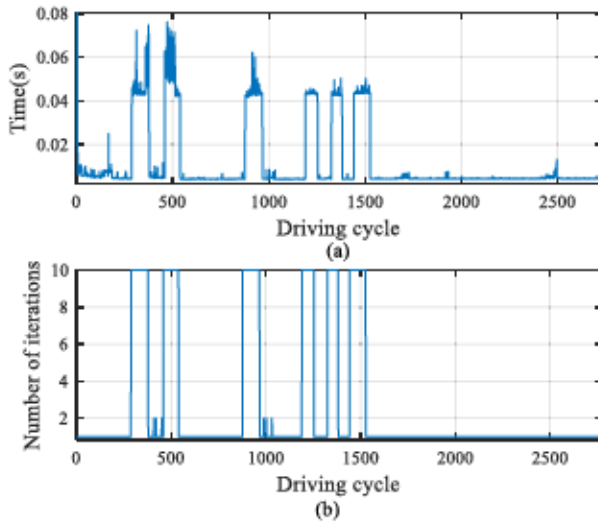


Fig. 12. (a) The computation time trajectory, (b) the number of iterations.

computational burden is much less. Moreover, the end-user price of D-APP is 27.74% lower than SQP while benefiting from a substantial decline in case of the computational time (71.31%) and the number of iterations (68.76%). # denotes the number of iterations in the optimization algorithms (SQP, APP), and  $S_{SoC}$  is the punishment term to recharge the battery pack. Based on our experience, despite slight differences between the centralized APP (17)–(19) and the D-APP (20)–(25), the final results of both approaches are almost the same while the D-APP is faster. To have a clear understanding, here, the number of iterations and the computational time evaluation according to the  $M_1$  are illustrated in Fig. 12. It is evident that the computational time is related to the number of iterations.

Based on the obtained results, the decentralized method has less computational time which shows that this method is a reasonable and practical candidate in the real-time PAS optimization applications.

Fig. 13 presents the price trajectories of different sources under a long test. The final end-user cost is approximately \$0.2134,

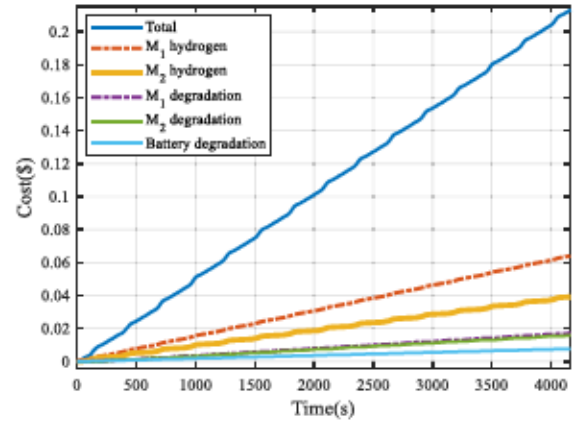


Fig. 13. Optimal price trajectories: the total end-user, the hydrogen of  $M_1$ , the hydrogen of  $M_2$ , the degradation of  $M_1$ , and the degradation of  $M_2$ , the battery degradation.

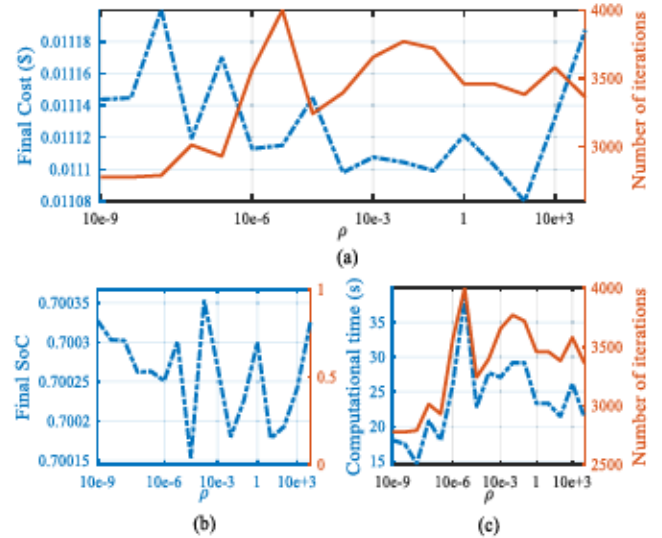


Fig. 14. The investigation of the parameter  $\rho$  in the DCO performances.

to which the total hydrogen price of \$0.1033 contributes most (48.41% of the end-user expense). Between these two, the  $M_1$  with about \$0.0641 (30.04% of the end-user cost) contributes more compared to the  $M_2$  with about \$0.0392 (18.37% of the final cost). The second largest cost is the modules degradation cost of nearly \$0.0330 (15.46% of the end-user cost). The battery degradation cost is around \$0.0077 (3.61% of the final cost). It is the lowest cost, compared to the ones related to the modules. The punishment term to recharge the battery pack is approximately \$0.0694 (32.52% of the final cost).

### B. Impact of Parameter Tuning

The effect of tuning  $\rho$  on the end-user price and the computational performance is scrutinized in this subsection. Fig. 14 describes a detailed analysis of  $\rho$  in a wide range, from  $10^{-9}$  to  $10^7$ . Fig. 14(a) shows the relation of  $\rho$  with the final cost (\$) and the computational time (s). In Fig. 14(b), to verify that all the comparisons finish with the nearly same final state



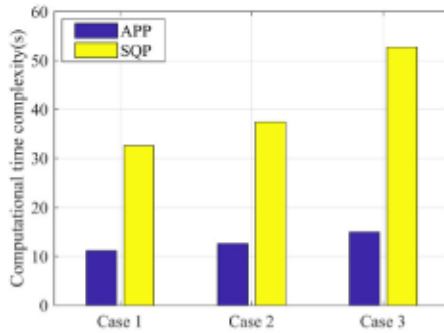


Fig. 15. The comparison of the computational burdens.

variable, the battery SoC evolution is presented. Fig. 14(c) shows a comparison between the computational complexity (s) and the number of iterations. It is apparent that they have the same pattern.

Generally, considering the modular powertrain problem and the hardware characteristics,  $\rho$  shows a significant influence over the performance where an improper  $\rho$  could lead to slower convergence and higher final cost. The end-user cost gradually decreases as  $\rho$  grows. However, the computational complexity (s) becomes progressively heavy, particularly when  $\rho$  exceeds  $10 e^{-5}$ . On the basis of our experience,  $\rho$  in the range of  $10 e^{-8}$ – $10 e^{-7}$  is more suitable for the DCO problem and relying on our analyses,  $\rho = 10 e^{-7}$  is selected as the optimal value.

### C. Sensitivity Analysis

In this subsection, a sensitivity analysis of the proposed D-APP method with SQP is conducted. In this regard, different cost functions are taken into consideration: 1) hydrogen, 2) hydrogen and FCS degradation, 3) hydrogen, FCS and battery degradation. As shown in Fig. 15, in case (2), the computational time of D-APP rises by almost 6.3378% in comparison with case (1) while the computational time of SQP increases by nearly 24.2079% compared to case (1). Moreover, the computational time of D-APP grows by around 10.5112% in case (3), compared to case (1). However, in case (2), the computational time of SQP increases by approximately 62.4511% compared to case (1). This analysis shows that D-APP has less sensitivity to a complex function with several constraints, which is important in practical real-time applications.

## VI. EXPERIMENTAL IMPLEMENTATION

To verify the results, the D-APP has been implemented in the PAS layer of the developed scaled-down test bench via LabVIEW. As demonstrated in Fig. 1.(b), the test bench is equipped with two open-cathode 500-W Horizon PEMFCs ( $M_1$  and  $M_2$ ) and a battery unit, composed of six series 12-V, 18-Ah batteries. The voltage of  $M_1$  oscillates between 14.1 and 22.7 V, and the voltage of  $M_2$  varies between 14.5 and 23.4 V, while the voltage of the DC-bus is given by the battery unit. The two boost converters are from Zahn Electronics. Each module has its PAS unit inside the National Instrument CompactRIO (NI 9022). The D-APP iteratively calculates the optimal references

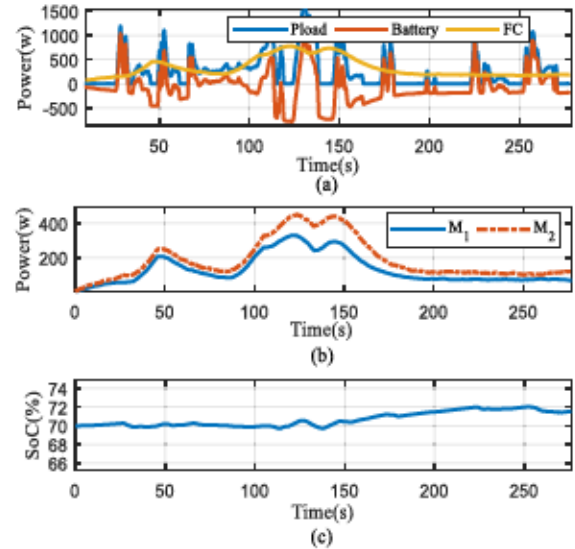


Fig. 16. Optimal results under real driving profile via the developed test bench: (a) power profiles, (b) the modules split powers, (c) the SoC.

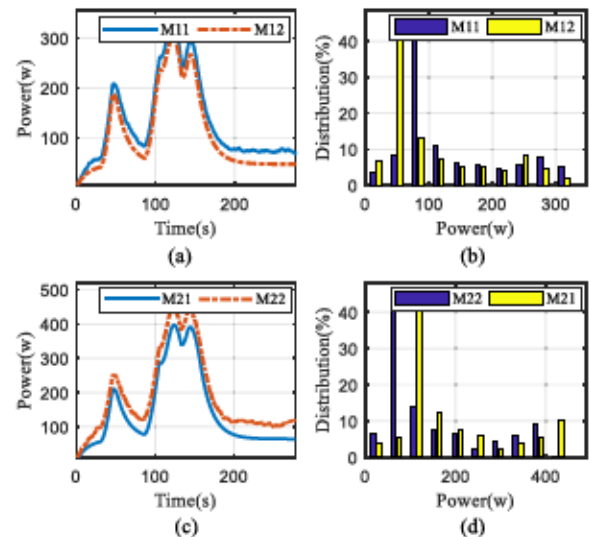


Fig. 17. The trajectories and the distribution of the power profiles.

in parallel. The optimal reference of each module,  $P_{Ref}^{M1}$  and  $P_{Ref}^{M2}$ , is updated at every control instant with an interval of 10 Hz. The results under the real profile is presented in Fig. 16 and Fig. 17. These results verify the validation of the real-time implementation of the D-APP as well as the correctness of the previous theoretical discussions.

## VII. CONCLUSION

In this paper, a DCO algorithm for MFCVs is suggested to address a multi-objective PAS optimization problem. In the proposed decentralized framework, a novel distributed normalized cost function, including hydrogen consumption and health-conscious constraints of the FC modules and the battery pack, is minimized via a fully D-APP algorithm. The effectiveness of the D-APP algorithm is validated via several numerical studies, such

as the effect of parameter tuning and driving behavior. Moreover, the performance of the proposed approach is compared with DP strategy, as an off-line method, and SQP, as a centralized method. This comparison shows that D-APP is able to achieve an end-user price very near to DP while it is a real-time method. Moreover, compared to SQP, the decentralized method leads to less computational time and also provides less sensitivity in case of having complex function with several constraints. Finally, an experimental validation is performed on a developed test bench which justifies the effectiveness of the proposed D-APP.

Looking forward, a number of recommendations can be made to extend the contributions of this paper:

- The proposed decentralized algorithm can be combined with an advanced MPC method to enhance the inherent robustness against uncertainty in both of vehicle model and projection of future driving conditions.
- Another future direction can be integrating the proposed approach with advanced prognostic frameworks which consider variable loading condition to further prolong the lifetime of the power sources.
- In this work, the robustness and the modularity points of view have not been demonstrated yet. Therefore, a comprehensive study regarding the raised matters will be performed in future.

## REFERENCES

- [1] S. F. Tie and C. W. Tan, "A review of energy sources and energy management system in electric vehicles," *Renewable Sustain. Energy Rev.*, vol. 20, pp. 82–102, Apr. 2013.
- [2] W. Su, H. Eichi, W. Zeng, and M. Chow, "A survey on the electrification of transportation in a smart grid environment," *IEEE Trans. Ind. Informat.*, vol. 8, pp. 1–10, Feb. 2012.
- [3] U. Eberle, B. Müller, and R. Helmolt, "Fuel cell electric vehicles and hydrogen infrastructure: Status 2012," *Energy Environ. Sci.*, vol. 5, pp. 8790–8798, 2012.
- [4] B. Geng, J. K. Mills, and D. Sun, "Two-stage energy management control of fuel cell plug-in hybrid electric vehicles considering fuel cell longevity," *IEEE Trans. Veh. Technol.*, vol. 61, pp. 498–508, Feb. 2012.
- [5] H. B. Jensen, E. Schaltz, P. S. Koustrup, S. J. Andreasen, and S. K. Kaer, "Evaluation of fuel-cell range extender impact on hybrid electrical vehicle performance," *IEEE Trans. Veh. Technol.*, vol. 62, pp. 50–60, Jan. 2013.
- [6] S. Ziaeejad, Y. Sangsefidi, and A. Mehrizi-Sani, "Fuel cell-based auxiliary power unit: EMS, sizing, and current estimator-based controller," *IEEE Trans. Veh. Technol.*, vol. 65, pp. 4826–4835, Jun. 2016.
- [7] D. Zhou, A. Al-Durra, F. Gao, A. Ravey, I. Matraji, and M. Godoy Simões, "Online energy management strategy of fuel cell hybrid electric vehicles based on data fusion approach," *J. Power Sources*, vol. 366, pp. 278–291, Oct. 2017.
- [8] R. Wai, S. Jhung, J. Liaw, and Y. Chang, "Intelligent optimal energy management system for hybrid power sources including fuel cell and battery," *IEEE Trans. Power Electron.*, vol. 28, pp. 3231–3244, Jul. 2013.
- [9] Y. Yan, Q. Li, W. Chen, B. Su, J. Liu, and L. Ma, "Optimal energy management and control in multimode equivalent energy consumption of fuel cell/supercapacitor of hybrid electric tram," *IEEE Trans. Ind. Electron.*, vol. 66, pp. 6065–6076, Aug. 2019.
- [10] E. Tazelaar, B. Veenhuizen, P. vandenBosch, and M. Grimminck, "Analytical solution of the energy management for fuel cell hybrid propulsion systems," *IEEE Trans. Veh. Technol.*, vol. 61, pp. 1986–1998, Jun. 2012.
- [11] X. Hu, C. Zou, X. Tang, T. Liu, and L. Hu, "Cost-optimal energy management of hybrid electric vehicles using fuel cell/battery health-aware predictive control," *IEEE Trans. Power Electron.*, vol. 35, no. 1, pp. 382–392, Jan. 2020.
- [12] J. Chen, C. Xu, C. Wu, and W. Xu, "Adaptive fuzzy logic control of fuel-cell-battery hybrid systems for electric vehicles," *IEEE Trans. Ind. Informat.*, vol. 14, no. 1, pp. 292–300, Jan. 2018.
- [13] C. Wu, J. Chen, C. Xu, and Z. Liu, "Real-time adaptive control of a fuel cell/battery hybrid power system with guaranteed stability," *IEEE Trans. Control Syst. Technol.*, vol. 25, no. 4, pp. 1394–1405, Jul. 2017.
- [14] X. Meng, Q. Li, G. Zhang, T. Wang, W. Chen, and T. Cao, "A dual-mode energy management strategy considering fuel cell degradation for energy consumption and fuel cell efficiency comprehensive optimization of hybrid vehicle," *IEEE Access*, vol. 7, pp. 134475–134487, 2019.
- [15] M. G. Carignano, V. Roda, R. Costa-Castelló, L. Valino, A. Lozano, and F. Barreras, "Assessment of energy management in a fuel cell/battery hybrid vehicle," *IEEE Access*, vol. 7, pp. 16110–16122, 2019.
- [16] N. Sulaiman, M. A. Hannan, A. Mohamed, E. H. Majlan, and W. R. Wan Daud, "A review on energy management system for fuel cell hybrid electric vehicle: Issues and challenges," *Renewable Sustain. Energy Rev.*, vol. 52, pp. 802–814, 2015.
- [17] M. Yue, S. Jemci, R. Gouriveau, and N. Zerhouni, "Review on health-conscious energy management strategies for fuel cell hybrid electric vehicles: Degradation models and strategies," *Int. J. Hydrogen Energy*, vol. 44, pp. 6844–6861, 2019.
- [18] M. Jouin, R. Gouriveau, D. Hissel, M.-C. Péra, and N. Zerhouni, "Prognostics of PEM fuel cell in a particle filtering framework," *Int. J. Hydrogen Energy*, vol. 39, pp. 481–494, 2014.
- [19] E. Lechartier, E. Laffly, M.-C. Péra, R. Gouriveau, D. Hissel, and N. Zerhouni, "Proton exchange membrane fuel cell behavioral model suitable for prognostics," *Int. J. Hydrogen Energy*, vol. 40, pp. 8384–8397, 2015.
- [20] R. E. Silva *et al.*, "Proton exchange membrane fuel cell degradation prediction based on adaptive neuro-fuzzy inference systems," *Int. J. Hydrogen Energy*, vol. 39, pp. 11128–11144, 2014.
- [21] K. Javed, R. Gouriveau, N. Zerhouni, and D. Hissel, "Prognostics of proton exchange membrane fuel cells stack using an ensemble of constraints based connectionist networks," *J. Power Sources*, vol. 324, pp. 745–757, 2016.
- [22] Y. Cheng, N. Zerhouni, and C. Lu, "A hybrid remaining useful life prognostic method for proton exchange membrane fuel cell," *Int. J. Hydrogen Energy*, vol. 43, pp. 12314–12327, Jul. 2018.
- [23] A. K. Soltani, M. Kandidayeni, L. Boulon, and D. L. St-Pierre, "Modular energy systems in vehicular applications," *Energy Procedia*, vol. 162, pp. 14–23, 2019.
- [24] A. O. M. Fernandez, M. Kandidayeni, L. Boulon, and H. Chaoui, "An adaptive state machine based energy management strategy for a multi-stack fuel cell hybrid electric vehicle," *IEEE Trans. Veh. Technol.*, vol. 69, no. 1, pp. 220–234, Jan. 2020.
- [25] H. Zhang, X. Li, X. Liu, and J. Yan, "Enhancing fuel cell durability for fuel cell plug-in hybrid electric vehicles through strategic power management," *Appl. Energy*, vol. 241, pp. 483–490, 2019.
- [26] T. Wang *et al.*, "Adaptive current distribution method for parallel-connected PEMFC generation system considering performance consistency," *Energy Convers. Manage.*, vol. 196, pp. 866–877, 2019.
- [27] Q. Li, T. Wang, C. Dai, W. Chen, and L. Ma, "Power management strategy based on adaptive droop control for a fuel cell-battery-supercapacitor hybrid tramway," *IEEE Trans. Veh. Technol.*, vol. 67, pp. 5658–5670, 2018.
- [28] N. Marx, L. Boulon, F. Gustin, D. Hissel, and K. Agbossou, "A review of multi-stack and modular fuel cell systems: Interests, application areas and on-going research activities," *Int. J. Hydrogen Energy*, vol. 39, pp. 12101–12111, Aug. 2014.
- [29] T. Wang, Q. Li, L. Yin, and W. Chen, "Hydrogen consumption minimization method based on the online identification for multi-stack PEMFCs system," *Int. J. Hydrogen Energy*, vol. 44, pp. 5074–5081, 2019.
- [30] S. East and M. Cannon, "Energy management in plug-in hybrid electric vehicles: Convex optimization algorithms for model predictive control," *IEEE Trans. Control Syst. Technol.*, pp. 1–13, Aug. 2019.
- [31] X. Wu, X. Hu, X. Yin, L. Li, Z. Zeng, and V. Pickert, "Convex programming energy management and components sizing of a plug-in fuel cell urban logistics vehicle," *J. Power Sources*, vol. 423, pp. 358–366, 2019.
- [32] H. Chen, J. Chen, Z. Liu, and H. Lu, "Real-time optimal energy management for a fuel cell/battery hybrid system," *Asian J. Control*, vol. 21, pp. 1847–1856, 2019.
- [33] S. East and M. Cannon, "Fast optimal energy management with engine on/off decisions for plug-in hybrid electric vehicles," *IEEE Control Syst. Lett.*, vol. 3, no. 4, pp. 1047–1079, Oct. 2019.
- [34] T. C. J. Romijn, M. C. F. Donkers, J. T. B. A. Kessels, and S. Weiland, "A distributed optimization approach for complete vehicle energy management," *IEEE Trans. Control Syst. Technol.*, vol. 27, no. 3, pp. 964–980, May 2019.



- [35] H. Yin, C. Zhao, and C. Ma, "Decentralized real-time energy management for a reconfigurable multiple-source energy system," *IEEE Trans. Ind. Informat.*, vol. 14, no. 9, pp. 4128–4137, Sep. 2018.
- [36] H. Yin, C. Zhao, M. Li, C. Ma, and M.-Y. Chow, "A game theory approach to energy management of an engine-generator/battery/ultracapacitor hybrid energy system," *IEEE Trans. Ind. Electron.*, vol. 63, no. 7, pp. 4266–4277, Jul. 2016.
- [37] B. H. Kim and R. Baldick, "Coarse-grained distributed optimal power flow," *IEEE Trans. Power Syst.*, vol. 12, no. 2, pp. 932–939, May 1997.
- [38] D. Hur, J. Park, and B. H. Kim, "Evaluation of convergence rate in the auxiliary problem principle for distributed optimal power flow," *IEEE Proc. Gener. Transmiss. Distrib.*, vol. 149, no. 5, pp. 525–532, Sep. 2002.
- [39] G. Cohen, "Auxiliary problem principle and decomposition of optimization problems," *J. Optim. Theory Appl.*, vol. 32, pp. 277–305, Nov. 1980.
- [40] F. Martel, S. Kelouwani, Y. Dubé, and K. Agbossou, "Optimal economy-based battery degradation management dynamics for fuel-cell plug-in hybrid electric vehicles," *J. Power Sources*, vol. 274, pp. 367–381, 2015.
- [41] M. Kandidayeni, A. O. M. Fernandez, A. Khalatbarisoltani, L. Boulon, S. Kelouwani, and H. Chaoui, "An online energy management strategy for a fuel cell/battery vehicle considering the driving pattern and performance drift impacts," *IEEE Trans. Veh. Technol.*, vol. 68, no. 12, pp. 11427–11438, Dec. 2019.
- [42] S. Ebbesen, P. Elbert, and L. Guzzella, "Battery state-of-health perceptible energy management for hybrid electric vehicles," *IEEE Trans. Veh. Technol.*, vol. 61, no. 7, pp. 2893–2900, Sep. 2012.
- [43] H. Chen, P. Pei, and M. Song, "Lifetime prediction and the economic lifetime of proton exchange membrane fuel cells," *Appl. Energy*, vol. 142, pp. 154–163, Mar. 2015.
- [44] N. Herr *et al.*, "Decision process to manage useful life of multi-stacks fuel cell systems under service constraint," *Renewable Energy*, vol. 105, pp. 590–600, 2017.
- [45] A. Khalatbarisoltani, L. Boulon, D. L. St-Pierre, and X. Hu, "Decentralized implementation of an optimal energy management strategy in interconnected modular fuel cell systems," in *Proc. IEEE Veh. Power Propulsion Conf.*, 2019, pp. 1–5.
- [46] S. Satyapal, "US department of energy hydrogen and fuel cell technology overview," presented at the 14th International Hydrogen and Fuel Cell Expo (FC EXPO 2018), 2018.
- [47] US DRIVE, *Fuel Cell Technical Team Roadmap*. Department of Energy, USA, 2017.
- [48] K. Mongird *et al.*, "Energy Storage Technology and Cost Characterization Report," Richland, WA, USA: Pacific Northwest National Lab.(PNNL), 2019.



**Arash Khalatbarisoltani** (Member, IEEE) received the master's degree in mechatronics from Arak University, Arak, Iran, in 2016. He is currently working toward the Ph.D. degree with the Hydrogen Research Institute (IRH) and the Department of Electrical and Computer Engineering, Université du Québec à Trois-Rivières (UQTR), Trois-Rivières, QC, Canada. His research interests include optimal control, decentralized systems, fuel cell systems, energy management, renewable energy, and intelligent transport systems. He had three years research experience,

especially in renewable vehicles and fuel cell systems. He published seven scientific papers in SCI journals, such as the IEEE TRANSACTIONS ON VEHICULAR TECHNOLOGY, *Energy Procedia*, and *Energy*. He presented his research works in several international conferences, such as the IEEE Vehicle Power and Propulsion Conference (VPPC), International Conference on Fundamentals & Development of Fuel Cells (FDPC). He received the excellent student scholarship of Université du Québec à Trois-rivières for his Ph.D. program. He is a Reviewer in multiple high impact factor SCI journals, selectively including the IEEE TRANSACTIONS ON VEHICULAR TECHNOLOGY, *Renewable & Sustainable Energy Reviews*, IEEE ACCESS, *Applied Energy*, and *IET Electrical Systems in Transportation*. He did an internship with Chongqing Automotive Collaborative Innovation Center, Chongqing University, China, under supervising of Prof. Xiaosong Hu.



**Mohsen Kandidayeni** (Member, IEEE) was born in Tehran, Iran, in 1989. His educational journey has spanned through different paths. He received the B.S. degree in mechanical engineering and the master's degree in mechatronics from Arak University, Arak, Iran, in 2011 and 2014, respectively, and the Ph.D. degree in electrical engineering from Hydrogen Research Institute, University of Quebec, Trois-Rivières (UQTR), QC, Canada, in 2020. In 2016, he joined the Hydrogen Research Institute, UQTR. He is currently a Postdoctoral Researcher with Electric-Transport, Energy Storage and Conversion Lab (e-TEESC), Université de Sherbrooke and a Research Assistant Member with Hydrogen Research Institute, UQTR. He was a straight-A student during his master's and Ph.D. programs. Moreover, he has been the Recipient of several awards/honors during his educational path, such as a doctoral scholarship from the Fonds de recherche du Québec-Nature et technologies (FRQNT), a postdoctoral scholarship from FRQNT, an excellence student grant from UQTR, and the third prize in Energy Research Challenge from the Quebec Ministry of Energy and Natural Resources. He has been actively involved in conducting research through authoring, coauthoring, and reviewing several papers in different prestigious scientific journals and also participating in various international conferences. His research interests include energy-related topics, such as hybrid electric vehicles, fuel cell systems, energy management, multiphysics systems, modeling, and control.



**Loïc Boulon** (Senior Member, IEEE) received the master's degree in electrical and automatic control engineering from the University of Lille, Lille, France, in 2006, and the Ph.D. degree in electrical engineering from the University of Franche-Comté, Besançon, France. Since 2010, he has been a Professor with UQTR (Full Professor since 2016) and he works with the Hydrogen Research Institute (Deputy Director since 2019). His work deals with modeling, control and energy management of multiphysics systems. His research interests include hybrid electric vehicles, energy and power sources (fuel cell systems, batteries, and ultracapacitors).

He has authored or coauthored more than 120 scientific papers in peer-reviewed international journals and international conferences and given more than 35 invited conferences all over the world. Since 2019, he has been the world most cited authors of the topic "Proton exchange membrane fuel cells (PEMFC); Fuel cells; Cell stack" in Elsevier SciVal. In 2015, he was the General Chair of the IEEE-Vehicular Power and Propulsion Conference, Montréal, QC, Canada. He is now VP-Motor Vehicles of the IEEE Vehicular Technology Society and he found the "International Summer School on Energetic Efficiency of Connected Vehicles" and the "IEEE Vehicular Technology Society Motor Vehicle Challenge." He is the holder of the Canada Research Chair in Energy Sources for the Vehicles of the future.



**Xiaosong Hu** (Senior Member, IEEE) received the Ph.D. degree in automotive engineering from the Beijing Institute of Technology, Beijing, China, in 2012. He did scientific research and completed the Ph.D. dissertation with the Automotive Research Center, University of Michigan, Ann Arbor, MI, USA, between 2010 and 2012. He is currently a Professor with the State Key Laboratory of Mechanical Transmissions and the Department of Automotive Engineering, Chongqing University, Chongqing, China. He was a Postdoctoral Researcher with the Department of Civil and Environmental Engineering, University of California, Berkeley, CA, USA, between 2014 and 2015, as well as with the Swedish Hybrid Vehicle Center and the Department of Signals and Systems, Chalmers University of Technology, Gothenburg, Sweden, between 2012 and 2014. He was also a Visiting Postdoctoral Researcher with the Institute for Dynamic Systems and Control, Swiss Federal Institute of Technology (ETH), Zurich, Switzerland, in 2014. His research interests include modeling and control of alternative power-trains and energy storage systems. He was the Recipient of several prestigious awards/honors, including Emerging Sustainability Leaders Award in 2016, EU Marie Curie Fellowship in 2015, ASME DSCD Energy Systems Best Paper Award in 2015, and Beijing Best Ph.D. Dissertation Award in 2013.

## **Chapitre 3 - A Comparison of Decentralized ADMM Optimization Algorithms for Power Allocation in Modular Fuel Cell Vehicles**

### **3.1 Introduction**

A comprehensive comparison of two state-of-art decentralized optimization algorithms based on the augmented Lagrangian decomposition technique is offered in this section's manuscript. Notwithstanding the previous optimization study, which straightforwardly examines a decentralized EMS, the main contribution of this study is to carefully assess the modularity and robustness of the decentralized convex optimization-based methods. Subsequently, the evaluation and outcome analysis of the decentralized scheme regarding different optimization parameters and baseline costs are reported to demonstrate the developed fully decentralized schemes' effectiveness compared to the centralized ones.

### **3.2 Methodology**

This paper puts forward a comparative study of two convex optimization frameworks based on the alternating direction method of multipliers (ADMM) for solving a multi-objective power allocation strategy (PAS) problem in a modular FCV (MFCV). The all-propose analysis of the optimization results has been achieved through two key stages. First and foremost, the optimization procedures of the two EMSs and their structure have been summarized. After that, a detailed investigation into the features of the two decentralized optimization algorithms has been conducted through various case studies that consider the robustness and modularity of the decentralized frameworks.



The utilized decomposition approaches are Consensus ADMM (C-ADMM) and Proximal Jacobian ADMM (PJ-ADMM). ADMM is fundamentally inspired by a decomposition-coordination procedure, in which an optimization problem is broken down into smaller subproblems. Then, the subproblems are solved to converge into the same results as the initial problem. Firstly, to apply the algorithms in our case study, an augmented Lagrangian function of the power-split problem is derived. Subsequently, the corresponding function is decomposed, and the broken-down terms are minimized over sequential processes. Finally, the dual variables are updated. This procedure continues until the convergence criteria are satisfied.

Figure 3-2 and Figure 3-1 depict the information flow in C-ADMM and PJ-ADMM.

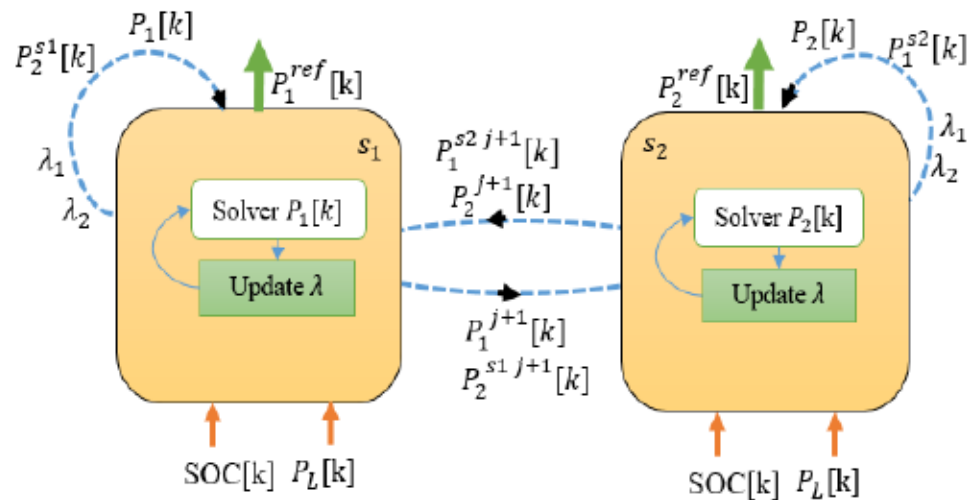


Figure 3-1 The parallel communication procedure of the decentralized PJ-ADMM.

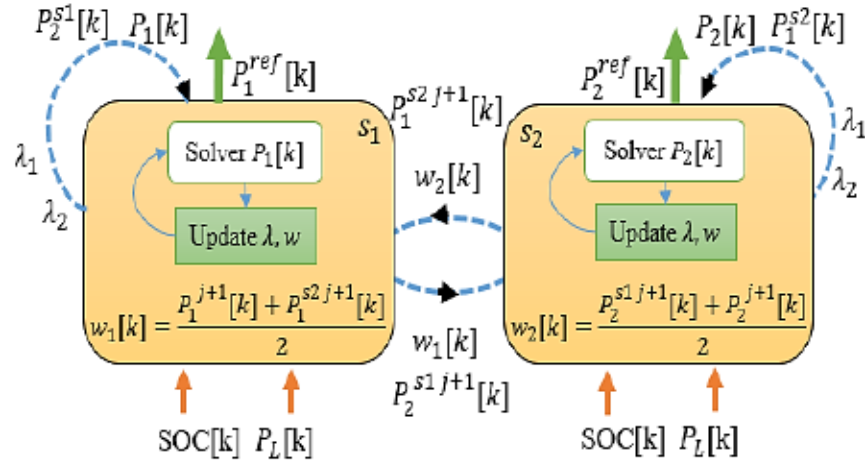


Figure 3-2 The information flow between the FC modules via the C-ADMM.

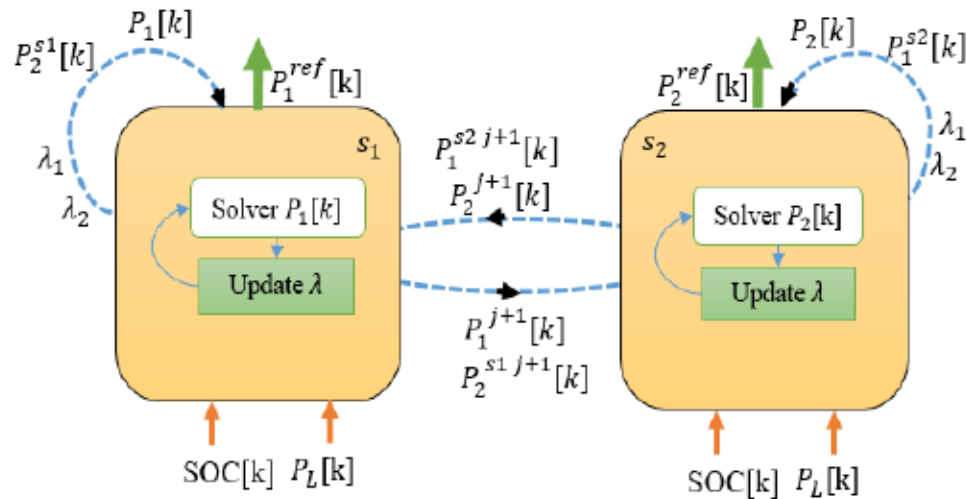


Figure 3-1 The parallel communication procedure of the decentralized PJ-ADMM.

### 3.3 Synopsis of the analyses of the results

Figure 3-3 compares the output powers and SoC variation obtained by C-ADMM and PJ-ADMM. The SoC level of the battery pack oscillates between 69% and 72%, which is less than approximately a 3% variation. Although the obtained SOC variations by C-ADMM and PJ-ADMM are similar, a slight deviation can be observed in the SOC levels from 50 s to 150 s. It is due to more cumulative costs in the PJ-ADMM algorithm. After the 150s, the SOC fluctuations become almost equal because the answers of decentralized convex optimization

algorithms (DCOAs) are similar. Another point is that the drawn power from the PEMFC modules is increased after the 250s to keep the SOC fluctuation close enough to the initial value.

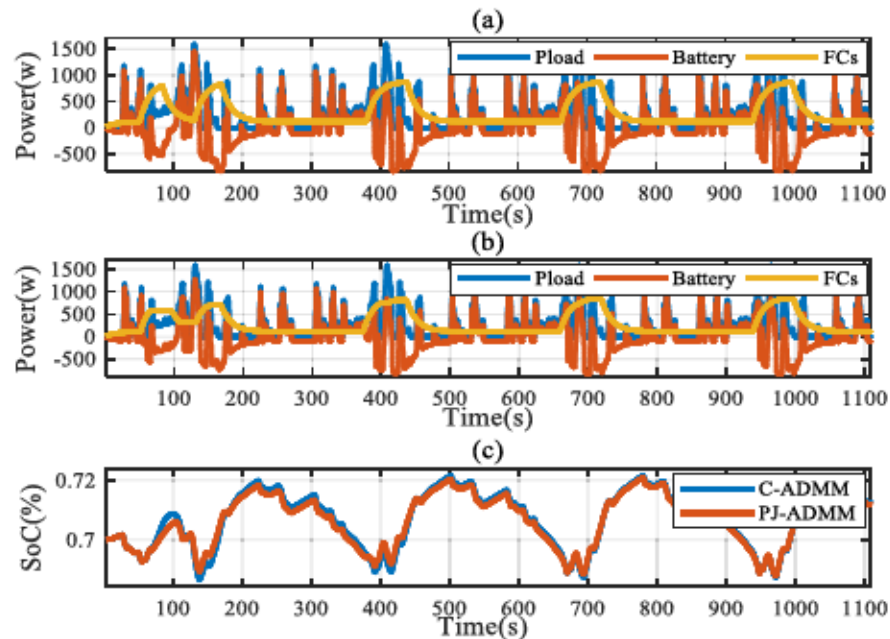


Figure 3-3 Optimal PASs results: (a) the profiles based on C-ADMM, (b) the profiles based on PJ-ADMM, and (c) the SoC evaluations.

The proposed DCOA methods are marginally better than SQP and have shown a very close performance to DP in terms of the total cost. However, in terms of computational time, the decentralized structures of the introduced DCOA methods have made them much faster than SQP, where the computational burden has been reduced by 78.4% and 84.1% when using C-ADMM and PJ-ADMM, respectively. The computational time in PJ-ADMM is 5.7% lower than in C-ADMM because of the proximal term.

### 3.4 Outcomes

The study of two decentralized optimization approaches has brought about the following points.

- Describing the principle highlights to devise a proficient modular EMS for the FCV applications.
- Demonstrating the benefits of the decentralized EMSs with an electrical fault, parameter initialization, and price changes.

The explanation, as mentioned earlier, is presented through an article in the following section.

**Article 2:** Comparison of Decentralized ADMM Optimization Algorithms for Power Allocation in Modular Fuel Cell Vehicles

**Authors:** Arash Khalatbarisoltani, Mohsen Kandidayeni, Loïc Boulon, and Xiaosong Hu

**Journal:** IEEE/ASME Transactions on Mechatronics

**Publication date:** September 2021

### 3.1 Conclusion




This chapter comprehensively analyzes two novel fully decentralized convex optimization algorithms (DCOA). Firstly, a general PAS problem is formulated, including hydrogen consumption, FC modules, and battery unit lifetime. Secondly, two multi-block alternating direction methods of multipliers (ADMM) algorithms are selected due to their fast convergence, parallel structure, modularity, and robustness. These features make them



feasible solutions in a MFCS. Subsequently, an in-depth comparative analysis, considering the real driving cycle and parameters and the sensitivity analysis regarding the dynamic fault and different price scenarios, is performed to fully disclose these algorithms' benefits.

Moreover, the performance of the algorithms is compared with DP and SQP. Both simulations and the experiments unveil that the fully decentralized modular schemes perform better than DP and SQP. Moreover, PJ-ADMM is more practical in real-time applications due to its fast response and robustness. This chapter has been mainly focused on a comprehensive analysis of two fully decentralized convex algorithms with a single-step optimization. The proposed decentralized procedures have the potential to be combined with an advanced multi-step MPC method to enhance the optimization performance and the inherent robustness against uncertainty in predicting future driving profiles. Additionally, the hyperparameters of the decentralized controller can be tuned to improve the optimization speed further. Consequently, the next chapter will present an adaptive look-ahead decentralized MPC.

# Comparison of Decentralized ADMM Optimization Algorithms for Power Allocation in Modular Fuel Cell Vehicles

Arash Khalatbarisoltani , *Member, IEEE*, Mohsen Kandidayeni , *Member, IEEE*, Loïc Boulon, *Senior Member, IEEE*, and Xiaosong Hu , *Senior Member, IEEE*

**Abstract**—The advanced modular powertrains are envisioned as primary part of future hybrid fuel cell vehicles (FCVs). The existing papers in the literature solely cope with the hardware side of modularity, while the software side is also vital to capitalize on the total capacity of these powertrains. Driven by this motivation, this article puts forward a comparative study of two novel decentralized convex optimization frameworks based on alternating direction method of multipliers (ADMM) to solve a multi-objective power allocation strategy (PAS) problem in a modular FCV (MFCV). The MFCV in this article is composed of two fuel cell (FC) stacks and a battery pack. Despite the existing centralized strategies for such a modular system, this manuscript proposes two decentralized PASs (Dec-PASs) based on Consensus ADMM (C-ADMM) and Proximal Jacobian ADMM (PJ-ADMM) to bridge the gap regarding the appreciation of modularity in software terms. Herein, after formulating the central PAS optimization problem, the principle of utilizing such decentralized algorithms is presented in detail. Subsequently, the performance of the proposed Dec-PASs is examined through several numerical simulations as well as experiments on a developed small-scale

test bench. The obtained results illustrate that decomposition into decentralized forms enables solving the complex PAS optimization problem faster and provides modularity and flexibility. Furthermore, the proposed Dec-PASs can cope with fault and malfunction and thus augment the durability and robustness of modular powertrain systems.

**Index Terms**—Alternating direction method of multipliers (ADMM), distributed optimization, energy management, fuel cell hybrid vehicle, proton exchange membrane fuel cell (PEMFC).

## I. INTRODUCTION

### A. General Context

ONE of the largest sources of greenhouse gas emissions is burning fossil fuels for the transportation sector. In this regard, electrification of transportation through different hybrid and pure electric vehicle technologies has come under attention [1]. Fuel cell vehicles (FCVs), which are generally composed of a fuel cell system (FCS) as the primary power source and an energy storage system (battery and/or supercapacitor) as the secondary one, are considered as one of the promising solutions to mitigate this critical concern [2], [3]. Among different FCSs, proton exchange membrane (PEM) fuel cell (FC) has been the most appropriate candidate for this application due to its efficiency, power density, low noise, and low-temperature operation range [4]. The lithium-ion battery is also the dominant battery technology in this domain due to its high energy and power density and low self-discharge rate [5]. Since the power sources of an FCV have different energetic characteristics, the use of a power allocation strategy (PAS) is crucial to minimize the total cost (hydrogen consumption and degradation of the components) [6], [7]. A large number of studies have been done on the design of PASs for FCVs, such as rule-based [8], [9], fuzzy-based [10]–[14], optimization-based [15]–[19], predictive-based [20]–[23], and adaptive strategies [24]. The majority of these studies are based on centralized PASs (Cen-PAS) designed for a single-stack FCV. Hence, they are vulnerable to the malfunction of the power sources, which can occur in such a configuration. This weakness exacerbates in high-power applications, like buses and trucks, since many cells must be stacked to meet the requested power. Consequently, with

Manuscript received June 24, 2020; revised October 22, 2020, April 1, 2021, and July 28, 2021; accepted August 12, 2021. This work was supported in part by the Natural Sciences and Engineering Research Council of Canada (NSERC) and in part by the Canada Research Chairs program. The work of Xiaosong Hu was supported in part by the Chongqing Natural Science Foundation for Distinguished Young Scholars under Grant cstc2019jcyj0010 and in part by Chongqing Science and Technology Bureau, China. Recommended by Technical Editor D. Chen and Senior Editor X. Chen. (Corresponding authors: Xiaosong Hu and Loïc Boulon.)

Arash Khalatbarisoltani and Loïc Boulon are with the Hydrogen Research Institute, Department of Electrical and Computer Engineering, Université du Québec à Trois-Rivières, QC G8Z 4M3, Canada (e-mail: arash.khalatbarisoltani@uqtr.ca; loic.boulon@uqtr.ca).

Mohsen Kandidayeni is with the Electric-Transport Energy Storage and Conversion Lab, Université de Sherbrooke, Sherbrooke, QC J1K 2R1, Canada, and also with the UQTR Hydrogen Research Institute, Université du Québec à Trois-Rivières, Trois-Rivières, QC G8Z 4M3, Canada (e-mail: mohsen.kandidayeni@usherbrooke.ca).

Xiaosong Hu is with the State Key Laboratory for Mechanical Transmission, Department of Automotive Engineering, Chongqing University, Chongqing 400044, China, and also with the Advanced Vehicle Engineering Centre, Cranfield University, MK43 0AL Cranfield U.K. (e-mail: xiaosonghu@ieee.org).

Color versions of one or more figure in this article are available at <https://doi.org/10.1109/TMECH.2021.3105950>.

Digital Object Identifier 10.1109/TMECH.2021.3105950



all the advantageous of the single-stack FCSs, it is necessary to advance them in terms of durability, modularity, and efficiency.

### B. Literature Study

One of the proposed promising solutions in this regard is the use of modular FCSs (MFCSS) [25]. Unlike the typical FCVs, the modular FCVs consist of several connected low-power FCs rather than a high-power one along with an energy storage system. In [26], a survey of the MFCSS with different power conditioning topologies and fluidic architectures is provided and concluded that these systems offer better efficiency and lower hydrogen consumption than the single-stack ones. Moreover, the inherent redundancy of the MFCSS leads to the increase of robustness and reliability in case of malfunction occurrence in one of the FCs and/or the converters. On the other hand, the extra degrees of freedom in the MFCSS necessitate the design of advanced PASs to optimize the end-user costs and fulfill the powertrain system requirements.

There are several research efforts based on the Cen-PASs for MFCVs. For instance, in [27], three PASs, namely daisy chain, equal distribution, and optimal splitting, are compared for an MFCV, and it is shown that the optimal splitting achieves the best performance. In [28], a rule-based PAS is utilized for an MFCV and concluded that this strategy is suitable for high hybridization ratios. In [29], four FCSs have been connected via power converters to the DC bus using a maximum power point tracking controller for each stack. In [30], a hysteresis PAS is developed for an MFCV composed of three FCSs and a battery pack. The primary purpose of the suggested PAS is to make the operation time of the three FCSs equal while reducing the number of on-off cycles. In [31], an adaptive state machine PAS is proposed to distribute the power among four FCSs and a battery pack. Simultaneously, the FCSs are constantly monitored in terms of their maximum power and efficiency points. In [32], an adaptive current distribution method based on a droop control technique is proposed for two FCSs to decline the degradation rate.

Although the discussed modular powertrains bring about modularity and reliability from electrical and fluidic (hardware) points of view, they do not guarantee these aspects in their management and control units (software). These Cen-PASs are susceptible to a precipitously single point of failure through their software programs. Moreover, the additional degrees of freedom make these Cen-PASs substantially complex and time-consuming to be solved in real-time, which is a critical aspect in the FCV applications. Therefore, there has been a growing trend in the literature to gradually shift from Cen-PASs to decentralized PASs (Dec-PASs). For instance, in [33], [34], two Dec-PASs based on game theory are proposed. However, the main drawback of these strategies is that the players are selfish and may not converge to their optimal results. Furthermore, these Dec-PASs cannot entirely satisfy the nonlinearities in the behaviour and the constraints of different sources. Another worth noting problem with these strategies is that they need a lot of data exchange which is not feasible for the onboard applications. In [35], a droop-based Dec-PAS is proposed for seeking optimal power-sharing. However, this approach cannot perform well in

a wide range of operations and does not consider the longevity of the powertrain system.

To evade the abovementioned problems in other domains with multisource systems, such as smart grids [36], [37], special attention has been given to decentralized convex optimization (DCO) algorithms [38]. One of the most famous classical decomposition methods in this regard is the one introduced in [39] based on Lagrangian relaxation. However, this method has slow convergence. Several other methods, such as auxiliary problem principle (APP) [40], consensus-based algorithm [41], Karush—Kuhn—Tucker (KKT) conditions [42], and alternating direction method of multipliers (ADMM) [43], [44], have been proposed to enhance the convergence rate. Among them, ADMM has attracted a lot of attentions since it can guarantee the global convergence and does not require a significant amount of data exchange in spite of other algorithms. This method amalgamates dual decomposition with the multipliers technique and the augmented Lagrangian approach. ADMM decomposition-based method can be categorized into Gauss-Seidel ADMM (GS-ADMM), Variable Splitting ADMM (VS-ADMM), and Jacobian ADMM (J-ADMM) [45]. GS-ADMM cannot be straightforwardly applied to an optimization problem with more than three subproblems and hence cannot guarantee the convergence in this case [45]. VS-ADMM is also not practical for large-size optimization problems, and J-ADMM may diverge for various problems although its updating procedure is parallel. In this regard, J-ADMM and GS-ADMM have been advanced to Proximal Jacobian ADMM (PJ-ADMM) and Consensus ADMM (C-ADMM), respectively, to be more practical for the distributed optimization problems. The update processes of PJ-ADMM and C-ADMM are parallel, and convergence performance can be guaranteed simultaneously [46]. These two DCO-based algorithms offer several advantages compared to centralized ones. First, parallel execution feature enables them to solve complex optimization problems with less computational effort. Second, they can autonomously adapt to new changes which provides robustness in case of any subsystem failure.

In [47], [48], two classic ADMM algorithms are suggested for solving Cen-PASs in hybrid electric vehicles. However, their central control units do not offer modularity, plug & play aspect, and robustness in terms of software. In [49], an APP-based scheme is proposed for a modular FCV. However, this decentralized approach will not provide satisfying results in convergence speed compared to other advanced DCO algorithms, such as PJ-ADMM and C-ADMM.

### C. Contribution

In the light of the discussed papers, it can be stated that there is a lack of discussion on designing Dec-PAS via DCOs in the domain of MFCVs. To the best of the authors' knowledge, this work is one of the leading attempts, if any, to propose a practical framework for designing Dec-PASs in MFCVs. In this respect, a detailed comparison of two Dec-PASs based on C-ADMM and PJ-ADMM is put forward for an MFCV. These two decomposition-based approaches are singled out due to their parallel updating process, fast convergence speed, ability to handle constraints, and global convergence performance.



The proposed Dec-PASs are compared with an offline optimal PAS (dynamic programming (DP)) and a Cen-PAS (sequential quadratic programming (SQP)). The performance of these fully Dec-PASs is thoroughly explored in terms of final cost under a real driving profile. Since the ADMM-based decentralized approaches are highly sensitive to their parameters tuning, this vital characteristic is thoroughly investigated. Moreover, to further highlight the DCO-based PAS capabilities, the best Dec-PAS is selected for price sensitivity and dynamic fault robustness analyses. It is worth reminding that the performance of the PJ-ADMM algorithm has been evaluated using a developed experimental test bench, as opposed to most of similar manuscripts in the literature, which are solely based on simulation.

#### D. Organization

The rest of this article is organized as follows. In Section II, the configuration and modeling of the MFCV are described in detail. Section III presents the general formulation of the multi-objective PAS optimization problem. Section IV describes the two utilized decentralized ADMM-based PAS frameworks. In Section V, a detailed comparison of several cases is conducted to scrutinize the performance of the proposed DCO-based PASs. Section VI demonstrates the implementation results via a developed small-scale test bench to validate the theoretical background. Finally, Section VII concludes this article.

## II. MFCV POWERTRAIN CONFIGURATION AND MODELING

### A. Powertrain Structure and Modeling

To investigate the performance of the proposed Dec-PASs, a modular FC test bench based on an electric vehicle is established [50], as shown in Fig. 1. The developed small-scale test bench comprises two FC modules, a battery pack, a programmable dc electronic load, and a multirange programmable dc power supply for simulating the requested load profile. The critical components of each FC module are a 500-W open-cathode PEMFCS (Horizon, model: H-500), a smoothing inductor, and an adjustable unidirectional boost dc-dc converter (Zahn Electronics<sup>TM</sup>, model: DC5036-SU). Moreover, six series 12V/18Ah battery packs provide the voltage of the dc-bus. Each module has its autonomous Dec-PAS inside of a National Instrument CompactRIO (NI9022). The optimal reference of each module is calculated at each control instant with an interval of 10 Hz. The power equilibrium of the FC modules and the battery unit is formulated as follows:

$$\sum_{m=1}^M P_{m,k} D_{m,k} + P_{B,k} = P_{L,k} \quad (1)$$

where  $P_m, m \in M, M = \{1, 2\}$  denotes the generated power by each one of the 500-W FCSs,  $D_m$  is the control signal of the boost converters,  $P_B$  is the power provided by the battery unit,  $P_L$  is the requested power from the propulsion system, and  $k$  is the time instant.

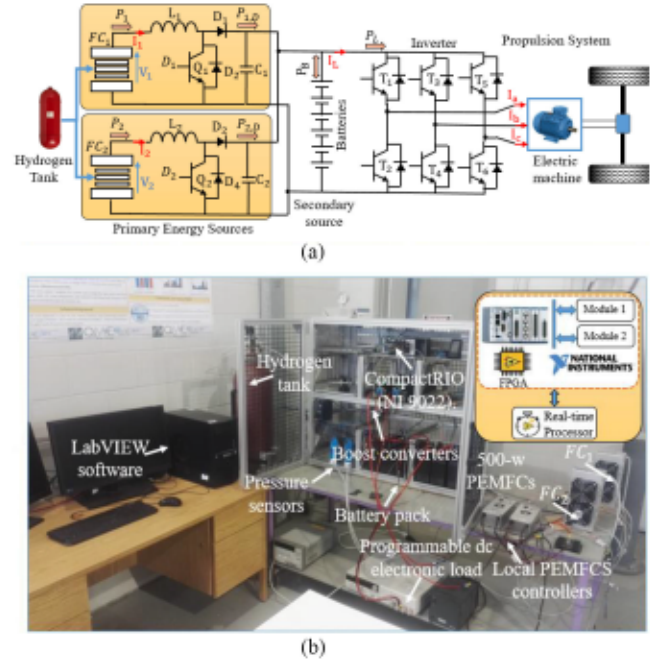


Fig. 1. Developed small-scale test bench. (a) Schematic of the powertrain system. (b) Developed test bench.

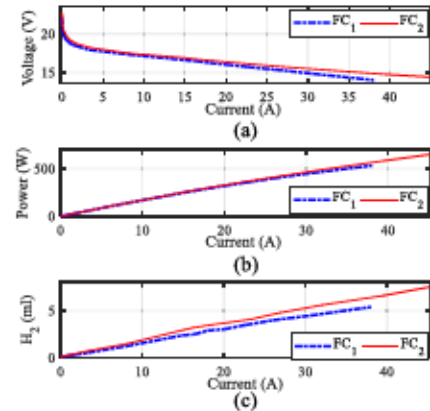


Fig. 2. Characteristic curves of the two real FC modules. (a) Polarization curves. (b) Power curves. (c) Hydrogen curves.

### B. FCS Modeling and Constraints

In this article, each of the 500-W FCSs,  $FC_m$ , are modeled as a voltage source where their polarization curves and the hydrogen mass flows versus requested current are described by experimentally validated quasi-static curves, as shown in Fig. 2. As explained in [14], the output power of an H-500 Horizon FCS is obtained by subtracting the power of the FC stack from the consumed power by the cooling fans and the hydrogen valve. The consumed power by the purge valve is ignored as it has a fixed cyclic purging (every ten seconds for a duration of 100 ms). In this article, the blowers and ancillaries of the FCSs are not explicitly modeled. Nevertheless, their energetic performances are taken into consideration by the static characteristics of the



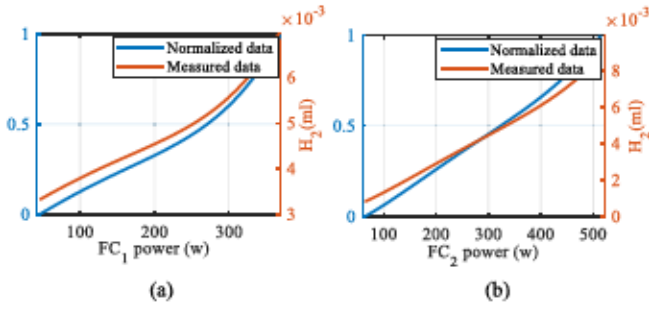


Fig. 3. Measured and normalized hydrogen consumption curves of the developed test bench. (a)  $FC_1$  and (b)  $FC_2$ .

TABLE I

TECHNICAL SPECIFICATION OF THE OPEN-CATHODE PEMFC STACKS (H-500)

Number of cells= 24	Hydrogen pressure= 0.45-0.55 bar
Rated power=500 W	External temperature= 5-30 °C
Rated performance= 14.4 V @35 A	Max stack temperature= 65 °C
Output voltage range= 12 V-24 V	Humidification= Self-humidified
Reactants= Hydrogen and Air	Cooling= Air (cooling fan)
Flow rate at max power= 6.5 L/min	Efficiency of stack= 40% @ 14.4V

FCSs. In other words, the presented characteristics in Fig. 2 belong to the FCSs considering the fans and hydrogen valve. The technical data of the utilized FCSs are reported in Table I. Fig. 3 demonstrates the measured and normalized hydrogen consumptions of the FC modules.

The following enforces power and slew rate limits:

$$P_{m,min} \leq P_{m,k} \leq P_{m,max} \quad (2.a)$$

$$R_{d,m}\Delta t \leq P_{m,k} - P_{m,(k-1)} \leq R_{u,m}\Delta t \quad (2.b)$$

where  $P_{m,min}$  and  $P_{m,max}$  are the minimum and maximum values for  $P_m$ ,  $R_{d,m}$  and  $R_{u,m}$  are boundaries of the slew rates, and  $\Delta t$  indicates the time step. As explained in [14], for rising, a dynamic limitation of 10% of the maximum power per second, and for falling, 30% of the maximum power per second have been considered for the operation of the FC stack. These constraints prevent the FC stack from sudden changes, which can result in degradation.

### C. Battery Modeling and Constraints

A first-order RC model of the battery pack is formulated by

$$I_{B,k} = \frac{V_{0,k} - R_s I_{B,k} - V_{B,k}}{R_c} + C_c \frac{d}{dt} (V_{0,k} - R_s I_{B,k} - V_{B,k}) \quad (3)$$

where  $I_B$  is the battery pack current,  $V_0$  is the open-circuit voltage,  $R_s$  is the series ohmic resistance,  $V_B$  is the output terminal voltage,  $R_c$  denotes the polarization resistance, and  $C_c$  is the polarization capacitor. The following imposes power and slew rate limits:

$$P_{B,min} \leq P_{B,k} \leq P_{B,max} \quad (4.a)$$

$$R_{d,B}\Delta t \leq P_{B,k} - P_{B,(k-1)} \leq R_{u,B}\Delta t \quad (4.b)$$

where  $P_{B,min}$  and  $P_{B,max}$  are the minimum and maximum limits of  $P_B$ , respectively, and  $R_{d,B}$  and  $R_{u,B}$  are the slew rate boundaries of  $P_B$ . The following presents the state of charge ( $SoC$ ) calculation formula along with the constraints on the battery  $SoC$  level:

$$SoC_{k+1} = SoC_k - \frac{P_{B,k}\Delta t}{Q_B V_{B,k} 3600} \quad (5.a)$$

$$SoC_{min} \leq SoC_k \leq SoC_{max} \quad (5.b)$$

where  $SoC_{min}$  and  $SoC_{max}$  denote the minimum and maximum limits of  $SoC$ , respectively,  $SoC_k = 0$  is the initial  $SoC$  level, and  $Q_B$  represents the battery capacity. The battery lifetime is affected by the depth of discharge ( $DoD$ ) and is defined as an initial capacity drop (reaching 80% of the initial capacity). The state of health ( $SoH$ ) is calculated by

$$SoH_{k+1} = SoH_k - \frac{|P_{B,k}|\Delta t}{2n_B Q_B V_{B,k} 3600} \quad (6.a)$$

$$SoH_{min} \leq SoH_k \quad (6.b)$$

where  $SoH_{min}$  and  $SoH_k = 0$  indicate the minimum and initial  $SoH$ , respectively, and  $n_B$  is the total number of cycles during the whole lifetime of the battery pack. The parameters of the battery pack have been obtained from experimental tests ( $V_0 = 12.21$  V,  $R_s = 0.0141$   $\Omega$ ,  $Q_B = 18.2A$  h, and  $R_c = 0.0177$   $\Omega$ ).

### D. Boost Converter Modeling and Characteristics

The two converters are modeled as follows:

$$L_m \frac{d}{dt} I_{m,k} = V_{m,k} - V_{h,m,k} - r_m I_{m,k} \quad (7)$$

$$\begin{cases} V_{h,m,k} = m_{h,m} V_{B,k} \\ I_{h,m,k} = m_{h,m} I_{m,k} \eta_m^z \end{cases} z = \begin{cases} 1, & \text{if } P_m > 0 \\ -1, & \text{if } P_m < 0 \end{cases}$$

where  $I_m$  and  $V_m$  are the current and voltage of  $FC_m$ , respectively,  $L_m$  presents the smoothing inductor inductance,  $r_m$  is the smoothing inductor resistance,  $\eta_{h,m}$  is the average efficiency, and  $m_{h,m}$  is the modulation ratio of the converters. The estimated parameters of the boost converters are  $L_m = 1.1$  mH,  $r_m = 23.9$  m $\Omega$ , and  $\eta_m = 96.21\%$ .

## III. PROCESS OF DEVELOPING THE GENERAL PAS PROBLEM AND THE EVALUATION FUNCTION

This section first presents a standard framework for formulating the main PAS optimization problem (8). Next, an evaluation function (9) is defined to measure all the main criteria used in different optimization methods in the same way.

### A. Formulation of the Central PAS Problem

The multiobjective optimization problem of the MFCV can be written as follows:

$$\min_{P_1, \dots, P_M, P_B} \sum_{m=1}^M g(c_{m,k} + c_{B,k}) \quad (8.a)$$

s.t.  $\sum_{m=1}^M A_m P_m = c$ , other equality, and inequality constraints

where  $g$  is a convex approximation cost function to be minimized, including the FC modules' normalized hydrogen consumption, and the normalized degradation of the modules,  $c_{m,k}$ , and the battery system,  $c_{B,k}$ , which are formulated as follows:

$$c_{m,k} = s_{h,m,k} + s_{d,m,k}, \quad c_{B,k} = s_{B,k} + s_{SoC,k} \quad (8.b)$$

where  $P_m \in \mathbb{R}^{N_m}$  stands for the control actions,  $A_m \in \mathbb{R}^{M \times N_m}$  and  $c \in \mathbb{R}^M$  apply the powertrain and the coupling constraints to the modules, respectively,  $k$  stands for each simulation moment, and  $s_{h,m,k}$  is the normalized hydrogen consumption function, calculated by

$$s_{h,m,k} = \frac{h_{m,k} - h_{m,min}}{h_{m,max} - h_{m,min}} \quad (8.c)$$

where  $h_{m,k}$ ,  $h_{m,min}$ , and  $h_{m,max}$  are the hydrogen consumption, and the minimum and maximum limits of  $FC_m$ , respectively. The normalized  $FC_m$  degradation term,  $s_{d,m}$ , which includes two normalized cost shaping functions, the low-power degradation,  $s_{d,m}^l$ , and the high-power degradation,  $s_{d,m}^h$ , are formulated by

$$s_{d,m,k} = \alpha_l s_{d,m,k}^l + \alpha_h s_{d,m,k}^h \quad (8.d)$$

where  $s_{d,m}^l$  and  $s_{d,m}^h$  are computed by

$$s_{d,m,k}^l = 1 - \frac{(P_{m,k} - P_{m,min})^2}{(P_{m,max} - P_{m,min})^2} \quad (8.e)$$

$$s_{d,m,k}^h = 1 - \frac{(P_{m,k} - P_{m,max})^2}{(P_{m,max} - P_{m,min})^2} \quad (8.f)$$

where  $\alpha_l$  and  $\alpha_h$  are the constant coefficients, computed by

$$\alpha_l = \frac{\varepsilon_l}{\varepsilon_l + \varepsilon_h}, \quad \alpha_h = \frac{\varepsilon_h}{\varepsilon_l + \varepsilon_h} \quad (8.g)$$

where  $\varepsilon_l$  and  $\varepsilon_h$  are the low-power and high-power cell degradation rates, respectively. The degradation terms are adopted from the previous studies since several long-duration aging tests, which are beyond the scope of this research work, are needed to determine them. These values are modified based on the number of cells in the utilized FCSs. The values of these variables ( $\varepsilon_l = 8.662 \mu V/h$  and  $\varepsilon_h = 10 \mu V/h$ ) have been obtained from [51], [52]. The normalized battery pack degradation function,  $s_B$ , is calculated by

$$s_{B,k} = \frac{P_{L,k}}{P_{L,max}} \quad (8.h)$$

where  $P_{L,max}$  denotes the maximum value of  $P_L$ .  $s_{SoC}$  is a punishment term to measure the SoC level variation, which is defined by

$$s_{SoC,k} = \beta (SoC_k - SoC_{k=0})^2 \quad (8.i)$$

where  $SoC_{k=0}$  is the initial SoC, and  $\beta$  is a big positive coefficient.

## B. Defined Evaluation Function

The end-user cost,  $S_T$ , in USD, is calculated by

$$S_T = \left( \sum_K \sum_m S_{H,m,k} + S_{d,m,k} + S_{B,k} \right) + S_{SoC} \quad (9.a)$$

The hydrogen cost of each module,  $S_{H,m}$ , is computed by

$$S_{H,m,k} = h_{m,k} C_{H_2} \Delta t \quad (9.b)$$

where  $h_{m,k}$  is the hydrogen consumption,  $C_{H_2}$  is the hydrogen price, and  $\Delta t$  indicates the time step. The degradation cost of each module,  $S_{d,m,k}$ , is calculated by

$$S_{d,m,k} = S_{d,m,k}^l + S_{d,m,k}^h \quad (9.c)$$

where  $S_{d,m,k}^l$  and  $S_{d,m,k}^h$  are costs of low-power and high-power degradation, given by

$$S_{d,m,k}^l = \frac{n_m \varepsilon_l C_{FC,m} \Delta t \mu_{l,m}}{3600 V_{n,m}} \quad (9.d)$$

$$S_{d,m,k}^h = \frac{n_m \varepsilon_h C_{FC,m} \Delta t \mu_{h,m}}{3600 V_{n,m}} \quad (9.d)$$

where  $n_m$  represents the numbers of cells in each  $FC_m$ ,  $V_{n,m}$  is 10% of the nominal  $FC_m$  voltage drop, and  $C_{FC_m}$  is FCS cost.  $\mu_{l,m}$  and  $\mu_{h,m}$  are equal to

$$\mu_{l,m} = \begin{cases} 1, & \text{if } P_{min,m} \leq P_{m,k} \leq 0.2 P_{nom,m} \\ 0, & \text{otherwise.} \end{cases} \quad (9.e)$$

$$\mu_{h,m} = \begin{cases} 1, & \text{if } 0.8 P_{nom,m} \leq P_{m,k} \leq P_{max,m} \\ 0, & \text{otherwise.} \end{cases} \quad (9.f)$$

where  $P_{nom,m}$  is the output power recommended by the manufacturing company for nominal use of the FCS [52]. The battery degradation cost,  $S_B$ , is determined by

$$S_{B,k} = C_B (SoH_{B,k} - SoH_{B,0}) \quad (9.g)$$

where  $C_B$  is the battery price. The punishment term,  $s_{SoC}$ , is to recharge the battery to reach the initial SoC by  $FC_m$  while operating at their maximum efficiency points. The reference prices are  $C_{H_2} = 3.9254 \$/Kg$  [53],  $C_B = 189 \$/kWh$  [54], and  $C_{FC_m} = 35 \$/kW$  [55].

## IV. FORMULATION OF THE GENERAL ADMM PAS FRAMEWORKS

In this section, the utilized DCO algorithms are described. To apply the DCO-based algorithms, firstly, the augmented Lagrangian functions of the power-split problem are derived. Subsequently, the corresponding functions are decomposed, and the broken-down terms are minimized. Finally, the dual variables are updated. These procedures continue until the convergence criteria are satisfied.

It is worth noting that for the following two subsections, each variable with the index of  $j$  means the current value at the  $j^{\text{th}}$  iteration, and each variable with the index of  $j+1$  denotes the new value.  $k$  is the position in the selected driving profile.  $P_{1,k}$  and  $P_{1,k}^{s_1}$  are related to  $FC_1$ , and  $P_{2,k}^{s_1}$  and  $P_{2,k}$  are linked



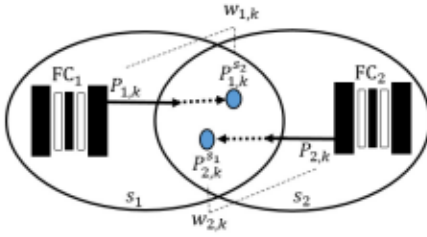


Fig. 4. Description of real, virtual, and global variables in the MFCS.

to  $FC_2$ . During the optimization process, each decentralized controller calculates the power of  $FC_1$  and  $FC_2$  at the same time. For instance, the decentralized controller 1 solves its subproblem for one iteration and calculates the output power  $P_{1,k}$  for its module and  $P_{2,k}^{s1}$  for the neighboring module. The decentralized controller 2 solves its subproblem for one iteration and calculates the output power  $P_{2,k}$  for its module and  $P_{1,k}^{s2}$  for the neighboring module. During the exchange step,  $P_{1,k}^{s2}$  is sent to  $FC_1$  and  $P_{2,k}^{s1}$  is sent to  $FC_2$ . Then, these values will be used in the next iteration of the optimization procedure. These shared variables are used to ensure that all the constraints are fulfilled for the final results in the  $k^{th}$  step. The final power of  $P_{1,k}$  and  $P_{2,k}$  will be sent to the converters as  $P_{1,k}^{ref}$  and  $P_{2,k}^{ref}$  to control the modules and the rest of the requested power will be supplied by  $P_B$ . These final values will be used for the  $k^{th}$  step. For each  $k$ , during the optimization iterations, the state variables of the modular powertrain system are supposed to be unchanged. However, these values will be updated in the next step ( $k + 1$ ).

### A. C-ADMM-Based PAS

As shown in Fig. 4, the central PAS is decomposed into two coupled subproblems,  $s_m$ . Since the coupling constraints are not separable,  $P_{m,k}$  is copied into its neighboring module and linked with a global power vector,  $w_{G,k} = \{w_{1,k}, w_{2,k}\}$ . In this respect,  $P_{1,k}$  is copied into  $s_2$ ,  $P_{1,k}^{s2}$ , as a virtual power, and  $w_{1,k}$  is defined to link them.  $P_{2,k}$  is also duplicated into  $s_1$ ,  $P_{2,k}^{s1}$ , and  $w_{2,k}$  connects them.

The following guarantees that the duplicated powers in  $s_1$  and  $s_2$  are equal with each other [44]

$$P_{1,k} - w_{1,k} = 0, P_{2,k}^{s1} - w_{2,k} = 0 \quad (10.a)$$

$$P_{1,k}^{s2} - w_{1,k} = 0, P_{2,k} - w_{2,k} = 0. \quad (10.b)$$

After defining the global power variable constraints, the distributed parallel form of C-ADMM is defined by (11) and (12).

*The  $FC_1$  module equations*

$$P_{1,k}^{j+1}, P_{2,k}^{s1,j+1} = \min(c_{1,k} (P_{1,k}, P_{2,k}^{s1}) + c_{B,k} (P_{B,k}) + \lambda_1^{s1,j} P_{1,k} + \lambda_2^{s1,j} P_{2,k}^{s1} + \frac{\rho}{2} \left( (P_{1,k} - w_{1,k}^j)^2 + (P_{2,k}^{s1} - w_{2,k}^j)^2 \right)) \quad (11.a)$$

$$w_{1,k}^{j+1} = \frac{P_{1,k}^{j+1} + P_{1,k}^{s1,j+1}}{2} \quad (11.b)$$

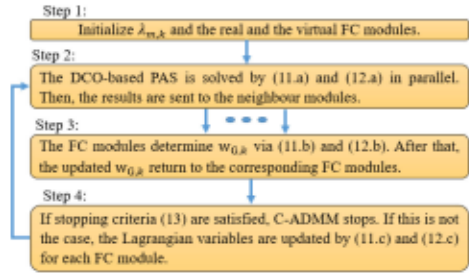


Fig. 5. Step-by-step flowchart of the decentralized C-ADMM algorithm.

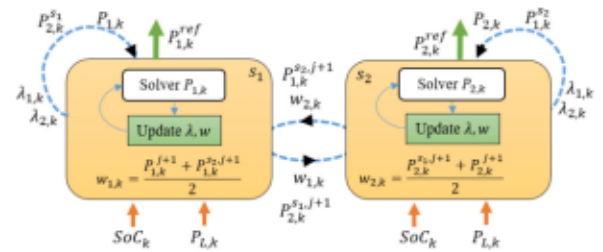


Fig. 6. Information flow between the FC modules via C-ADMM.

$$\lambda_{1,k}^{s1,j+1} = \lambda_{1,k}^{s1,j} + \rho (P_{1,k}^{j+1} - w_{1,k}^{j+1}) \quad (11.c)$$

$$\lambda_{2,k}^{s1,j+1} = \lambda_{2,k}^{s1,j} + \rho (P_{2,k}^{j+1} - w_{2,k}^{j+1}).$$

*The  $FC_2$  module equations*

$$P_{1,k}^{s2,j+1}, P_{2,k}^{j+1} = \min(c_{2,k} (P_{1,k}^{s2}, P_{2,k}) + c_{B,k} (P_{B,k})$$

$$\lambda_1^{s2,j} P_{1,k}^{s2} + \lambda_2^{s2,j} P_{2,k} + \frac{\rho}{2} \left( (P_{1,k}^{s2} - w_{1,k}^j)^2 + (P_{2,k} - w_{2,k}^j)^2 \right)) \quad (12.a)$$

$$w_{2,k}^{j+1} = \frac{P_{2,k}^{j+1} + P_{2,k}^{s1,j+1}}{2} \quad (12.b)$$

$$\lambda_{1,k}^{s2,j+1} = \lambda_{1,k}^{s2,j} + \rho (P_{1,k}^{j+1} - w_{1,k}^{j+1}) \quad (12.c)$$

$$\lambda_{2,k}^{s2,j+1} = \lambda_{2,k}^{s2,j} + \rho (P_{2,k}^{j+1} - w_{2,k}^{j+1})$$

where  $\lambda_{m,k}$  represents the Lagrangian multipliers, and  $\rho$  is a positive tuning value. Equations (11.b) and (12.b) define the global power vector,  $w_{G,k}$ , calculated based on the average of all the linked modules, and  $j$  denotes the number of iterations [44]. The optimization convergence is defined by the following, where  $\mu_1$  and  $\mu_2$  are the limiting values:

$$\|\lambda_{m,k}^{j+1} - \lambda_{m,k}^j\|_2^2 \leq \mu_1, \rho \|P_{m,k}^{j+1} - P_{m,k}^j\|_2^2 \leq \mu_2. \quad (13)$$

Fig. 5 presents the flowchart of the C-ADMM algorithm in four steps. Fig. 6 depicts the flow of information in C-ADMM, where the virtual powers are sent to the neighboring modules. Then, the global powers are calculated and returned in parallel.

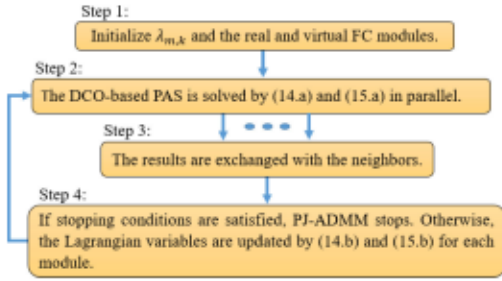


Fig. 7. Update process of the PJ-ADMM-based PAS.

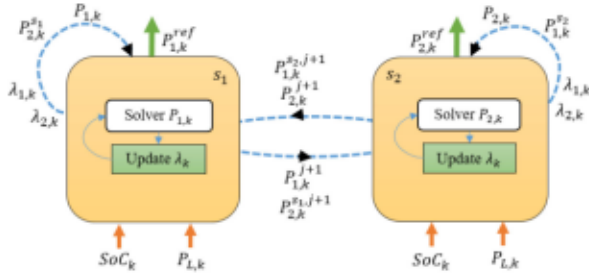


Fig. 8. Parallel communications of the decentralized PJ-ADMM PAS.

## B. PJ-ADMM-Based PAS

To improve the convergence of ADMM, PJ-ADMM is proposed in [45]. The formulation and parallel updating procedure are presented as follow.

The  $FC_1$  module equations

$$\begin{aligned}
 P_{1,k}^{j+1}, P_{2,k}^{s_1,j+1} &= \min(c_{1,k} (P_{1,k}, P_{2,k}^{s_1}) + c_{B,k} (P_{B,k})) \\
 &+ \frac{\rho}{2} \|P_{1,k} - P_{1,k}^{s_2,j} - \lambda_{1,k}^j\|_2^2 + \frac{1}{2} \|P_{1,k} - P_{1,k}^j\|_{P_{xt}}^2 \\
 &+ \frac{\rho}{2} \|P_{2,k}^{s_1} - P_{2,k}^j - \lambda_{2,k}^j\|_2^2 + \frac{1}{2} \|P_{2,k}^{s_1} - P_{2,k}^{s_1,j}\|_{P_{xt}}^2 \quad (14.a)
 \end{aligned}$$

$$\begin{aligned}
 \lambda_{2,k}^{j+1} &= \lambda_{2,k}^j - \gamma (P_{2,k}^{s_1,j+1} - P_{2,k}^{j+1}) \\
 \lambda_{1,k}^{j+1} &= \lambda_{1,k}^j - \gamma (P_{1,k}^{j+1} - P_{1,k}^{s_2,j+1}) \quad (14.b)
 \end{aligned}$$

The  $FC_2$  module equations

$$\begin{aligned}
 P_{1,k}^{s_2,j+1}, P_{2,k}^{j+1} &= \min(c_{2,k} (P_{1,k}^{s_2}, P_{2,k}) + c_{B,k} (P_{B,k})) \\
 &+ \frac{\rho}{2} \|P_{1,k}^{s_2} - P_{1,k}^j - \lambda_{1,k}^j\|_2^2 + \frac{1}{2} \|P_{1,k}^{s_2} - P_{1,k}^{s_2,j}\|_{P_{xt}}^2 \\
 &+ \frac{\rho}{2} \|P_{2,k} - P_{2,k}^{s_1,j} - \lambda_{2,k}^j\|_2^2 + \frac{1}{2} \|P_{2,k} - P_{2,k}^j\|_{P_{xt}}^2 \quad (15.a)
 \end{aligned}$$

$$\begin{aligned}
 \lambda_{1,k}^{j+1} &= \lambda_{1,k}^j - \gamma (P_{1,k}^{s_2,j+1} - P_{1,k}^{j+1}) \\
 \lambda_{2,k}^{j+1} &= \lambda_{2,k}^j - \gamma (P_{2,k}^{j+1} - P_{2,k}^{s_1,j+1}) \quad (15.b)
 \end{aligned}$$

where  $P_{xt}$  presents a positive and symmetric semidefinite matrix, and  $\gamma$  indicates a positive damping parameter. Figs. 7 and 8 illustrate the step-by-step update process and the inter-module communications of the DCO-based PAS.

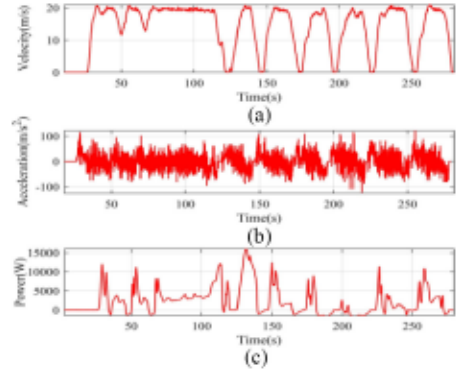


Fig. 9. Real driving profil . (a) Velocity. (b) Acceleration. (c) Power.

## V. SIMULATION RESULTS AND DISCUSSION

To unveil the capability of the DCO algorithms, first, a comprehensive analysis of the two proposed PASs is performed in MATLAB software. In this sense, the developed approaches are compared with DP as an offline optimization method and SQP as a centralized convex programming algorithm. Subsequently, due to the inherent sensitivity of the ADMM-based optimization approaches to parameter tuning, this critical point is investigated for PJ-ADMM and C-ADMM. Next, the most potential algorithm is selected to scrutinize the effect of price sensitivity and fault occurrence in the performance of the PAS. It is essential to mention that the computational time extensively depends on the utilized PC hardware (Processor = Corei5, 2.30 GHz, and RAM = 4.00 GB). Except for the parameter tuning analysis subsection, the same initial values are applied to all the considered cases to establish an unbiased comparison.

### A. Optimal Performance Analysis

A real driving cycle is utilized to inspect the performance of the developed DCO-based PASs, as shown in Fig. 9. Since the maximum power of the selected driving profile is higher than the developed test bench limitations, the power profile is scaled down by ten during the simulation and implementation steps.

The optimized power trajectories using C-ADMM and PJ-ADMM are shown in Fig. 10(a) and (b). As it can be seen, the modules collaborate and primarily operate at the efficient regions to fulfill the requested power and minimize the multiobjective cost functions. However, due to the slow response of the modules, the secondary source supplies the fast dynamic response and peaks. Fig. 10(c) compares the  $SoC$  variations obtained by C-ADMM and PJ-ADMM. The  $SoC$  of the battery pack oscillates between 69 and 72%, less than approximately 3% variation. Although the obtained  $SoC$  variations by C-ADMM and PJ-ADMM are similar, a slight deviation can be observed in the  $SoC$  levels from 50 to 150 s. It is due to more cumulative costs in the PJ-ADMM algorithm. After 150 s, the  $SoC$  fluctuations become almost equal because the responses of the DCO-based algorithms are similar. Another point is that the drawn power from the FC modules are increased after 250 s to keep the  $SoC$  fluctuations close enough to the initial values.



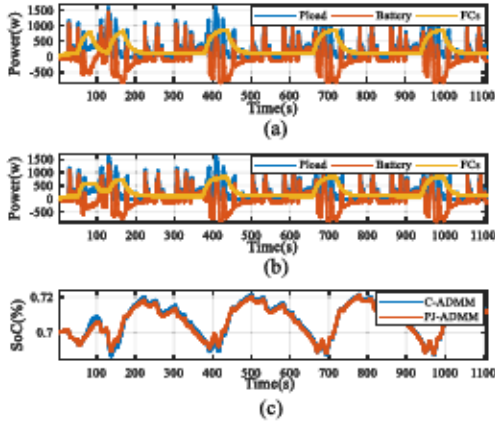


Fig. 10. Optimal PASs results ( $P_{load}$ : The requested power,  $FC_s$ : The power provided by the modules,  $Battery$ : The battery power). (a) Profile based on C-ADMM. (b) The profile based on PJ-ADMM. (c) The  $SoC$  evaluations.

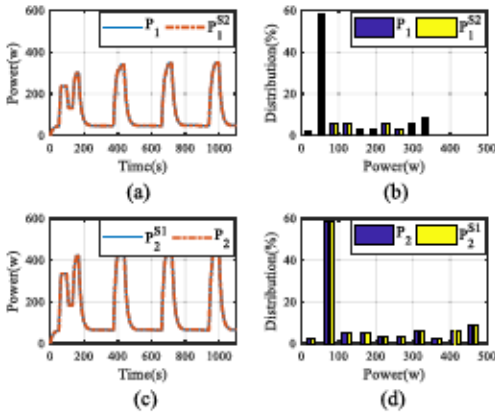


Fig. 11. Optimized power and power distributions of the modules using C-ADMM. (a) Power profile of  $FC_1$ . (b) The distribution of  $FC_1$ . (c) The power profile of  $FC_2$ . (d) The distribution of  $FC_2$ .

As an example, the time series and the distribution of the power in the real and virtual FCs are presented for C-ADMM case study in Fig. 11.  $P_1$  and  $P_1^{s2}$  are the real and the virtual power profile of  $FC_1$ , and  $P_2$  and  $P_2^{s1}$  are the real and the virtual power profile of  $FC_2$ , respectively. It is evident from this figure that the real power and virtual power of the modules are well-matched. Moreover, the request power from the FCs is almost located in high efficient regions. Since the convergence speed of the C-ADMM algorithm is faster than the modular powertrain dynamics, the virtual power of FCs gets very close to the real one. It can also be realized that since  $FC_2$  has a higher level of maximum output power and efficiency, it is more utilized than  $FC_1$ .

The computation time and the number of iterations according to  $FC_1$  are illustrated in Fig. 12. The detailed computing performance and final price of the developed PASs are presented in Table II, where T is the computation time per second, and is the number of iterations. As shown in Table II, the proposed DCO algorithms are marginally better than SQP and have shown a very close performance to DP in terms of the total cost. However, in terms of computational time, the decentralized structures of the

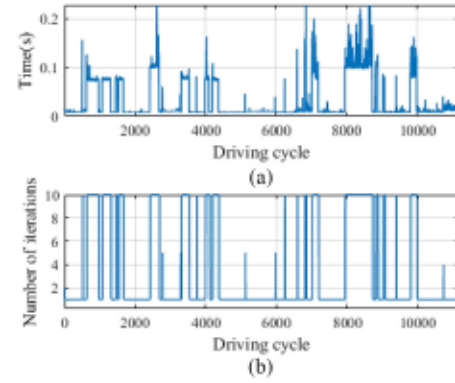


Fig. 12. (a) Computational time. (b) Number of iterations.

TABLE II  
DETAILED COMPUTING PERFORMANCE AND FINAL PRICE

	DP	SQP	C-ADMM		PJ-ADMM	
	$FC_1 + FC_2$	$FC_1 + FC_2$	$FC_1$	$FC_2$	$FC_1$	$FC_2$
T	4160.5	208.4	45.9	45.9	31.7	33.6
#	-	2463	968	972	932	963
$S_{H,m}$	0.0254	0.0298	0.0174	0.01	0.0173	0.0109
$S_{d,m}$	0.0091	0.0101	0.0062	0.0039	0.0062	0.0036
$S_B$	0.0055	0.0043	0.0051		0.0041	
$S_{SoC}$	0	0.0008	0.0006		0.0005	
$S_T$	0.040	0.045	0.0432		0.0426	

proposed PASs have made them much faster than SQP, where the computational burdens have been reduced by 78.4% and 84.1% concerning C-ADMM and PJ-ADMM, respectively. The computational time in PJ-ADMM is 5.7% lower than C-ADMM because of the proximal term [45]. SQP is the slowest optimization method with an operation time per iteration of 0.08 s. C-ADMM and PJ-ADMM are faster than SQP with 0.04 and 0.03 s, respectively. The associated total costs based on PJ-ADMM and C-ADMM are \$0.0426 and \$0.0432, which are 4.4118% and 5.8824% higher than DP, respectively. These minor differences are derived from the single-step optimization and the convex modeling approximations. The hydrogen consumptions are the highest cost, where  $FC_1$  and  $FC_2$  contribute \$0.0173 and \$0.0109 under PJ-ADMM and \$0.0174 and \$0.010 under C-ADMM, respectively. The second-largest expenses are related to the modules' degradations, which are approximately \$0.0096 and \$0.0098 by PJ-ADMM and C-ADMM, respectively. The degradation costs of the battery pack using PJ-ADMM and C-ADMM are about \$0.0048 and \$0.005, respectively, which constitute 11.3% and 11.6% of the final costs. The C-ADMM and PJ-ADMM cost terms equally decline because of the normalized cost functions. It should be pronounced that DCOs can assist the modules to prolong the FCSs lifetime and minimize the final costs. Fig. 13 provides the optimized cumulative cost changes by utilizing the PJ-ADMM algorithm.

## B. Parameter Tuning Analysis

In this section, the effects of the DCO-based PASs parameters on the total cost and the computational time are cautiously examined. A set of simulations are performed to seek appropriate

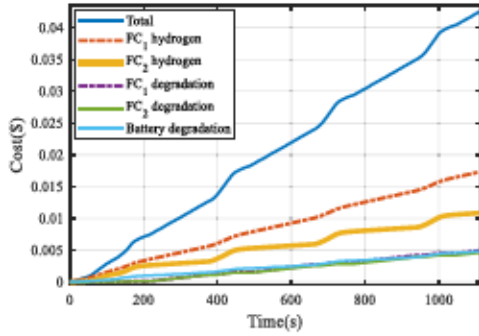


Fig. 13. Cost evaluation of the PJ-ADMM algorithm.

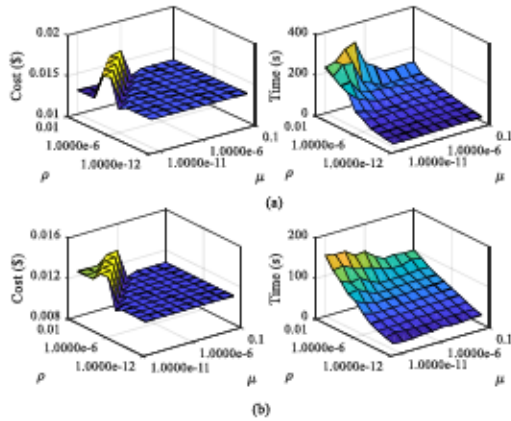


Fig. 14. Variation with  $\rho$  and  $\mu$  of the final cost and the processing time. (a) C-ADMM and (b) PJ-ADMM.

ranges for  $\rho$  and  $\mu$ . The obtained outcomes are presented in Fig. 14. Overall, the costs present upward trends with some fluctuations when  $\rho$  increases and  $\mu$  declines. Furthermore, the computational time experiences incremental trends in both cases, specifically when  $\mu$  passes  $1.0 \times 10^{-6}$ . Consequently, the selected  $\rho$  and  $\mu$  ranges require a balance between the final cost and the data processing efficiency.

### C. Price Sensitivity and Optimization Criteria Analysis

For the sake of exploring the influence of price changes and optimization goals over the behavior of the DCO-based PASs, a straightforward and effective investigation of PJ-ADMM is performed in this section. Fig. 15 illustrates the cost and optimization criteria evaluation. The current situation in 2020, shown by the red dashed line, is considered the baseline. The upcoming trend after five years in 2025 is considered a means of comparison with two different probable case studies. The first case study is related to a cheaper PEMFC stack price ( $-20\%$ ) trend, which is plotted by the blue dashed line because of applying several cost-effective strategies from FC stack manufacturers. The second case study assumes a surge in the hydrogen price ( $+20\%$ ), depicted by the yellow-solid line, due to the growth of the FCV production numbers and the penetration of the hydrogen-powered system life. The criteria of the DCO-based algorithms are defined through  $\eta$ , where  $\eta = 0$  shows

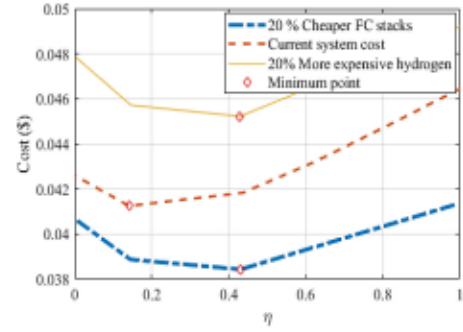


Fig. 15. Final cost evaluation according to different price and optimization objective scenarios.

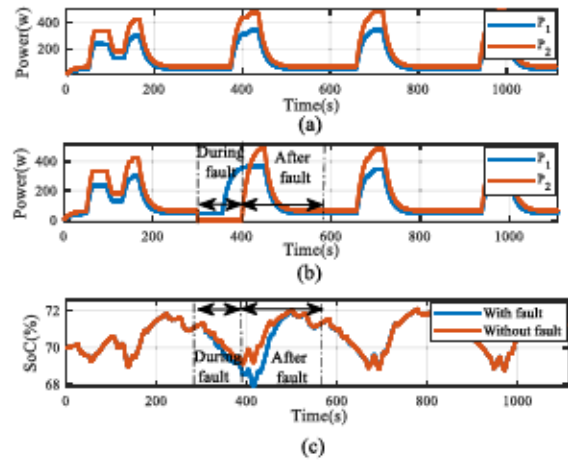


Fig. 16. Comparison between standard and fault operations of the Dec-PAS based on PJ-ADMM. (a) Power profile evolutions in case of regular operation. (b) The power profile trajectories in case of dynamic electrical fault operation. (c) The *SoC* levels of the battery pack.

the optimization is only hydrogen-consumption-oriented, and  $\eta = 1$  means the optimization is only health-aware-oriented. It is pronounced that compared to the baseline price, a  $20\%$  decrease in the FC stack price reduces the minimal value to around  $7.32\%$ . Moreover, a  $20\%$  increase in the hydrogen price augments the optimal value to around  $9.76\%$ . The optimal  $\eta = 0.18$  is increased in both of the case studies. In future, adaptive and comprehensive DCO PASs can be established while considering short-term and long-term price trajectories.

### D. Fault-Resilient Analysis

To evaluate the robustness and modularity (plug & play), a comparison between regular and faulty operation of PJ-ADMM is performed in this subsection. This article takes only electrical fault conditions into account, which will affect the system's total output power. For this purpose, a dynamic electrical fault is imposed to  $FC_2$  for  $100$  s. Fig. 16 depicts the power trajectories and the *SoC* fluctuations of the well-behaved and misbehaved modules during and after the electrical fault. Throughout the fault occurrence, the functional module and battery unit collaborate to converge to the optimal power. After passing the electrical



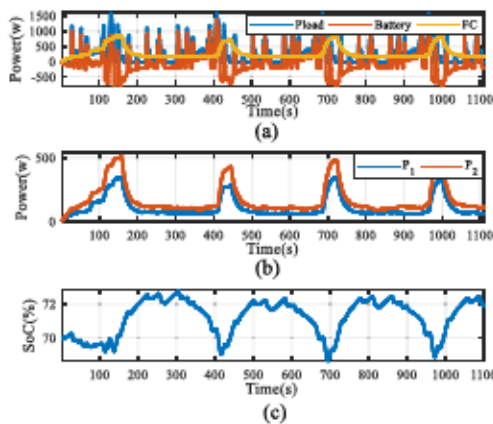


Fig. 17. Implementation results of the developed PAS based on PJ-ADMM. (a) Power profile. (b) The modules' power profile. (c) The *SoC* level fluctuation.

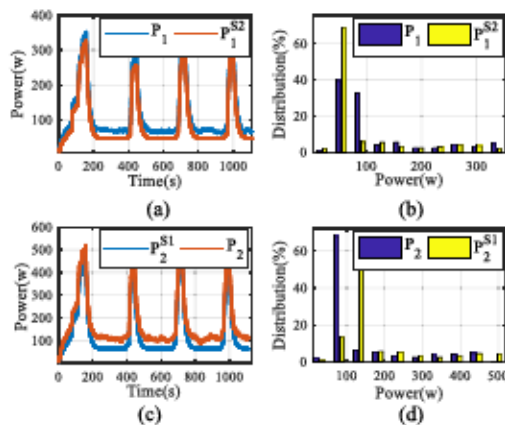


Fig. 18. Experimental results of the PJ-ADMM approach. (a) Power profile of  $FC_1$ . (b) The distribution of  $FC_1$ . (c) The power profile of  $FC_2$ . (d) The distribution of  $FC_2$ .

fault condition, due to the parallel structure of PJ-ADMM, this algorithm can conveniently follow the requested power profile. Therefore, if one of the modules stops regular operation for a specific duration and gets back to regular operation again, the Dec-PAS can keep working without making any problems for the powertrain system. It is an intriguing clue that applying these decentralized approaches at module-level fault operation needs further investigations.

## VI. EXPERIMENTAL IMPLEMENTATION

An experimental test based on FPGA implementation is conducted under the real driving profile to verify the simulation results. In this regard, PJ-ADMM is singled out due to its superior performance compared to C-ADMM. Generally, the computational time and performance in the simulation step running on general-purpose hardware (PC) differ from a real-time field test for several reasons, such as processing capacity, memory, communication delay, and uncertainty in the powertrain components. The power trajectories and *SoC* oscillation are demonstrated in Fig. 17. Moreover, the power distributions are shown in Fig. 18.

The final cost of the PJ-ADMM-based PAS shows an extra cost of 6.62% compared to that of the offline one. The hydrogen consumption cost approximately forms 41.15% of the final cost. The degradation of FC modules is the second-highest cost, with about 27.84% of the final cost. The modular system operates in the low-power and high-efficiency region to mitigate the degradation expense and reduce hydrogen consumption. The suggested PAS works well to ensure the constraints of the powertrain components prolong their lifespans. The computational complexity of PJ-ADMM is about 63.25% lower than SQP. In this regard, it is a practical and suitable optimization algorithm for low-cost systems with limited onboard computational power. These results highlight the potential of the decentralized implementation schemes in real-time applications.

## VII. CONCLUSION

This article presents a comprehensive analysis of two Dec-PASs based on distributed convex optimization in an MFCV application. The two decomposition-based algorithms (C-ADMM and PJ-ADMM) are selected due to their parallel updating optimization procedures and their global convergences. In this regard, a general PAS optimization problem with a convex approximation is formulated for a modular powertrain system, including hydrogen consumption and lifetime of the FC modules as well as the lifetime of the battery unit. After that, the decentralized optimization frameworks for solving the power-splitting problem are presented. To evaluate the performance of the proposed Dec-PASs under real driving profile, an in-depth comparative analysis of costs and computational times are presented compared to DP and SQP.

Additionally, due to the importance of parameter tuning in the ADMM-based optimization algorithms, this feature in C-ADMM and PJ-ADMM is investigated. Since the PJ-ADMM algorithm has reached a better general performance than C-ADMM under the discussed scenarios, it is also used for two further sensitivity analyses in terms of dynamic fault and price fluctuation case studies. Finally, the experimental results unveil that the implemented PJ-ADMM decentralized scheme achieves excellent performance compared to SQP. Considering the outcomes of this manuscript, the following directions are put forward for future endeavors.

- 1) The inclusion of future trip information in the DCO-based PAS framework. This idea requires developing a predictive-based control strategy and introducing a trip model with a high level of reliability and accuracy.
- 2) The integration of thermal models of FCSs and battery into the Dec-PAS and scrutinizing it from the perspective of different initial temperatures and health conditions.
- 3) Combining DCO-based PASs with fault detection algorithms to develop robust strategies for MFCV powertrains.

## REFERENCES

- [1] Z. P. Cano *et al.*, "Batteries and fuel cells for emerging electric vehicle markets," *Nature Energy*, vol. 3, no. 4, pp. 279–289, Apr. 2018.



- [2] H. S. Das, C. W. Tan, and A. H. M. Yatim, "Fuel cell hybrid electric vehicles: A review on power conditioning units and topologies," *Renewable Sustain. Energy Rev.*, vol. 76, no. C, pp. 268–291, Nov. 2017.
- [3] T. Hua *et al.*, "Status of hydrogen fuel cell electric buses worldwide," *J. Power Sources*, vol. 269, pp. 975–993, Dec. 2014.
- [4] U. Eberle, B. Müller, and R. Helmolt, "Fuel cell electric vehicles and hydrogen infrastructure: Status 2012," *Energy Environ. Sci.*, vol. 5, no. 10, pp. 8790–8798, Jul. 2012.
- [5] X. Hu, C. Zou, C. Zhang, and Y. Li, "Technological developments in batteries: A survey of principal roles, types, and management needs," *IEEE Power Energy Mag.*, vol. 15, no. 5, pp. 20–31, Sep/Oct. 2017.
- [6] N. Sulaiman, M. A. Hannan, A. Mohamed, E. H. Majlan, and W. R. Wan Daud, "A review on energy management system for fuel cell hybrid electric vehicle: Issues and challenges," *Renewable Sustain. Energy Rev.*, vol. 52, no. C, pp. 802–814, Dec. 2015.
- [7] H. Ramírez-Murillo, C. Restrepo, J. Calvente, A. Romero, and R. Giral, "Energy management of a fuel-cell serial-parallel hybrid system," *IEEE Trans. Ind. Electron.*, vol. 62, no. 8, pp. 5227–5235, Aug. 2015.
- [8] M. G. Carignano, V. Roda, R. Costa-Castelló, L. Valino, A. Lozano, and F. Barreras, "Assessment of energy management in a fuel cell/battery hybrid vehicle," *IEEE Access*, vol. 7, pp. 16110–16122, Jan. 2019.
- [9] C. Wu, J. Chen, C. Xu, and Z. Liu, "Real-Time adaptive control of a fuel cell/battery hybrid power system with guaranteed stability," *IEEE Trans. Control Syst. Technol.*, vol. 25, no. 4, pp. 1394–1405, Jul. 2017.
- [10] S. Ziacnejad, Y. Sangsefidi, and A. Mehrizi-Sani, "Fuel cell-based auxiliary power unit: EMS, sizing, and current estimator-based controller," *IEEE Trans. Veh. Technol.*, vol. 65, no. 6, pp. 4826–4835, Jun. 2016.
- [11] X. Meng, Q. Li, G. Zhang, T. Wang, W. Chen, and T. Cao, "A dual-mode energy management strategy considering fuel cell degradation for energy consumption and fuel cell efficiency comprehensive optimization of hybrid vehicle," *IEEE Access*, vol. 7, pp. 134475–134487, 2019.
- [12] R. Wai, S. Jung, J. Liaw, and Y. Chang, "Intelligent optimal energy management system for hybrid power sources including fuel cell and battery," *IEEE Trans. Power Electron.*, vol. 28, no. 7, pp. 3231–3244, Jul. 2013.
- [13] M. Kandidayeni, A. O. M. Fernandez, A. Khalatbarisoltani, L. Boulon, S. Kelouwani, and H. Chaoui, "An online energy management strategy for a fuel cell/battery vehicle considering the driving pattern and performance drift impacts," *IEEE Trans. Veh. Technol.*, vol. 68, no. 12, pp. 11427–11438, Dec. 2019.
- [14] M. Kandidayeni, A. M. Fernandez, L. Boulon, and S. Kelouwani, "Efficiency upgrade of hybrid fuel cell vehicles' energy management strategies by online systemic management of fuel cell," *IEEE Trans. Ind. Electron.*, vol. 68, no. 6, pp. 4941–4953, Jun. 2021.
- [15] H. Chen, J. Chen, Z. Liu, and H. Lu, "Real-time optimal energy management for a fuel cell/battery hybrid system," *Asian J. Control*, vol. 21, no. 4, pp. 1847–1856, Mar. 2019.
- [16] Y. Yan, Q. Li, W. Chen, B. Su, J. Liu, and L. Ma, "Optimal energy management and control in multimode equivalent energy consumption of fuel cell/supercapacitor of hybrid electric tram," *IEEE Trans. Ind. Electron.*, vol. 66, no. 8, pp. 6065–6076, Aug. 2019.
- [17] X. Han, H. He, J. Wu, J. Peng, and Y. Li, "Energy management based on reinforcement learning with double deep Q-learning for a hybrid electric tracked vehicle," *Appl. Energy*, vol. 254, 2019, Art. no. 113708.
- [18] E. Tazelaar, B. Veenhuizen, P. vandenBosch, and M. Grimminck, "Analytical solution of the energy management for fuel cell hybrid propulsion systems," *IEEE Trans. Veh. Technol.*, vol. 61, no. 5, pp. 1986–1998, Jun. 2012.
- [19] X. Hu, N. Murgovski, L. M. Johannesson, and B. Egardt, "Optimal dimensioning and power management of a fuel cell/battery hybrid bus via convex programming," *IEEE/ASME Trans. Mechatronics*, vol. 20, no. 1, pp. 457–468, Feb. 2014.
- [20] D. Zhou, A. Al-Durra, F. Gao, A. Ravey, I. Matraji, and M. G. Simões, "Online energy management strategy of fuel cell hybrid electric vehicles based on data fusion approach," *J. Power Sources*, vol. 366, pp. 278–291, Oct. 2017.
- [21] X. Hu, C. Zou, X. Tang, T. Liu, and L. Hu, "Cost-optimal energy management of hybrid electric vehicles using fuel cell/battery health-aware predictive control," *IEEE Trans. Power Electron.*, vol. 35, no. 1, pp. 382–392, Jan. 2020.
- [22] B. Geng, J. K. Mills, and D. Sun, "Two-Stage energy management control of fuel cell plug-in hybrid electric vehicles considering fuel cell longevity," *IEEE Trans. Veh. Technol.*, vol. 61, no. 2, pp. 498–508, Feb. 2012.
- [23] H. Chen, J. Chen, H. Lu, C. Yan, and Z. Liu, "A modified MPC-based optimal strategy of power management for fuel cell hybrid vehicles," *IEEE/ASME Trans. Mechatronics*, vol. 25, no. 4, pp. 2009–2018, Aug. 2020.
- [24] J. Chen, C. Xu, C. Wu, and W. Xu, "Adaptive fuzzy logic control of fuel-cell-battery hybrid systems for electric vehicles," *IEEE Trans. Ind. Inform.*, vol. 14, no. 1, pp. 292–300, Jan. 2018.
- [25] A. K. Soltani, M. Kandidayeni, L. Boulon, and D. L. St-Pierre, "Modular energy systems in vehicular applications," *Energy Procedia*, vol. 162, pp. 14–23, Apr. 2019.
- [26] N. Marx, L. Boulon, F. Gustin, D. Hissel, and K. Agbossou, "A review of multi-stack and modular fuel cell systems: Interests, application areas and on-going research activities," *Int. J. Hydrogen Energy*, vol. 39, no. 23, pp. 12101–12111, 2014.
- [27] J. E. Garcia, D. F. Herrera, L. Boulon, P. Sicard, and A. Hernandez, "Power sharing for efficiency optimisation into a multi fuel cell system," in *Proc. IEEE 23rd Int. Symp. Ind. Electron.*, 2014, pp. 218–223.
- [28] N. Marx, D. Hissel, F. Gustin, L. Boulon, and K. Agbossou, "On the sizing and energy management of an hybrid multistack fuel cell – battery system for automotive applications," *Int. J. Hydrogen Energy*, vol. 42, no. 2, pp. 1518–1526, Jan. 2017.
- [29] B. Somaiah and V. Agarwal, "Distributed maximum power extraction from fuel cell stack arrays using dedicated power converters in series and parallel configuration," *IEEE Trans. Energy Convers.*, vol. 31, no. 4, pp. 1442–1451, Dec. 2016.
- [30] H. Zhang, X. Li, X. Liu, and J. Yan, "Enhancing fuel cell durability for fuel cell plug-in hybrid electric vehicles through strategic power management," *Appl. Energy*, vol. 241, no. 6, pp. 483–490, May 2019.
- [31] A. O. M. Fernandez, M. Kandidayeni, L. Boulon, and H. Chaoui, "An adaptive state machine based energy management strategy for a multi-stack fuel cell hybrid electric vehicle," *IEEE Trans. Veh. Technol.*, vol. 69, no. 1, pp. 220–234, Jan. 2020.
- [32] T. Wang *et al.*, "Adaptive current distribution method for parallel-connected PEMFC generation system considering performance consistency," *Energy Convers. Manage.*, vol. 196, no. 27, pp. 866–877, Sep. 2019.
- [33] H. Yin, C. Zhao, and C. Ma, "Decentralized real-time energy management for a reconfigurable multiple-source energy system," *IEEE Trans. Ind. Inform.*, vol. 14, no. 9, pp. 4128–4137, Sep. 2018.
- [34] H. Yin, C. Zhao, M. Li, C. Ma, and M.-Y. Chow, "A game theory approach to energy management of an engine-generator/battery/supercapacitor hybrid energy system," *IEEE Trans. Ind. Electron.*, vol. 63, no. 7, pp. 4266–4277, Jul. 2016.
- [35] Q. Li, T. Wang, C. Dai, W. Chen, and L. Ma, "Power management strategy based on adaptive droop control for a fuel cell-battery-supercapacitor hybrid tramway," *IEEE Trans. Veh. Technol.*, vol. 67, no. 7, pp. 5658–5670, Jul. 2018.
- [36] D. K. Molzahn *et al.*, "A survey of distributed optimization and control algorithms for electric power systems," *IEEE Trans. Smart Grid*, vol. 8, no. 6, pp. 2941–2962, Nov. 2017.
- [37] A. Kargarian *et al.*, "Toward distributed/decentralized DC optimal power flow implementation in future electric power systems," *IEEE Trans. Smart Grid*, vol. 9, no. 4, pp. 2574–2594, Jul. 2018.
- [38] D. P. Bertsekas and A. Scientific, *Convex Optimization Algorithms*, Belmont, MA, USA: Athena Scientific, 2015.
- [39] A. J. Conejo and J. A. Aguado, "Multi-area coordinated decentralized DC optimal power flow," *IEEE Trans. Power Syst.*, vol. 13, no. 4, pp. 1272–1278, Nov. 1998.
- [40] G. Cohen, "Auxiliary problem principle and decomposition of optimization problems," *J. Optim. Theory Appl.*, vol. 32, no. 3, pp. 277–305, Nov. 1980.
- [41] Z. Zhang and M.-Y. Chow, "Convergence analysis of the incremental cost consensus algorithm under different communication network topologies in a smart grid," *IEEE Trans. Power Syst.*, vol. 27, no. 4, pp. 1761–1768, Nov. 2012.
- [42] F. J. Nogales, F. J. Prieto, and A. J. Conejo, "A decomposition methodology applied to the multi-area optimal power flow problem," *Ann. Oper. Res.*, vol. 120, no. 1, pp. 99–116, Apr. 2003.
- [43] D. Gabay and B. Mercier, "A dual algorithm for the solution of nonlinear variational problems via finite element approximation," *Comput. Math. Appl.*, vol. 2, no. 1, pp. 17–40, 1976.
- [44] S. Boyd, N. Parikh, E. Chu, B. Peleato, and J. Eckstein, "Distributed optimization and statistical learning via the alternating direction method of multipliers," *Found. Trends Mach. Learn.*, vol. 3, no. 1, pp. 1–122, 2011.



- [45] W. Deng, M.-J. Lai, Z. Peng, and W. Yin, "Parallel multi-block ADMM with  $o(1/k)$  convergence," *J. Sci. Comput.*, vol. 71, no. 2, pp. 712–736, 2017.
- [46] L. Liu and Z. Han, "Multi-block ADMM for big data optimization in smart grid," in *Proc. Int. Conf. Comput., Netw. Commun.*, 2015, pp. 556–561.
- [47] S. East and M. Cannon, "Fast optimal energy management with engine on/off decisions for plug-in hybrid electric vehicles," *IEEE Control Syst. Lett.*, vol. no. 3, no. 4, pp. 1074–1079, Oct. 2019.
- [48] S. East and M. Cannon, "Energy management in plug-in hybrid electric vehicles: Convex optimization algorithms for model predictive control," *IEEE Trans. Control Syst. Technol.*, vol. 28, no. 6, pp. 2191–2203, Nov. 2020.
- [49] A. Khalatbarisoltani, M. Kandidayeni, L. Boulon, and X. Hu, "Power allocation strategy based on decentralized convex optimization in modular fuel cell systems for vehicular applications," *IEEE Trans. Veh. Technol.*, vol. 69, no. 12, pp. 14563–14574, Dec. 2020.
- [50] F. Martel, S. Kelouwani, Y. Dubé, and K. Agbossou, "Optimal economy-based battery degradation management dynamics for fuel-cell plug-in hybrid electric vehicles," *J. Power Sources*, vol. 274, no. C, pp. 367–381, Jan. 2015.
- [51] H. Chen, P. Pei, and M. Song, "Lifetime prediction and the economic lifetime of proton exchange membrane fuel cells," *Appl. Energy*, vol. 142, pp. 154–163, Mar. 2015.
- [52] N. Herr *et al.*, "Decision process to manage useful life of multi-stacks fuel cell systems under service constraint," *Renewable Energy*, vol. 105, no. C, pp. 590–600, May 2017.
- [53] S. Satyapal, "U.S. department of energy hydrogen and fuel cell technology overview," Presented at The 14th International Hydrogen and Fuel Cell Expo (FC EXPO 2018), 2018.
- [54] K. Mongird *et al.*, *Energy Storage Technology and Cost Characterization Report*, Richland, WA, USA: Pacific Northwest National Lab, 2019.
- [55] T. Benjamin, R. Borup, N. Garland, C. Gittleman, B. Habibzadeh, and S. Hirano, "Fuel cell technical team roadmap," Energy.gov (Office of Energy Efficiency & Renewable Energy), 2017.



**Arash Khalatbarisoltani** (Member, IEEE) received the master's degree in mechatronics from Arak University, Arak, Iran, in 2016. He is currently working toward the Ph.D. degree with the Hydrogen Research Institute (IRH) and the Department of Electrical and Computer Engineering, Université du Québec à Trois-Rivières (UQTR), Trois-Rivières, QC, Canada.

His research interests include optimal control, decentralized systems, fuel cell systems, energy management, renewable energy, and intelligent transport systems.



**Mohsen Kandidayeni** (Member, IEEE) was born in Tehran, Iran, in 1989. He received the B.S. degree in mechanical engineering in 2011 and the master's degree in mechatronics from Arak University, Arak, Iran, in 2014, the Ph.D. degree in electrical engineering from the University of Quebec, Trois-Rivières (UQTR), QC, Canada, in 2020.

He joined the Hydrogen Research Institute, UQTR in 2016. He is currently a Postdoctoral Researcher with Electric-Transport, Energy

Storage, and Conversion Lab (e-TESC), Université de Sherbrooke, Sherbrooke, QC, Canada, and a Research Assistant Member with the Hydrogen Research Institute, UQTR. He has been actively involved in conducting research through authoring, coauthoring, and reviewing several papers in different prestigious scientific journals and also participating in various international conferences. His research interests include energy-related topics, such as hybrid electric vehicles, fuel cell systems, energy management, multiphysics systems, modeling, and control.

Dr. Kandidayeni was the recipient of several awards/honors during his educational path, such as a doctoral scholarship from the Fonds de recherche du Québec–Nature et technologies (FRQNT), a postdoctoral scholarship from FRQNT, an excellence student grant from UQTR, and the third prize in Energy Research Challenge from the Quebec Ministry of Energy and Natural Resources.



**Loïc Boulon** (Senior Member, IEEE) received the master's degree in electrical and automatic control engineering from the University of Lille, Lille, France, in 2006, the Ph.D. degree in electrical engineering from the University of Franche-Comté, Besançon, France.

Since 2010, he has been a Professor with University of Quebec, Trois-Rivières (UQTR), QC, Canada (Full Professor since 2016) and works with the Hydrogen Research Institute (Deputy Director since 2019). His work deals

with modeling, control, and energy management of multiphysics systems. He has published more than 120 scientific papers in peer-reviewed international journals and international conferences and has given over 35 invited conferences all over the world. His research interests include hybrid electric vehicles, energy and power sources (fuel cell systems, batteries, and ultracapacitors).

In 2015, Prof. Boulon was the General Chair of the IEEE-Vehicular Power and Propulsion Conference in Montréal (QC, Canada). He is now VP-Motor Vehicles of the IEEE Vehicular Technology Society, and he found the "International Summer School on Energetic Efficiency of Connected Vehicles" and the "IEEE VTS Motor Vehicle Challenge". He is the holder of the Canada Research Chair in Energy Sources for the Vehicles of the future. Since 2019, he is the world's most-cited author of the topic "Proton exchange membrane fuel cells (PEMFC); Fuel cells; Cell stack" in Elsevier SciVal.



**Xiaosong Hu** (Senior Member, IEEE) received the Ph.D. degree in automotive engineering from the Beijing Institute of Technology, Beijing, China, in 2012.

He did scientific research and completed the Ph.D. dissertation in Automotive Research Center at the University of Michigan, Ann Arbor, MI, USA, between 2010 and 2012. He is currently a Professor with the Department of Mechanical and Vehicle Engineering, Chongqing University, Chongqing, China. He was a Postdoctoral Researcher with the Department of Civil and Environmental Engineering, University of California, Berkeley, CA, USA, between 2014 and 2015,

as well as at the Swedish Hybrid Vehicle Center and the Department of Signals and Systems at Chalmers University of Technology, Gothenburg, Sweden, between 2012 and 2014. He was also a Visiting Postdoctoral Researcher with the Institute for Dynamic Systems and Control at Swiss Federal Institute of Technology (ETH), Zurich, Switzerland, in 2014. His research interests include modeling and control of alternative powertrains and energy storage systems.

Dr. Hu has been the recipient of numerous prestigious awards/honors, including Web of Science Highly-Cited Researcher by Clarivate Analytics, SAE Environmental Excellence in Transportation Award, IEEE ITSS Young Researcher Award, SAE Ralph Teator Educational Award, Emerging Sustainability Leaders Award, EU Marie Curie Fellowship, ASME DSCD Energy Systems Best Paper Award, and Beijing Best Ph.D. Dissertation Award. He is an IET Fellow.

# **Chapitre 4 - Look-Ahead Decentralized Safe-Learning Control for a Modular Powertrain Using Convex Optimization and Federated Reinforcement Learning**

## **4.1 Introduction**

This thesis explores different strengths and weaknesses related to the modular system, and a future-oriented concept is put forward using the distributed convex optimization approaches. After introducing the central idea of the decentralized optimization method in Chapter 2 and studying different algorithms to evaluate the advantages of the suggested methodology in Chapter 3, now this is the best moment to enhance the optimization algorithms' performance. All the work is based on one-step point optimization and does not include future information. This chapter will attempt to present the following point of view to combining the predictive model idea with the proposed fully decentralized strategy during the previous chapters. Nevertheless, two crucial sides to this combination need to be studied. Firstly, having a moving horizon will augment the computational time and will increase the number of iterations. Secondly, selecting the best hyperparameter value is highly related to the application and the general pattern of the disturbance to the under-control system. For these two reasons, a decentralized learning method is added to simultaneously adopt the optimal horizon length based on the current state of the powertrain system.

## **4.2 Methodology**

The fully decentralized lookahead allocation methodology to accomplish the third study is presented through the following stages.

- First, a multi-objective convex cost function for the power allocation problem is formulated by considering the hydrogen economy and powertrain lifespan factors.

Second, a decentralized predictive-based optimization algorithm is developed by utilizing a Lagrangian decomposition method to minimize the convex cost function simultaneously. In the proposed Dec-MPC, the main problem is decentralized into  $m \in \mathbf{M}$  subproblems, and each one is allocated to a FC module control unit, as shown in Figure 4-1. During the optimization process, an exchange of candidate output powers occurs through the module-to-module communication layer. This iterative process continues until an agreement is attained among the local control units, according to the determined stopping criterion. Then, the optimization process will be repeated and shifted to the next point.

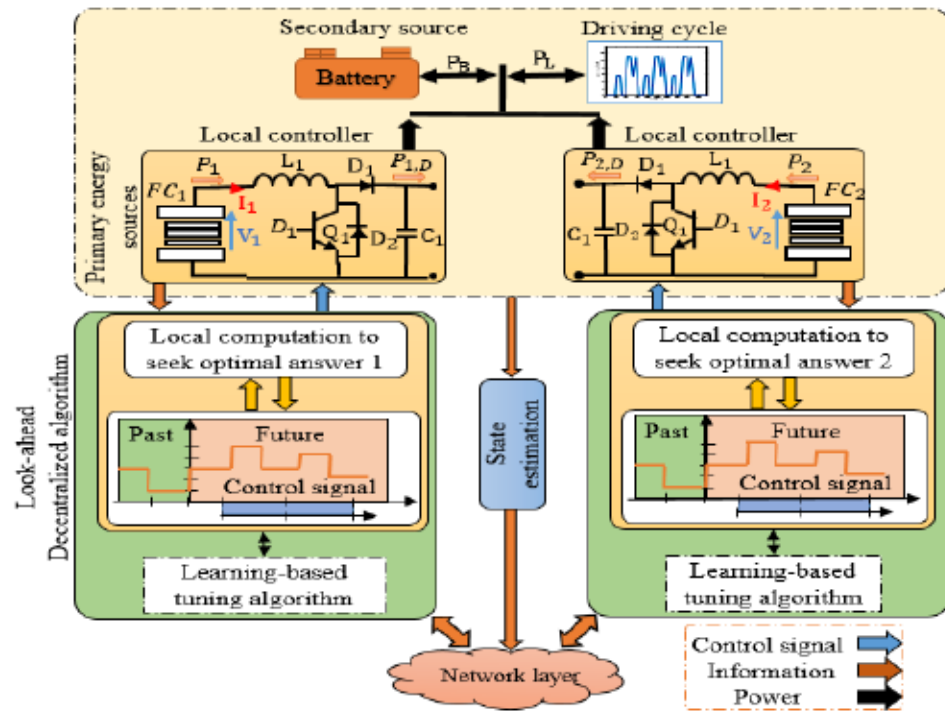


Figure 4-1 The adaptive look-ahead Dec-MPC framework and the modular powertrain system sequence operation.



The detailed procedure of Dec-MPC is presented in Figure 4-2. First, a cold-start initialization of  $\lambda_{m,\{i+1,\dots,i+k\}}$ ,  $P_{m,\{i+1,\dots,i+k\}}$ , and  $W_{m,\{i+1,\dots,i+k\}}$  is required for each module  $m$  ( $\forall m \in M$ ). The local PAS problems are solved to determine  $P_{m,\{i+1,\dots,i+k\}}$ . Then,  $W_{m,\{i+1,\dots,i+k\}}$  are calculated and sent to the neighbor module in parallel. After that,  $\lambda_{m,\{i+1,\dots,i+k\}}$  updates. If  $\|\lambda_m^{n+1} - \lambda_m^n\|_2^2 \leq \mu_1$  and  $\rho\|P_m^{n+1}[k] - P_m^n[k]\|_2^2 \leq \mu_2$ , where  $\mu_1$  and  $\mu_2$  are the limiting values, as the stopping criteria are fulfilled, the optimization processes stop and  $P_{m,i+1}$  is sent to the converters as  $P_m^{ref}$ . After that, the optimization windows shift for one time step. If not, the optimization process goes back to Step 3.

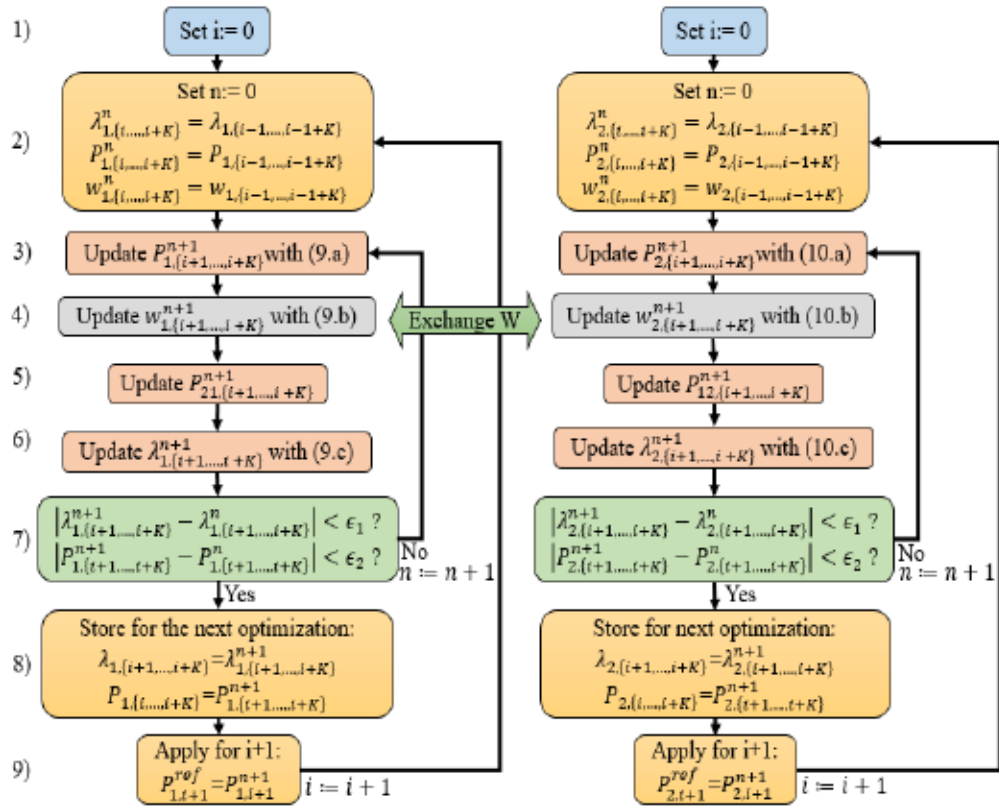


Figure 4-2 The systematic flowchart of the Dec-MPC algorithm.



- Third, a multi-agent safe learning technique is integrated to monitor the decentralized MPC performance and seek the best operational performance. This safe learning-based algorithm optimizes the hyperparameters of the control units based on the corresponding computational burden, final cost, and SoC level penalty. Safe Reinforcement Learning may be defined as establishing rules that maximize the likelihood of achieving a good return on investment on challenges. It is vital to maintain a high level of system performance and/or to adhere to safety restrictions during the learning and/or deployment stages [58]. A decentralized learning algorithm is built based on this notion of safe reinforcement learning by incorporating the decentralized MPC layer to get optimal outcomes. This topology aids the learning technique in converging on the FCS module's ideal outcomes. By considering the characteristics of the powertrain components, this safe learning technique ensures optimal outcomes. In this regard, state information from the environment that comprises the instance SoC level and average future power profile are exploited with different actions to reach the optimal answers. The decentralized strategy's learning mechanism is based on three standard driving cycles. There is only one real driving profile for the electric car under study. Furthermore, just three available standard driving profiles are well-suited to the selected light-duty electric vehicle. Indeed, to obtain a trustworthy outcome, it is critical to train the learning process using a database of real-world driving patterns. The result reported in this chapter is the first proof of the central concept. Integrating the new driving profiles is the first step to making the suggested method even better. The process of decentralized learning based on federated reinforcement learning (FRL) is indicated in Figure 4-3. To explain the FRL algorithm, an environment with  $\{FC_m\}_{m=1}^M$  modules is considered, where each module

has the training points  $\mathcal{O}_m = \left\{ \left( P_{avg_1}, SoC_1, r_1 \right), \dots, \left( P_{avg_l}, SoC_l, r_l \right) \right\}$  with  $l$  tagged samples and the weight parameter list  $\mathbf{W}^m$ . All modules  $\{FC_m\}_{m=1}^M$  are linked directly in a module-to-module style. Firstly, a cold-start initialization is applied to all modules  $\{FC_m\}_{m=1}^M$ , then it starts with training data  $\mathcal{O}_m$  in parallel for a small number of iterations (step 1). After that, each one pools its partially trained weight parameters  $\mathbf{W}^m$  to others (step 2) and merges all the received models by the weighted averaging technique, i.e.,  $\mathbf{W}^A = \sum_m \frac{1}{m} \mathbf{W}^m$  (step 3). In the end, the aggregated model  $\mathbf{W}^A$  is used by the modules to select the optimal prediction horizon length. Several rounds are executed until all FC modules' models converge (step 4). After completing the decentralized learning process, each FC module has its local model  $\mathbf{W}^i$  and the aggregated fine-tuned model  $\mathbf{W}^A$ . Whenever a new FC module is connected to the environment  $\{FC_m\}_{m=1}^M$ , the aggregated model  $\mathbf{W}^A$  will be shared to join the process (step 5) quickly.

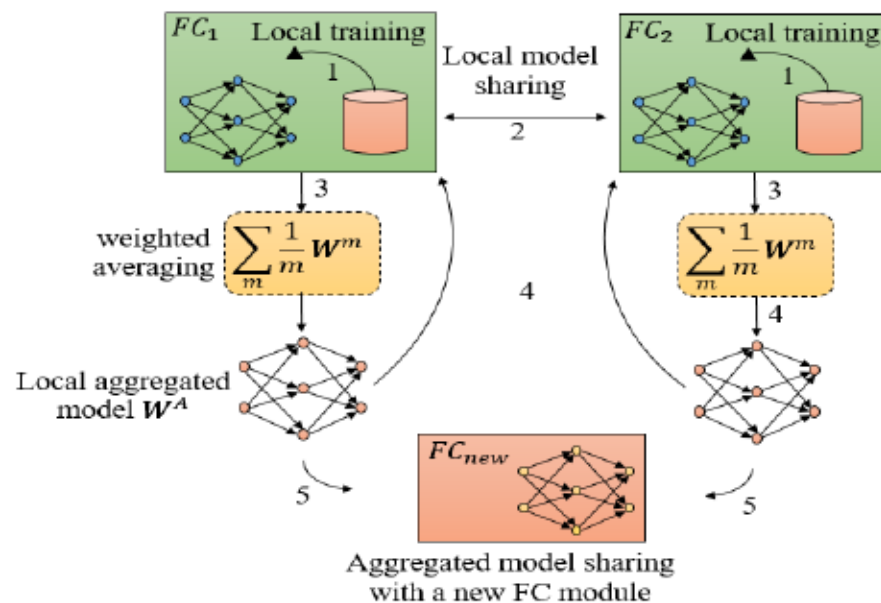


Figure 4-3 Visual representation of the module-to-module FRL algorithm and the learning steps.

- Fourth, the adaptive decentralized optimization algorithm has been implemented using a laboratory-scale test bench system to evaluate real implementation.

### 4.3 Synopsis of the analyses of the results

The optimized output answers of the powertrain components via Cen-MPC, fixed horizon, and safe-learning Dec-MPCs are illustrated in Figure 4-4. The prediction horizon length,  $K$ , is selected to be equal to 10 time-step for the Cen-MPC and the fixed-horizon Dec-MPC schemes. The maximum moving look-ahead horizon  $K$  of the learning-enabled Dec-MPC is also chosen to be equal to 10-time steps. It is evident from Figure 4-4 that the powers profiles and the SoC curves of the proposed decentralized approaches perfectly follow Cen-MPC with minor errors. For instance, the SoC curves of the fixed horizon and adjustable horizon Dec-MPCs accurately track Cen-MPC with under 0.0571 % and 0.0597 % errors.

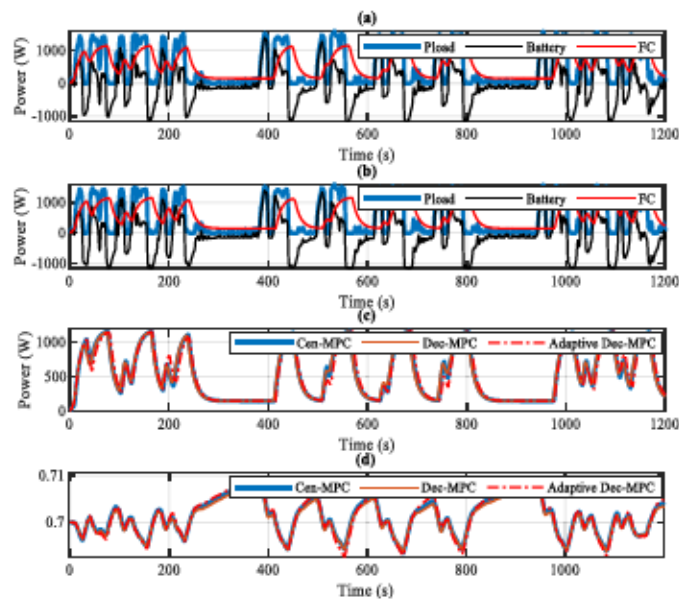


Figure 4-4 Optimized results of the MPC-based approaches: (a) the powers based on Dec-MPC, (b) the powers based on adaptive Dec-MPC, (c) the comparison between the total output modules powers of the FC modules, and (d) the comparison between SoC levels.



The exact final operational costs associated with the proposed decentralized algorithms compared to DP and Cen-MPC are listed in Table 4-I. The final costs of the suggested approaches have achieved a very close performance to the DP results. The final costs based on fixed-horizon and adaptive Dec-MPCs are \$0.0617 and \$0.0628, which are 5.89% and 7.75% greater than DP, respectively. Based on the obtained results, the final costs of the fixed-horizon and the adaptive Dec-MPCs are about 1.74% and 3.52% higher than Cen-MPC.

Table 4-I The detailed comparison of computational complexity and final price

	DP	Cen-MPC	Dec-MPC (Fixed-horizon)	Dec-MPC (Adaptive-horizon)
T	-	25.5914	14.6237	9.2473
$S_T$	0.0583	0.0609	0.0617	0.0628

A comparison of the final costs and the computational time based on different prediction horizon lengths (from 2 to 25) is depicted in Figure 4-5. Generally, the final costs and computational complexities demonstrate inverse behaviors as the moving optimization window length increases for all cases. If the prediction moving window length is selected too short, the calculated optimized power values result in unsatisfactory approximations of the infinite horizon result. The execution time of Cen-MPC grows at best linearly with raising the length of the looking-ahead window in comparison with others, significantly when the optimization horizon dimension exceeds 12s. The computational burden of adjustable Dec-MPC is about 61.54% and 76.95% fewer sensitivities than Dec-MPC and centralized one to the length of the moving horizon.

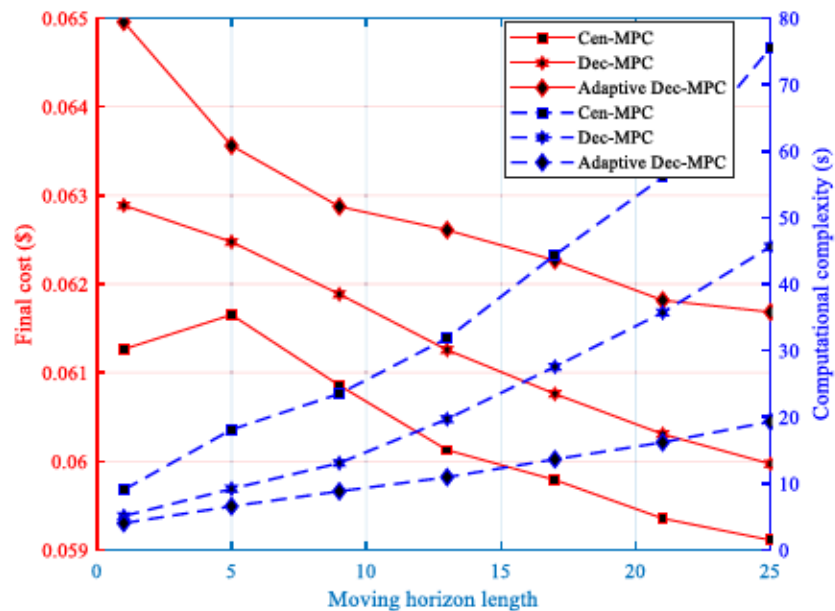


Figure 4-5 Optimal final cost and computational complexity of Cen-MPC, Dec-MPC, and adjustable Dec-MPC as functions of optimization window size.

#### 4.4 Outcomes

The results of an exhaustive investigation about an optimal module-level power allocation control focusing on merging the model predictive theory and reinforcement learning algorithm have brought about the following statements.

- The presented findings demonstrate the effectiveness and superiority of the proposed approach compared to the centralized MPC from final cost, computational time, and robustness elicited from numerous examinations of the targeted optimization problem.
- It gives a valuable knowledge of the top prospects and challenges of the adjustable decentralized EMS by analyzing functioning achievements and requirements.
- Experimentation with a developed test bench system has been another contribution of this study neglected in other relevant studies.

The subsequent paper gives the discussions mentioned above in the context of the suggested predictive power-splitting algorithm.

**Article 3:** Look-Ahead Decentralized Safe-Learning Control for a Modular Powertrain Using Convex Optimization and Federated Reinforcement Learning

**Authors:** Arash Khalatbarisoltani, Mohsen Kandidayeni, Loïc Boulon, and Xiaosong Hu

**Journal:** IEEE Transactions on Intelligent Transportation Systems (under review)

**Publication date:** -

#### 4.5 Conclusion

This chapter presents a lookahead D-PAS for coordinating two FC modules and one battery pack in a FCV application. Firstly, the look-ahead PAS problem is formulated as a convex problem. Secondly, the decentralized PAS is attained by applying a decomposition scheme based on C-ADMM without any central coordinator. During the DCO-based optimization process, the constraints of the powertrain components are scrutinized by projecting the temporary FC modules powers into the feasible working spaces. Each module communicates with the neighboring one to agree on the optimal solutions leading to a robust and reconfigurable power-splitting scheme. Then, a federated reinforcement learning-based tuning approach is proposed to improve the computational time of the D-PAS scheme. Finally, several numerical and experimental studies investigate the data processing time efficiencies, convergence performances, final optimal solution precisions, and module-to-module communication necessities of the D-PAS methods. The next chapter provides a general conclusion and the future direction of this work.



# Look-Ahead Decentralized Safe-Learning Control for a Modular Powertrain Using Convex Optimization and Federated Reinforcement Learning

*Arash Khalatbarisoltani, Member, IEEE, Mohsen Kandidayeni, Member, IEEE, Loïc Boulon, Senior Member, IEEE, Xiaosong Hu, Senior Member, IEEE*

## *4.5.1 Abstract*

Optimization-based power allocation strategy (PAS) facilitates knowledge to enhance the performance of fuel cell vehicles (FCVs) powertrain. Ongoing efforts predominantly concentrate on optimizing a centralized PAS (Cen-PAS) by numerous high-computational methods without adequately providing flexibility (plug & play) and robustness for the onboard powertrain components. To address these shortcomings, a forward-looking decentralized PAS (Dec-PAS) based on the consensus-based alternating direction method of multipliers (ADMM) is presented with an explicit consciousness of coordination of powertrain components' dynamic responses and considering the future driving profile information. The powertrain components using the multi-step scheme cooperate in converging the global optimum answers using a highly dynamic module-to-module communication layer in a fully decentralized configuration that is more robust and provides plug and play capability. Compared to a single-step decentralized optimization approach, the proposed predictive scheme, which considers future driving information, results in a more overall decline in the final costs of hydrogen consumption and degradation.

Additionally, to improve the processing time, a safe-learning algorithm is proposed to learn the optimal policy of the moving horizon dimensions in the Dec-PAS using a federated reinforcement learning (FRL) algorithm. The performance of the proposed framework is assessed for accuracy, convergence speed, and communication burden compared to Cen-PASs. Both numerical simulation and implementation results manifested the superiority of the recommended multi-step safe-learning-enabled Dec-PAS scheme over the centralized and fixed-horizon MPC approaches.

*Index Terms*— Alternating direction method of multipliers (ADMM), distributed optimization algorithms, energy management strategy (EMS), fuel cell hybrid electric vehicle (FC-HEV), model predictive control (MPC), proton exchange membrane fuel cell (PEMFC).

#### 4.5.2 Introduction

Owing to more exceeding concern throughout fossil fuel consumption and the consequential escalating requirements for more renewable resources, transportation as an essential sector is transitioning from internal combustion engine (ICE) vehicles to fuel cell vehicles (FCVs) [59]. Power allocation strategies (PASs) aim to enhance the operational performance and the lifetime of their powertrain components (fuel cell system (FCS), battery, and ultracapacitor) in the FCVs [60, 61]. Since the powertrain system of heavy-duty FCVs demands high-level powers, there is a need to employ a big-size FCS. Nevertheless, a multilayer FC stack diminishes the safety and reliability of the powertrain system. These drawbacks motivate to shift into modular energy systems (MESs) [13]. Although there are many efforts to advance the multi-stack FCSs (MSFCs) from hardware perspectives (for instance, connection topologies [1] and power-conditioning [5]), some issues still need to be

further addressed in terms of the software point of view. For this purpose, various power-splitting strategies are assigned through a centralized PAS (Cen-PAS) control unit, as shown in Figure 4-6(a), such as power point tracking [28], optimization [27, 30], state machine [32], hierarchical [34], hysteresis [35], and droop control [62]. However, when integrating the dynamic responses of components, it is indispensable to optimize over multiple time steps. Furthermore, adding driving cycle prediction to the PAS problem may improve the obtained optimization results. In this regard, various centralized model predictive control (Cen-MPC) approaches are suggested in the literature, for instance, standard [63-67], nonlinear [68, 69], hierarchical [70], mixed-integer [71], and multi-mode [72] MPC. The popularity of Cen-MPC predominantly stems from its proficiency to manage complex powertrains while respecting components' constraints and guaranteeing safe operation as two crucial points for the FCV applications. The primary impediment of Cen-MPC is that the computational complexity of solving the optimal power-splitting problem is comparatively significant, restricting the implementation. Furthermore, the hyperparameters of Cen-MPC require to be fine-tuned to the multi-objective power-splitting purpose. More importantly, due to the centralized control structure, Cen-PAS does not provide plug-and-play and robustness from software perspective. In this regard, it makes perfect sense to look for a decentralized PAS (Dec-PAS) method, as shown in Figure 4-6(b), where the main optimization problem is appropriately mapped into a subproblem for each of the module controllers.



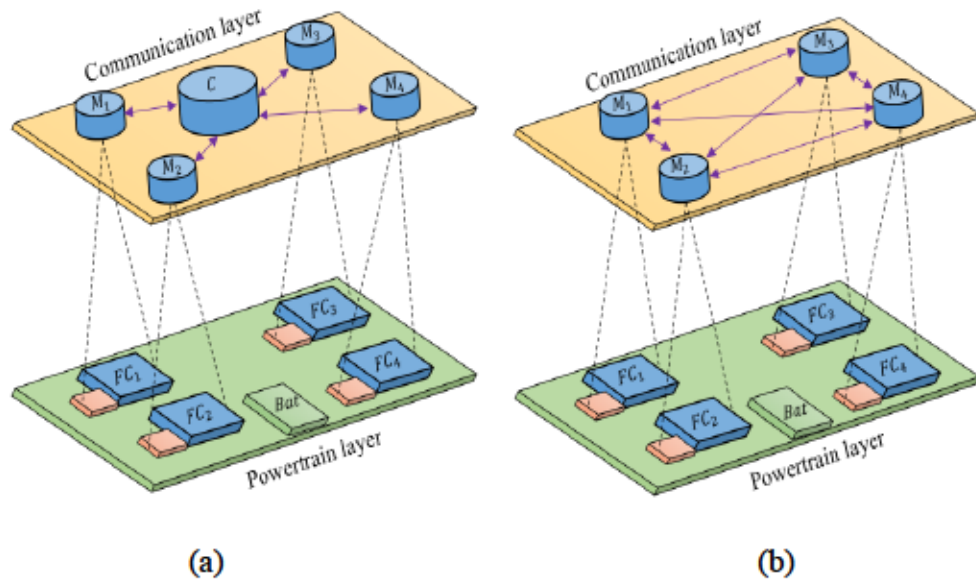


Figure 4-6 Diagram of the communications topologies and the underlying powertrain for Cen-PAS and Dec-PAS with four FC modules ( $FC_m, m = \{1, \dots, 4\}$ ) and one battery pack (Bat). a) Cen-PAS with four local control units ( $M_m, m = \{1, \dots, 4\}$ ) and one centralized unit (c), b) Dec-PAS without a centralized controller.

Decentralized decision-making approaches to distributed convex optimization (DCO) algorithms, such as Benders decomposition, Karush–Kuhn–Tucker optimality condition, Lagrangian relaxation, and consensus algorithm, have been put forward recently in the literature [73, 74]. As one of the popular decomposition techniques, the alternating direction method of multipliers (ADMM) method [75] obtains the convergence characteristics of the multipliers technique and the decomposability of Lagrangian relaxation. The most relevant study regarding the optimization-based Dec-PAS has been introduced in [76]. In [76], a single-step Dec-PAS based on an auxiliary problem principle (APP) method is introduced to address a PAS problem. This study is based on a single-step optimization method. Although efficiently bringing to bear the available battery pack capacity, preventing nearsighted optimization answers, and respecting system constraints, optimizing multiple-step strategies

is necessary. It seems to be beneficial to extend the single-step DCO-based PAS into a multi-step MPC-based one. Decomposing a complex PAS optimization problem into several cooperative sub-problems, which converges into the global optimum answer, can offer various benefits. A decentralized MPC (Dec-MPC) controller can manage the abnormal process in either an electrical fault or a failure of a processor unit, or even an internal stack malfunction.

Moreover, Den-PAS offers plug-and-play since its modular power network can be reconfigured without completely changing its control policies. In addition, since each local subproblem in a parallel optimization process has fewer shared variables, constraints, and control variables than Cen-MPC, the computational complexity burden will be enormously mitigated. In a Dec-MPC scheme, the size of the looking-ahead moving window is an imperative parameter, which selects how far into the future the decentralized optimization scheme assesses the outcomes of its control actions. This clue motivates integrating a learning-based algorithm with Dec-MPC to learn the optimal moving horizon police.

Reinforcement learning (RL) [77] as a powerful data-driven algorithm has devoted considerable attention in the FCV domain, for instance, direct [78-80], online recursive [81], and hierarchical [82, 83] RL. Notwithstanding, the RL-based approach has proven to be an advanced method, but it has not witnessed many practical applications in MFCVs. It is mainly because this learning-based PAS faces several difficulties. The operation safety concern in the training and implementation stages is important [84]. Several approaches are suggested to address this weakness, such as, coach-actor double critic [85], learning-based MPC [86, 87], robust MPC [88], parallel-constrained policy optimization [89], shielding [90, 91], and Lyapunov-based [92].

The contribution of this study is situated within formulating a lookahead decentralized MPC-based PAS framework and investigating how the FRL algorithm is assisting in learning the optimal policy to choose the prediction moving horizon size in a MFCV. In contrast with [76], to consider the intertemporal constraints and efficiently utilize the available battery pack capacity, the previous single-step DCO-based approach is extended into a multi-step decentralized with parallel moving horizons. The proposed method leads to an overall decline in the total system expense since predictive control responses in anticipation of the requested power in the future driving profile can be singled out. Also, integrating the receding prediction horizon into the decomposition technique facilitates good initial points, enhancing the optimization convergence speed. Moreover, since the main hyper-parameters affecting Dec-MPC's performance and the computational burden are the lengths of the prediction horizon, a safe-learning scheme that integrates federated reinforcement learning (FRL) algorithm with Dec-MPC is put forward. The FRL framework without a central unit cooperatively learns a shared control policy across the FC modules. The FC modules locally train based on the module-specific data for several epochs and then directly collaborate to build an aggregated and fined-tuned model. To the best of our knowledge, no research has been conducted to develop a Dec-MPC approach with safe-learning capability for a MFCV. Since the main idea of this study does not lie in introducing a predictive method, the DCO-based strategy is straightforwardly formulated by considering that the future power profile is precisely known. The rest of this paper proceeds as follows. The FCV powertrain modeling description is presented in Section II. Section III formulates the multi-step look-ahead PAS optimization problem. The suggested Dec-MPC framework is derived according to the consensus-based ADMM procedure in Section IV. The formulation of learning the optimal length of the Dec-MPC receding prediction horizon as a FRL framework is provided in

Section V. Comprehensive numerical simulations. Experimental results are presented in Section VI, and Section VII, respectively, accompanied by conclusions recapped about the proposed decentralized approach and prospects in Section VIII.

#### *4.5.3 FCV powertrain configuration and modeling*

To facilitate the general idea of transforming centralized power-splitting problem into Dec-MPC, a powertrain system comprises two parallel modules, and one battery unit is developed, as illustrated in Figure 4-7.

##### **4.5.3.1 Powertrain structure and modeling**

A modular test bench based on an electric vehicle is established [25]. The developed small-scale test bench comprises two modules, a battery pack, a programmable DC electronic load, and a multi-range programmable DC power supply for simulating the requested load profile. The critical components of each module are a 500-W open-cathode PEMFCS (H-500), a smoothing inductor, and an adjustable unidirectional boost DC-DC converter. Six series 12-V 18-Ah battery packs give the voltage of the DC bus. Each module has its autonomous Dec-MPC inside of a National Instrument CompactRIO. The optimal reference of each module is calculated at every control instant with an interval of 10 Hz.



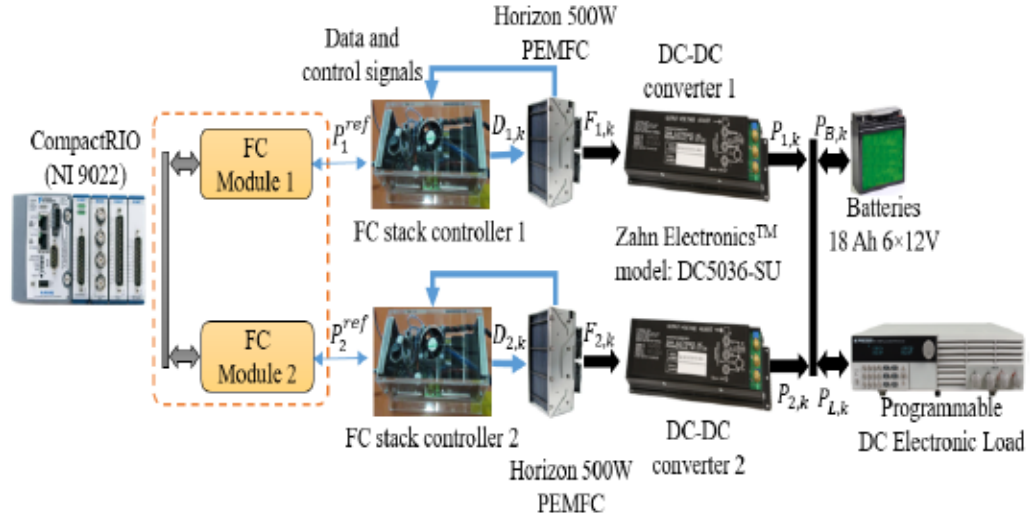


Figure 4-7 The schematic of the established small-scale modular test bench.

The power balance equation of the modules and the battery unit on the DC bus at each step of the optimization window ( $\forall k \in K$ ) is formulated in (1).

$$\sum_m P_{m,k} + P_{B,k} = P_{L,k}, \forall m \in M, \forall k \in K, \quad (1.a)$$

$$P_{m,k} = \eta_m (F_{m,k} D_{m,k} - P_{loss,k}), \forall m \in M, \forall k \in K, \quad (1.b)$$

where  $P_{m,k}$  ( $\forall m \in M, M = \{1,2\}$ ) denotes the power of each one of the modules  $FC_m$ .  $P_{B,k}$  ( $\forall k \in K$ ) denotes the power provided by the battery unit,  $P_{L,k}$  is the requested power from the propulsion system,  $F_{m,k}$  indicates the generated power of each of the 500-W FCSSs,  $\eta_m$  and  $D_{m,k}$  are the efficiency and the control signal of the boost converters, respectively,  $P_{loss,k}$  denotes the consumed power by the auxiliary of FCSSs.

#### 4.5.3.2 FCS modeling and constraints

In this work, each one of the 500-W FCSSs,  $FC_m$  ( $\forall m \in M$ ) are modeled as voltage sources where their polarization curves and the hydrogen mass flows versus requested

currents are described by experimentally validated quasi-static curves, as shown in Figure 4-8.

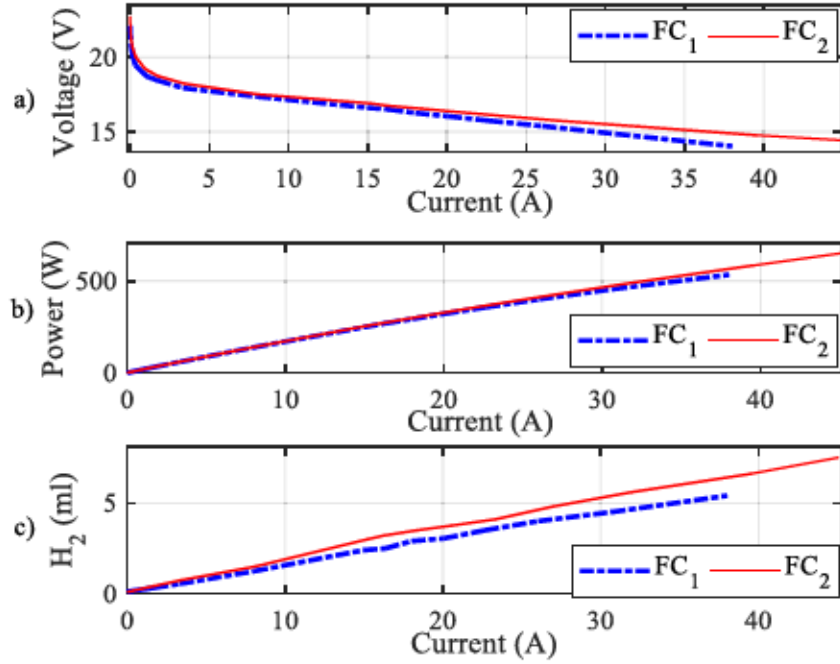


Figure 4-8 The characteristic curves of the two actual FCS modules: (a) polarization curves, (b) power curves, and (c) hydrogen curves.

Equation (2) demonstrates the upper, lower, and slew rate limits on instantaneous powers  $P_{m,k}$  ( $\forall m \in M, \forall k \in K$ ).

$$P_m^{min} \leq P_{m,k} \leq P_m^{max}, \forall m \in M, \forall k \in K, \quad (2.a)$$

$$P_{m,k} - P_{m,k-1} \leq R_m^{up} \Delta t, \forall m \in M, \forall k \in K, \quad (2.b)$$

$$P_{m,k-1} - P_{m,k} \leq R_m^{down} \Delta t, \forall m \in M, \forall k \in K, \quad (2.c)$$

where  $P_m^{min} \geq 0$  and  $P_m^{max} \geq 0$  are the minimum and maximum values of  $P_{m,k}$ ,  $R_m^{down} \leq 0$  and  $R_m^{up} \geq 0$  are boundaries of the slew rate, and  $\Delta t$  indicates the time step. These limitations

encumber the FCSs from repeatedly turning on/off and sudden changes, which can cause degradation costs.

#### 4.5.3.3 Battery modeling and constraints

The first-order RC model of the battery pack is formulated by

$$I_{B,k} = \frac{V_{0,k} - R_s I_{B,k} - V_{B,k}}{R_c} + C_c \frac{d}{dt} (V_{0,k} - R_s I_{B,k} - V_{B,k}), \forall k \in \mathbf{K}, \quad (3.a)$$

where  $I_B$  is the battery pack current,  $V_0$  is the open-circuit voltage,  $R_s$  is the series ohmic resistance,  $V_B$  is the terminal voltage,  $R_c$  denotes the polarization resistance, and  $C_c$  is the polarization capacitor. Equation (3) imposes power and slew rate limits for the battery unit  $P_{B,k}$ ,  $\forall k \in \mathbf{K}$ .

$$P_B^{min} \leq P_{B,k} \leq P_B^{max}, \forall k \in \mathbf{K}, \quad (3.b)$$

$$P_{B,k} - P_{B,k-1} \leq R_B^{up} \Delta t, \forall k \in \mathbf{K}, \quad (3.c)$$

$$P_{B,k-1} - P_{B,k} \leq R_B^{down} \Delta t, \forall k \in \mathbf{K}, \quad (3.d)$$

where  $P_B^{min} \leq 0$  and  $P_B^{max} \geq 0$  are the minimum and maximum limits of  $P_{B,k}$ , respectively, and  $R_B^{down}$  and  $R_B^{up}$  are the slew rate boundaries of  $P_{B,k}$ . Equation (4) presents the state of charge (SoC) calculation formula and the constraints on the battery SoC level.

$$SoC_{k+1} = SoC_k - \frac{P_{B,k} \Delta t}{Q_B V_{B,k} 3600}, \forall k \in \mathbf{K}, \quad (4.a)$$

$$SoC^{min} \leq SoC_k \leq SoC^{max}, \forall k \in \mathbf{K}, \quad (4.b)$$

where  $SoC^{min}$  and  $SoC^{max}$  denote the minimum and maximum limits of SoC, respectively, the initial SoC level  $SoC_{k=0}$  is  $SoC_0$ , and  $Q_B$  represent the battery capacity. The battery life

is affected by the depth of discharge (DOD) and is defined as an initial capacity drop (reaching 80% of the initial battery capacity). The state of health (*SoH*) is calculated by

$$SoH_{k+1} = SoH_k - \frac{|P_{B,k}|\Delta t}{2n_B Q_B V_{B,k} 3600}, \forall k \in K, \quad (5.a)$$

$$SoH^{min} \leq SoH_k, \forall k \in K, \quad (5.b)$$

where  $SoH^{min}$  is the minimum value and  $SoH_{k=0}$  is the initial SoH level, and  $n_B$  denotes the total number of cycles during the whole lifetime of the battery unit. The parameters of the battery unit obtained from experimental tests are listed in Table 4-II.

Table 4-II The approximated battery unit parameters.

$V_0 = 12.21 V$	$R_s = 0.014\Omega$	$V_B = 73.26$	$R_c = 0.017\Omega$
$C_c = 1792 F$	$Q_B = 18.2Ah$	$SoC^{min} = 0.65$	$SoC^{max} = 0.75$

#### 4.5.3.4 Boost converter modeling and characteristics

The two converters are modeled as follows:

$$L_m \frac{d}{dt} I_{m,k} = V_{m,k} - V_{h_{m,k}} - r_m I_{m,k}, \forall m \in M, \forall k \in K \quad (6.a)$$

$$V_{h,k} = m_{h,k} V_{B,k}, I_{h_{m,k}} = m_{h_{m,k}} I_{m,k} \eta_{h_k}, \quad (6.b)$$

where  $I_m$  and  $V_m$  are the current and voltage of  $FC_m$  ( $\forall m \in M$ ), respectively,  $L_m = 1.1 mH$  presents the smoothing inductor inductance,  $r_m = 23.9 m\Omega$  is the smoothing inductor resistance,  $\eta_h = 96.21\%$  is the average efficiency, and  $m_h$  is the modulation ratio of the converters.



#### 4.5.4 The general optimization problem formulation of the look-ahead PAS

In this section, the mathematical formula of the main PAS optimization problem for the multi-stack FCV, as illustrated in Figure 4-9, is provided and utilized in the subsequent sections to elicit the decentralized scheme.

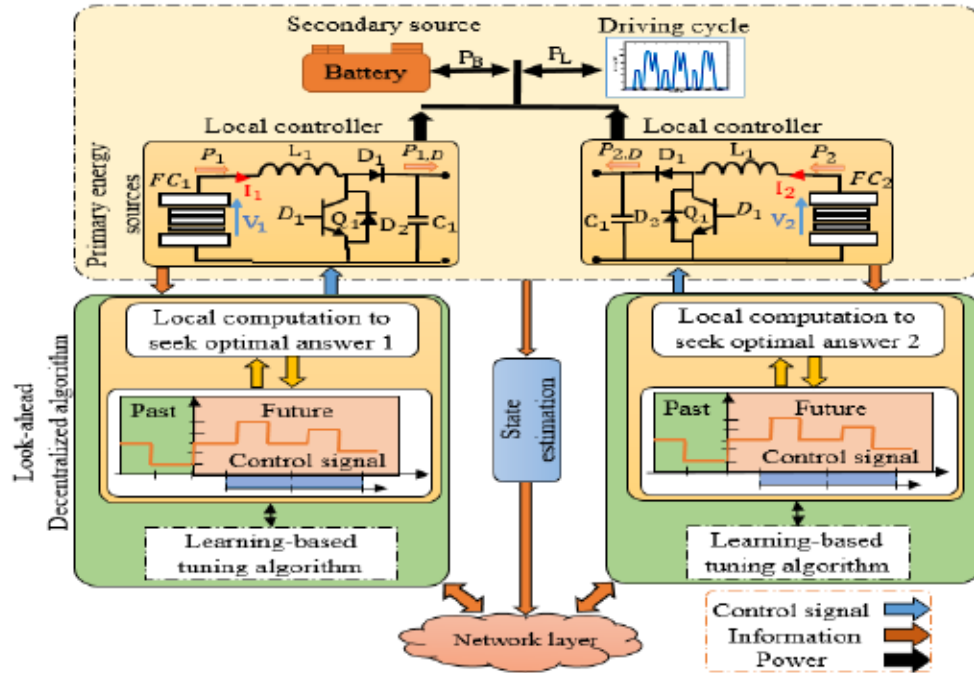


Figure 4-9 The adaptive look-ahead Dec-MPC framework and the modular powertrain system sequence operation.

The centralized convex-based multi-objective problem can be formulated in the following sequence.

$$\min_{P_{m,k} P_{B,k}} \sum_{k=0}^{K-1} \sum_{m=1}^M g(c_m(P_{m,k}) + c_B(P_{B,k})) \quad (7.a)$$

$$\text{s.t } \sum_m A_m P_{m,k} = c, \text{ other equality and inequality constraints}$$

where  $g$  is a symbolic convex approximation cost function that summarizes all the cost functions which equal to sum module and battery cost,  $c_m = s_{h_{m,k}} + s_{d_{m,k}}$  denotes the

hydrogen and degradation costs of  $FC_m (\forall m \in \mathbf{M})$ ,  $c_B = s_{B,k} + s_{SoC,k}$  is the battery unit degradation and SoC penalty costs,  $P_{m,k} \in \mathbb{R}^{N_m}$  stands for the power of the module  $m$ ,  $A_m \in \mathbb{R}^{M \times N_m}$  and  $c \in \mathbb{R}^M$  apply the powertrain and the coupling constraints, respectively,  $n \in N_m$  denotes the number of iterations.  $s_{h_{m,k}}$  is computed by  $H_{m,k} C_{H_2} \Delta t$ , where  $h_{m,k} = a_m^1 P_{m,k}^2 + a_m^2 P_{m,k} + a_m^3$  is a quadratic approximation function to calculate the hydrogen consumption cost with  $a_m^1, a_m^2, a_m^3 \geq 0$  and  $P_{m,k} \geq 0$  for  $FC_m (\forall m \in \mathbf{M})$  and  $C_{H_2}$  is hydrogen price, 3.92 \$/Kg [93].  $s_{d_{m,k}}$  includes the low-power degradation  $s_{d_{m,k}}^l$ , the high-power degradation  $s_{d_{m,k}}^h$ , and the load-change degradation  $s_{d_{m,k}}^t$ , formulated by

$$s_{d_{m,k}}^l = \frac{\varepsilon_l 0.5 C_{FC_m} \Delta t \mu_{l,m}}{3600 V_{n,m}}, \forall m \in \mathbf{M}, \forall k \in \mathbf{K}, \quad (7.b)$$

$$s_{d_{m,k}}^h = \frac{\varepsilon_h 0.5 C_{FC_m} \Delta t \mu_{h,m}}{3600 V_{n,m}}, \forall m \in \mathbf{M}, \forall k \in \mathbf{K}, \quad (7.c)$$

$$s_{d_{m,k}}^t = \frac{\varepsilon_t 0.5 C_{FC_m} \sum_{k=0}^{K-1} \sum_{m=1}^M |P_{m,k+1} - P_{m,k}|}{1000 n_m V_{n,m}}, \forall m \in \mathbf{M}, \forall k \in \mathbf{K} \quad (7.d)$$

where  $n_m$  represents cell numbers of,  $\mu_{l,m}$  and  $\mu_{h,m}$  are equal to

$$\mu_{l,m} = \begin{cases} 1, & \text{if } P_{min,m} \leq P_{m,k} \leq 0.2 P_{nom,m} \\ 0, & \text{otherwise.} \end{cases}, \quad (7.e)$$

$$\mu_{h,m} = \begin{cases} 1, & \text{if } 0.8 P_{nom,m} \leq P_{m,k} \leq P_{max,m} \\ 0, & \text{otherwise.} \end{cases}, \quad (7.f)$$

where  $V_{n,m}$  is 10 % of the nominal  $FC_m$  voltage drop,  $C_{FC_m} = 35$  \$/kW is the FCS cost [94].

The low-power, high-power, and load-change cell degradation rates are  $\varepsilon_l = 8.662 \mu V/h$ ,

$\varepsilon_h = 10 \mu V/h$ , and  $\varepsilon_t = 0.04185 \mu V/kW$ , respectively, adapted from [30, 95]. The battery

degradation cost,  $s_{B,k}$ , is determined by

$$s_{B,k} = c_B(\text{SoH}_{B,k} - \text{SoH}_{B,0}), \forall k \in \mathbf{K}, \quad (7.g)$$

where  $c_B = 189 \text{ \$/kWh}$  is the battery price [96],  $s_{\text{SoC}_k}$  is a punishment item to measure the SoC level variation, which is defined by

$$s_{\text{SoC}_k} = \beta(\text{SoC}_k - \text{SoC}_0)^2, \forall k \in \mathbf{K}, \quad (7.h)$$

where  $\text{SoC}_0$  is the initial SoC, and  $\beta$  is a large positive coefficient.

#### 4.5.5 Reformulation of Cen-MPC via C-ADMM

This section thoroughly explains reformulating the Cen-MPC problem (7) into a decentralized form using C-ADMM. Additionally, the communication principle and data flow are investigated comprehensively. In the proposed Dec-MPC, the main problem is decentralized into  $m \in \mathbf{M}$  subproblems, and each one is allocated to a FC module control unit. During the optimization process, an exchange of candidate output powers occurs through the module-to-module communication layer. This iterative process continues until an agreement is attained among the local control units, according to the determined stopping criterion. Then, the optimization process will be repeated and shifted to the next point, as illustrated in Figure 4-10.

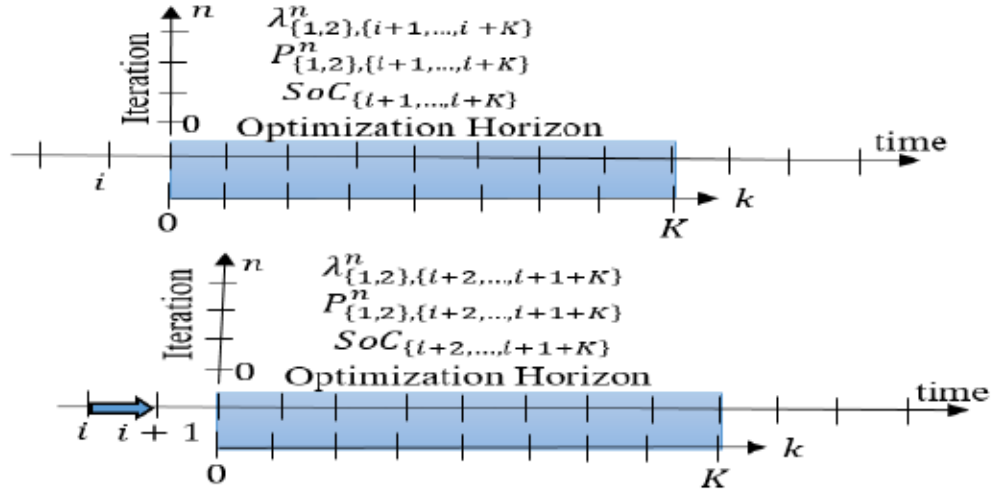


Figure 4-10 The employed decomposition technique.

Since the modules are coupled through (1) on the DC bus, the general problem (7) is not inherently decomposable. To tackle this issue, as demonstrated in Figure 4-11,  $P_{m,\{i+1,\dots,i+K\}}$  is duplicated into its neighboring module as a virtual power and coupled with a global power vector,  $W_{m,\{i+1,\dots,i+K\}} = \{w_{1,\{i+1,\dots,i+K\}}, w_{2,\{i+1,\dots,i+K\}}\}$ . As an example,  $P_{1,\{i+1,\dots,i+K\}}$  is copied into  $FC_2$  as a virtual power  $P_{12,\{i+1,\dots,i+K\}}$ , and  $w_{1,\{i+1,\dots,i+K\}}$  is defined to link them together. Equation (8) is added to guarantee that the duplicated variables are equal and the modified PAS converges to the same optimal optimization result [49].

$$P_{1,\{i+1,\dots,i+K\}}^n - w_{1,\{i+1,\dots,i+K\}}^n = 0, \forall k \in K, \quad (8.a)$$

$$P_{12,\{i+1,\dots,i+K\}}^n - w_{1,\{i+1,\dots,i+K\}}^n = 0, \forall k \in K, \quad (8.b)$$

$$P_{2,\{i+1,\dots,i+K\}}^n - w_{2,\{i+1,\dots,i+K\}}^n = 0, \forall k \in K \quad (8.c)$$

$$P_{21,\{i+1,\dots,i+K\}}^n - w_{2,\{i+1,\dots,i+K\}}^n = 0, \forall k \in K \quad (8.d)$$

To improve the convergence performance and ease the communication burden, the number of the optimization variables is reduced by assuming that the virtual variables are equal to



the previous global variables. For instance,  $P_{12,\{i+1,\dots,i+K\}}^{n+1}$  is equal to  $w_{1,\{i+1,\dots,i+K\}}^n$ . In this way, the centralized PAS problem can be transformed into two decentralized subproblems functions of  $P_{m,\{i+1,\dots,i+K\}}$  and  $W_{m,\{i+1,\dots,i+K\}}$ .

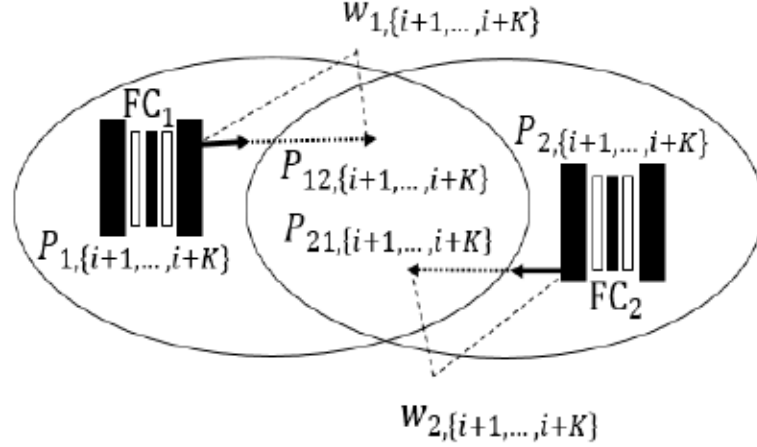


Figure 4-11 Visual representation of the multi-step MPC-based PAS.

The decentralized optimization process of (7)-(8) includes a three-step procedure, where  $\rho$  is a positive tuning value,  $n$  denotes the number of iterations, and  $\lambda_m$  are Lagrangian multipliers [49]. The equations related to modules 1 and 2 are given in (9) and (10), respectively.

$$P_{1,\{i+1,\dots,i+K\}}^{n+1} = \min \{ C_1(P_{1,\{i+1,\dots,i+K\}}, P_{21,\{i+1,\dots,i+K\}}^n) + C_B(P_{b,\{i+1,\dots,i+K\}}) + \quad (9.a)$$

$$\lambda_{1,\{i+1,\dots,i+K\}}^n P_{1,\{i+1,\dots,i+K\}} + \frac{\rho}{2} (P_{1,\{i+1,\dots,i+K\}} - w_{1,\{i+1,\dots,i+K\}}^n)^2 \}, \forall k \in K,$$

$$w_{1,\{i+1,\dots,i+K\}}^{n+1} = \frac{P_{1,\{i+1,\dots,i+K\}}^{n+1} + w_{1,\{i+1,\dots,i+K\}}^n}{2}, \forall k \in K \quad (9.b)$$

$$\lambda_{1,\{i+1,\dots,i+K\}}^{n+1} = \lambda_{1,\{i+1,\dots,i+K\}}^n + \rho (P_{1,\{i+1,\dots,i+K\}}^{n+1} - w_{1,\{i+1,\dots,i+K\}}^{n+1}), \forall k \in K \quad (9.c)$$

$$P_{2,\{i+1,\dots,i+K\}}^{n+1} = \min \{ C_2(P_{12,\{i+1,\dots,i+K\}}^n, P_{2,\{i+1,\dots,i+K\}}) + C_B(P_{b,\{i+1,\dots,i+K\}}) + \quad (10.a)$$

$$\lambda_{2,\{i+1,\dots,i+k\}}^n P_{2,\{i+1,\dots,i+k\}} + \frac{\rho}{2} (P_{2,\{i+1,\dots,i+k\}} - w_{2,\{i+1,\dots,i+k\}}^n)^2 \}, \forall k \in K$$

$$w_{2,\{i+1,\dots,i+k\}}^{n+1} = \frac{P_{2,\{i+1,\dots,i+k\}}^{n+1} + w_{2,\{i+1,\dots,i+k\}}^n}{2}, \forall k \in K \quad (10.b)$$

$$\lambda_{2,\{i+1,\dots,i+k\}}^{n+1} = \lambda_{2,\{i+1,\dots,i+k\}}^n + \rho (P_{2,\{i+1,\dots,i+k\}}^{n+1} - w_{2,\{i+1,\dots,i+k\}}^{n+1}), \forall k \in K. \quad (10.c)$$

where  $C_1$  and  $C_2$  are based on  $C_m$  which defines in the previous sections. The detailed procedure of Dec-MPC is presented in Figure 4-12. First, a cold-start initialization of  $\lambda_{m,\{i+1,\dots,i+k\}}$ ,  $P_{m,\{i+1,\dots,i+k\}}$ , and  $W_{m,\{i+1,\dots,i+k\}}$  is required for each module  $m$  ( $\forall m \in M$ ). The local PAS problems (9.a) and (10.a) are solved to determine  $P_{m,\{i+1,\dots,i+k\}}$ . Then, the  $W_{m,\{i+1,\dots,i+k\}}$  are calculated by (9.b) and (10.b) and sent to the neighbor module in parallel. After that,  $\lambda_{m,\{i+1,\dots,i+k\}}$  is updated using by (9.c) and (10.c). If  $\|\lambda_m^{n+1} - \lambda_m^n\|_2^2 \leq \mu_1$  and  $\rho \|P_m^{n+1}[k] - P_m^n[k]\|_2^2 \leq \mu_2$ , where  $\mu_1$  and  $\mu_2$  are the limiting values, as the stopping criteria are fulfilled, the optimization processes stop and  $P_{m,i+1}$  sends to the converters as  $P_m^{ref}$ . After that, the optimization windows shift for one time step. If not, the optimization process goes back to Step 3.

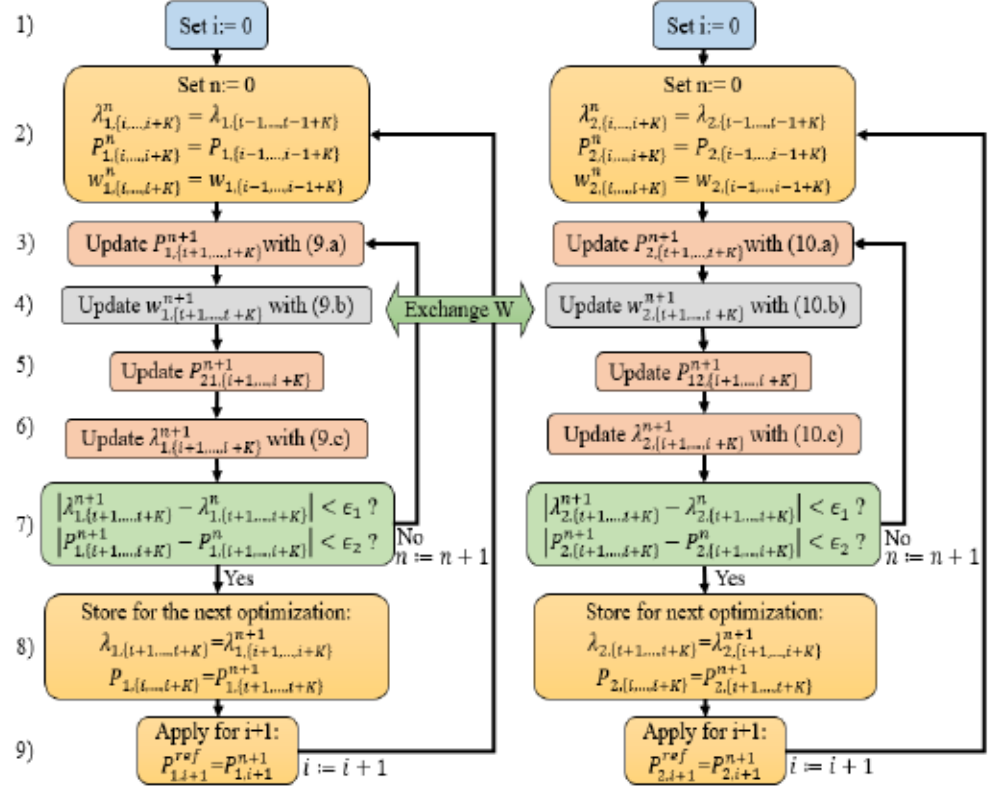


Figure 4-12 The step-by-step flowchart of the Dec-MPC algorithm.

#### 4.5.6 General description of the hyper-parameters tuning algorithm based on Federated reinforcement learning

As the primary hyperparameter of the proposed DCO-based PAS approach, the length of the moving window significantly impacts the optimization accuracy and speed. In this regard, a learning approach based on FRL is proposed to tune this hyperparameter optimally. A Markov decision process (MDP) is formulated for the tuning process as a tuple  $(\mathcal{S}^m, \mathcal{A}^m, P, R, T)$ , where  $\mathcal{S}^m$  denotes the set of states  $s \in \mathcal{S}^m = \{P_{avg,i}, SoC_i\} (\forall i \in I, \forall m \in M)$ , where  $P_{avg}$  and  $SoC$  are the average requested power for the maximum optimization horizon length and the current  $SoC$  value, respectively,  $\mathcal{A}^m$  represents the action set  $a \in \mathcal{A}^m = \{K\}$ , where

$K$  is the prediction horizon.  $P(s_{i+1}|s_i, a_i): \mathcal{S}^m \times \mathcal{A}^m \rightarrow P(s)$  ( $\forall i \in I, \forall m \in M$ ) are the probability of transitioning into  $s_{i+1} \in \mathcal{S}^m$  at time  $i + 1$  when the decentralized PAS units take action  $a_i \in \mathcal{A}^m$  in the state  $s_i \in \mathcal{S}^m$  at time  $i$ ,  $R_i(s_i, a_i, s_{i+1}): \mathcal{S}^m \times \mathcal{A}^m \times \mathcal{S}^m \rightarrow \mathbb{R}$ ,  $r_{m,i} = -1 \times (\alpha_1 t_{m,i} + \alpha_2 c_{m,i} + \alpha_3 (SoC_{i+H} - SoC_0)^2)$  ( $\forall i \in I, \forall m \in M$ ) is the reward value obtained when an action  $a_i \in \mathcal{A}^m$  is taken, with  $\{\alpha_d\}_{d=1}^3$  are weighting variables,  $t_{m,i}$  denotes the computational time of module  $m$  at the time step  $i$ ,  $c_{m,i}$  is the sum of the cost of module  $m$  and the battery unit at the time step  $i$ , and the last term is the cost associated with sustaining the SoC level. The primary objective of the FRL method is to determine the optimal hyper-parameter tuning strategy  $\pi_\theta^*$  [97]. The main parameter we are focused on is finding the optimization horizon window size. The procedure of two sequence optimization steps of the proposed predictive-based method is visualized in Figure 4-13.

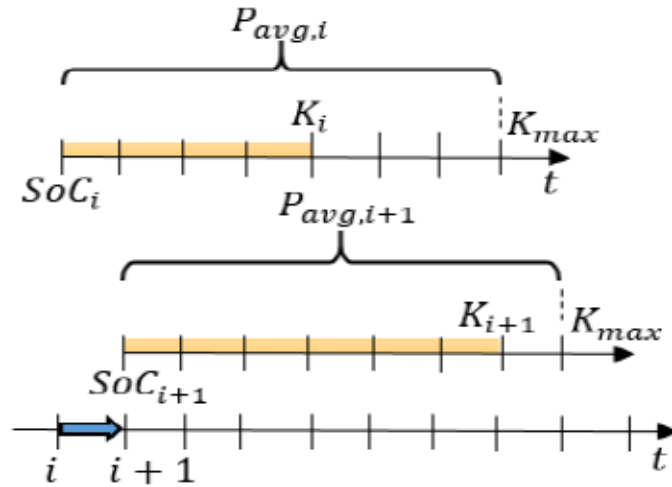


Figure 4-13 The general operation of the FRL-based approach to seeking the optimal hyperparameter based on the current powertrain states ( $P_{avg}$  and  $SoC$ ) in two sequence optimization steps.

The process of decentralized learning based on FRL is indicated in Figure 4-14. To explain the FRL algorithm, an environment with  $\{FC_m\}_{m=1}^M$  modules is considered, where



each module has the training points  $\mathcal{O}_m = \{(P_{avg_1}, SoC_1, r_1), \dots, (P_{avg_l}, SoC_l, r_l)\}$  with  $l$  tagged samples and the weight parameter list  $W^m$ . All modules  $\{FC_m\}_{m=1}^M$  are linked directly in a module-to-module style. Firstly, a cold-start initialization is applied to all modules  $\{FC_m\}_{m=1}^M$ , then it starts with training data  $\mathcal{O}_m$  in parallel for a small number of iterations (step 1). After that, each one pools its partially trained weight parameters  $W^m$  to others (step 2), and merges all the received models by the weighted averaging technique, i.e.,  $W^A = \sum_m \frac{1}{m} W^m$  (step 3). In the end, the aggregated model  $W^A$  is used by the modules to select the optimal prediction horizon length. Several rounds are executed until all FC modules' models converge (step 4). After completing the decentralized learning process, each FC module has its local model  $W^i$  and the aggregated fine-tuned model  $W^A$ . Whenever a new FC module is connected to the environment  $\{FC_m\}_{m=1}^M$ , the aggregated model  $W^A$  will be shared to join the process (step 5) quickly.

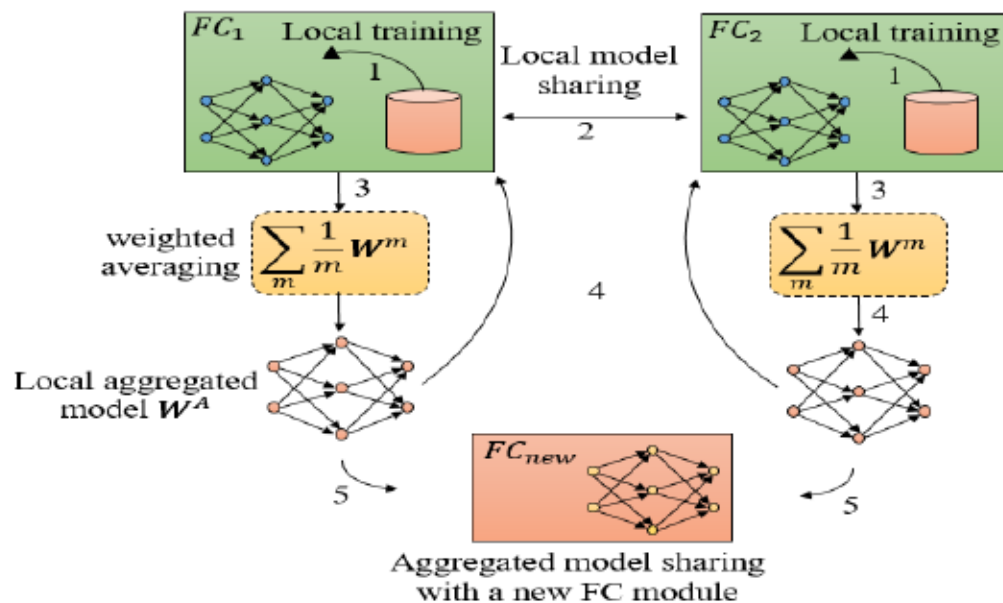


Figure 4-14 Visual representation of the module-to-module FRL algorithm and the learning steps.

#### 4.5.7 Results and Discussions on Numerical case studies

This section explicitly elucidated the optimization results of the fixed horizon and safe-learning-based Dec-MPC frameworks. Dynamic programming (DP) and Cen-MPC are implemented on the same PAS problem for comparison purposes. The result based on DP is accepted as the optimal global solution. The Cen-MPC answer is used to appraise the optimal solution accuracy, convergence speed, and communication performance of the DCO-based MPCs. To quantitatively scrutinize the operation of the proposed methods, the processing times are compared on a desktop PC (Processor= Intel Core i5, 2.30 GHz, RAM= 4 GB, MATLAB R2018). For investigation, a real driving profile from [98] is singled out, as shown in Figure 4-15.

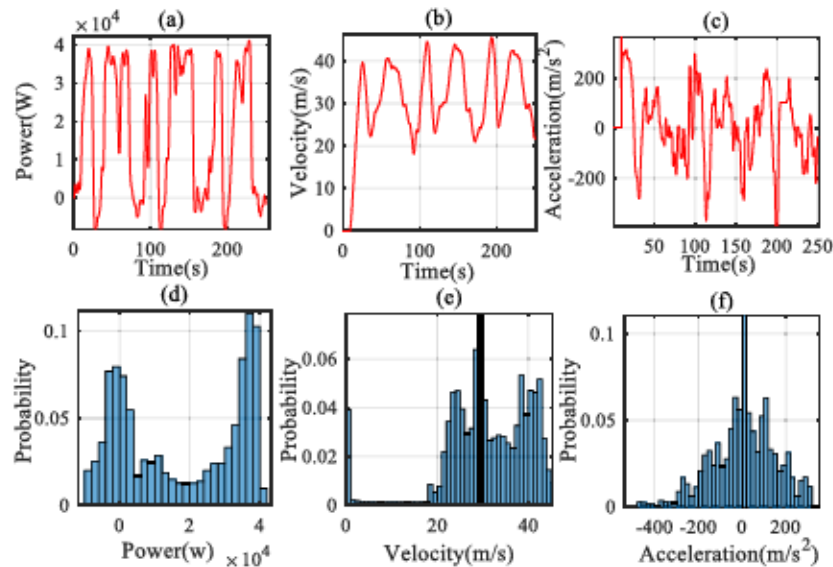


Figure 4-15 The real profile characteristics: (a) power, (b) velocity, (c) acceleration, (d) power distribution, (e) velocity distribution, and (f) acceleration distribution.

#### 4.5.7.1 Regular Operation Optimized Results

The optimized output answers of the powertrain components via Cen-MPC, fixed horizon, and safe-learning Dec-MPCs are illustrated in Figure 4-16. The prediction horizon length  $K$  is selected to be equal to 10 time-step for the Cen-MPC and fixed-horizon Dec-MPC schemes. The maximum moving lookahead horizon  $K$  of the learning-enabled Dec-MPC is also equal to 10 time-steps. It is evident that the power profiles and the SoC curves of the proposed decentralized approaches perfectly follow Cen-MPC with minor errors. For instance, the SoC curves of the fixed horizon and adjustable Dec-MPCs accurately track Cen-MPC with under 0.0571 % and 0.0597 % errors.

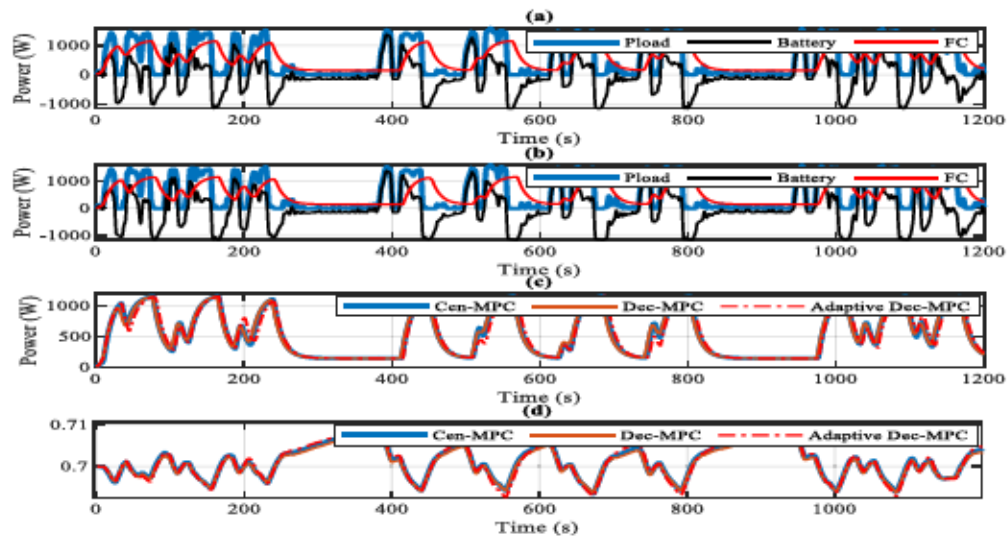


Figure 4-16 Optimized results of the MPC-based approaches: (a) the powers based on Dec-MPC, (b) the powers based on adaptive Dec-MPC, (c) the comparison between the total output modules powers of the FC modules, and (d) the comparison between SoC levels.

Figure 4-17(a) presents the computational time of Cen-MPC and the proposed PASs under the selected real driving profile. As can be observed, the computational times of the fixed horizon and learning-enabled Dec-MPCs take an average of 0.0139s and 0.0096s, respectively, to converge for each execution. In comparison, Cen-MPC takes 0.0233s with the same stopping criteria, which demonstrates the computational complexities are reduced by about 40.4040 % and 58.9062 % compared to Cen-MPC. That is because the proposed decentralized method opens up the possibility to scrutinize feasible management fast-response policies with cooperation between the FC modules that minimize the overall costs of the powertrain while considering the fair distribution of incremental expenses. Figure 4-17 (b) shows that the learning-enabled Dec-MPC iteration is reduced by 11.8384%. In this study, a high-speed solution has been selected for primary convergence conditions of the adaptive-horizon Dec-MPC. If the output power errors deviation from the optimized powers obtained from the benchmark Cen-MPC can be tolerated more, FRL-based Dec-MPC can improve the convergence speed. More iterative iterations would be indispensable if accuracy was selected as the optimization design criterion. Based on the selected cost function, the learning-enabled decentralized scheme reaches an appropriate policy to choose the prediction horizon length optimally. A comparison between the trajectories of the moving look-ahead horizons for the developed MPC-based PASs is presented in Figure 4-17(c). It is evident that different zones of the moving horizon state space ( $P_{avg}, SoC$ ) of adaptive Dec-MPC requires various prediction dimensions to seek nearly optimal powers. The distribution of the moving horizon regarding the prediction length is illustrated in Figure 4-17(d).



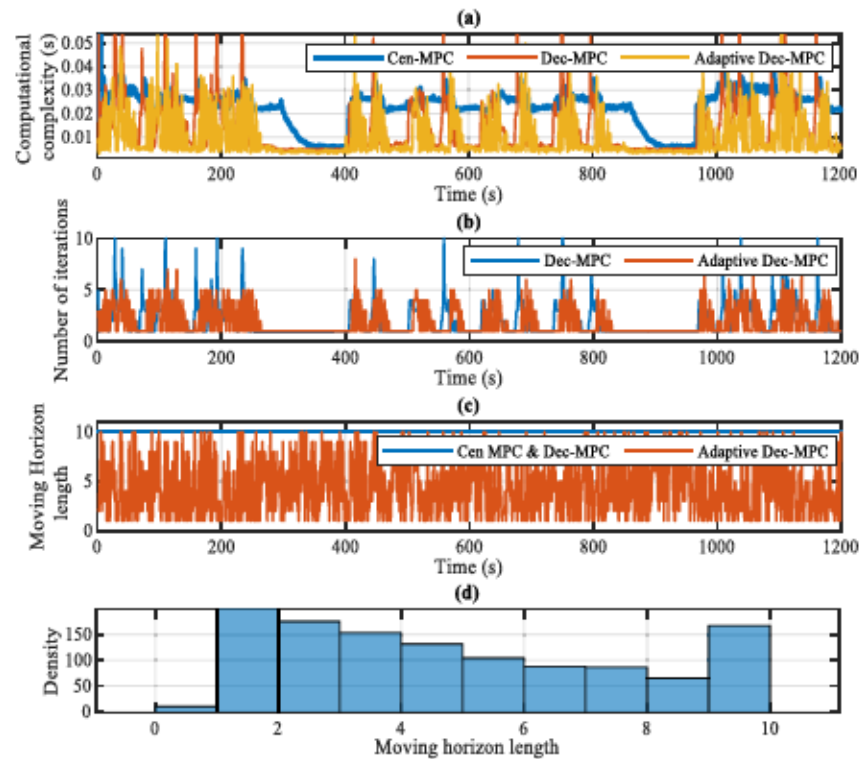


Figure 4-17 (a) The computational complexity of the developed MPC-based approaches, (b) the number of iterations based on the DCO-based MPCs, (c) the moving horizon trajectories, and (d) the distribution of the lookahead horizon decided by the FRL control policy.

The exact final operational costs associated with the proposed decentralized algorithms compared to DP and Cen-MPC are listed in Table 4-III. The final prices of the suggested approaches have achieved a very close performance to the DP results. The final costs based on fixed-horizon and adaptive Dec-MPCs are \$0.0617 and \$0.0628, which are 5.89% and 7.75% greater than DP, respectively. Based on these results, the final costs of the fixed-horizon and adaptive Dec-MPCs are about 1.74% and 3.52% higher than Cen-MPC.

Table 4-III The detailed comparison of computational complexity and final price

	DP	Cen-MPC	Dec-MPC (Fixed-horizon)	Dec-MPC (Adaptive-horizon)
T	-	25.5914	14.6237	9.2473
$S_T$	0.0583	0.0609	0.0617	0.0628

#### 4.5.7.2 Impact of prediction horizon length

This subsection examines how learning the optimal prediction window policies impact the optimization performance and computational complexity of the MPC-based approaches. A comparison of the final costs and the computational complexities based on different prediction horizon lengths (from 2 to 25) are depicted in Figure 4-18. Generally, the final costs and computational complexities demonstrate inverse behaviors as the moving optimization window length increases for all cases. If the prediction moving window length is selected too short, the calculated optimized power values result in unsatisfactory approximations of the infinite horizon result. The execution time of Cen-MPC grows at best linearly with raising the length of the looking-ahead window in comparison with others, significantly when the optimization horizon dimension exceeds 12s. The computational burden of adjustable Dec-MPC is about 61.54% and 76.95% fewer sensitivities than Dec-MPC and centralized one to the length of the moving horizon.

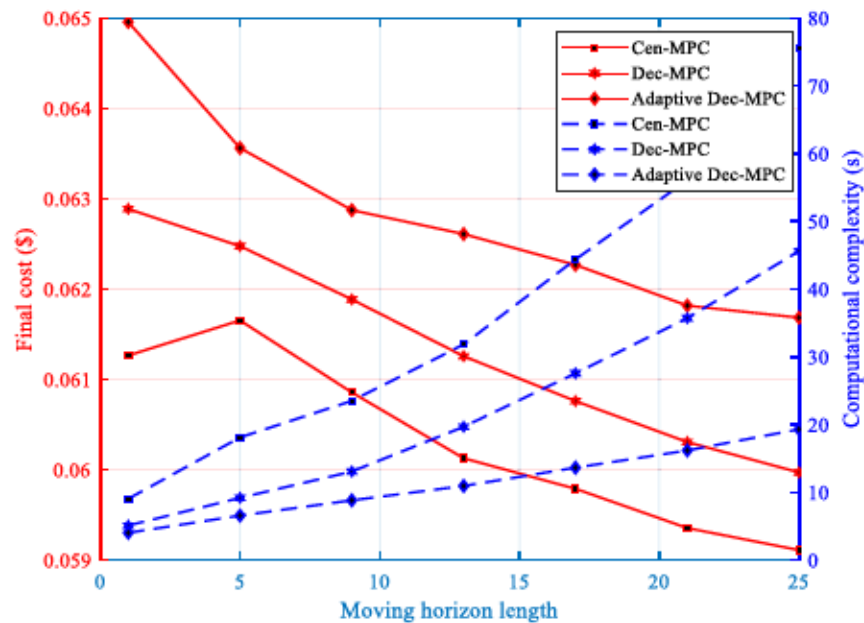


Figure 4-18 Optimal final cost and computational complexity of Cen-MPC, Dec-MPC, and adjustable Dec-MPC as functions of optimization window size.

#### 4.5.8 Experimental implementation

To assess the decentralized lookahead PASs, a small-scale experiment is carried out using the developed modular test bench under the selected real driving profile to verify the previous numerical studies. The output powers and SoC level of the learning-enabled Dec-MPC are presented in Figure 4-19. In addition, the power distributions of the FC modules are illustrated in Figure 4-20. As shown in Figure 4-19 and Figure 4-20, the modules primarily operate close to efficiency zones to diminish the hydrogen economy. The power ramping of the modules met the defined constraints entirely. The battery pack is mainly responsible for charging in the low-power zones and discharging in high-power conditions, offering reduced modules' dimensioning.

Additionally, the battery unit is in charge of balancing the fast-dynamic load fluctuations. The oscillation level of the battery SoC demonstrates that the adaptive Dec-MPC contributes to the cooperation of their two modules to reach the minimum deviations from the initial SoC levels. The total cost of the FRL-based Dec-MPC scheme (\$0.0668) demonstrates an additional charge of 6.32% compared to the simulation result. The computational time of the adaptive Dec-MPC strategy is about 50.07% lower than the Cen-MPC method.

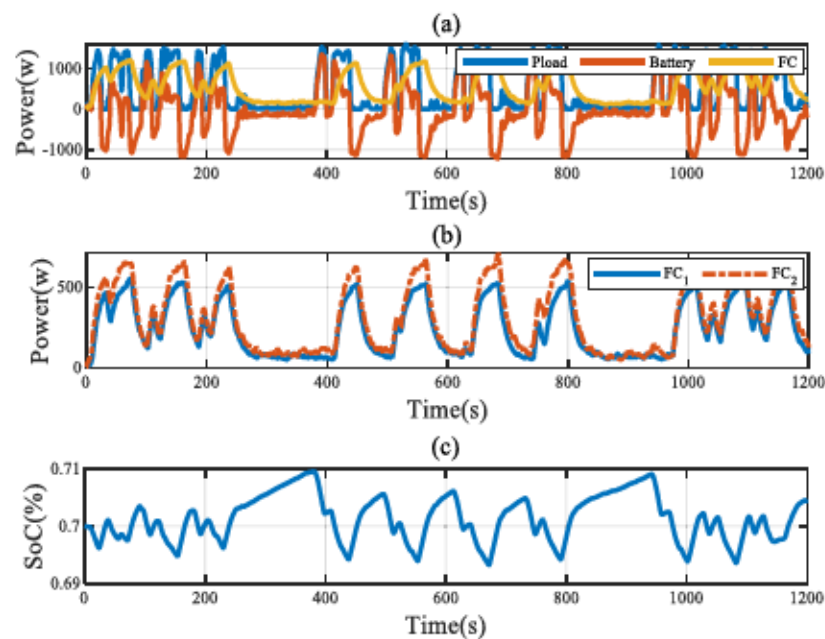


Figure 4-19 The experimental results of the suggested Dec-MPC: (a) the output power profiles, (b) the FC modules' power profiles, and (c) the SoC level fluctuations.



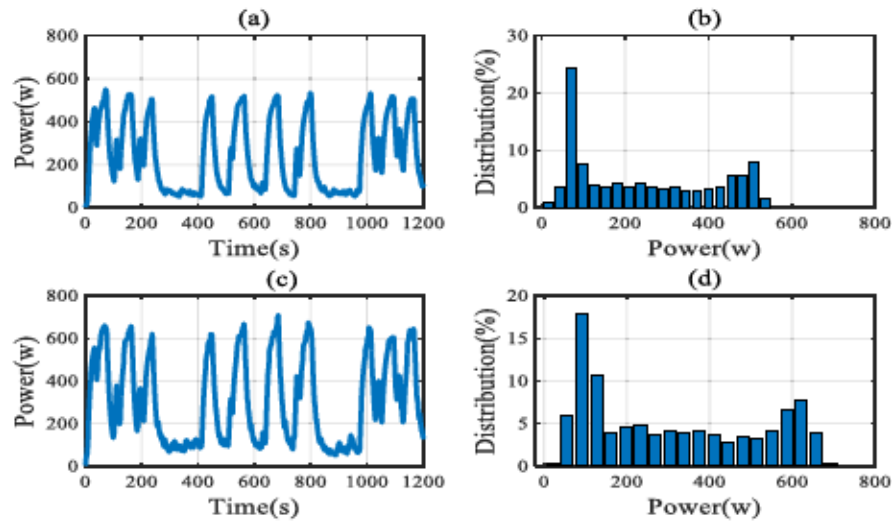


Figure 4-20 The experimental results of the learning-enabled Dec-MPC approach: (a) the power profile of  $FC_1$ , (b) the distribution of  $FC_1$ , (c) the power profile of  $FC_2$ , and (d) the distribution of  $FC_2$ .

#### 4.5.9 Conclusion

This paper presents a look-ahead safe-learning-enabled Dec-MPC for coordinating two FC modules and one battery pack in a FCV application. The cumulative operational cost, which includes the hydrogen consumption and degradation costs, is minimized in a fully decentralized MPC framework. The studied problem is formulated as a multi-step convex problem with several constraints. Then, the decentralized PAS is attained by applying a decomposition scheme based on C-ADMM without any central coordinator. During the DCO-based optimization process, the limitations on the powertrain components are scrutinized by projecting the temporary FC modules powers into the feasible working spaces. Each module communicates with the neighboring one concerning future power responses to

agree on optimal solutions, leading to a higher cost-optimal, robust, and reconfigurable power splitting scheme.

Additionally, to improve the computational time of the Dec-MPC strategy, a learning-based hyperparameter tuning approach is proposed. Several numerical and experimental studies investigate the data processing time efficiencies, convergence performances, final optimal solution precisions, and module-to-module communication necessities of the Dec-MPC methods. The introduced DCO-based procedure will be extended for solving a non-convex PAS optimization problem with uncertainty for future works. Additionally, asynchronous updating features will be explored.

#### 4.5.10 References

- [1] Z. P. Cano, D. Banham, S. Ye, A. Hintennach, J. Lu, M. Fowler, *et al.*, "Batteries and fuel cells for emerging electric vehicle markets," *Nature Energy*, vol. 3, pp. 279-289, 2018/04/01 2018.
- [2] N. Sulaiman, M. A. Hannan, A. Mohamed, E. H. Majlan, and W. R. Wan Daud, "A review on energy management system for fuel cell hybrid electric vehicle: Issues and challenges," *Renewable and Sustainable Energy Reviews*, vol. 52, pp. 802-814, 2015/12/01/ 2015.
- [3] H. S. Das, C. W. Tan, and A. H. M. Yatim, "Fuel cell hybrid electric vehicles: A review on power conditioning units and topologies," *Renewable and Sustainable Energy Reviews*, vol. 76, pp. 268-291, 2017/09/01/ 2017.
- [4] A. K. Soltani, M. Kandidayeni, L. Boulon, and D. L. St-Pierre, "Modular Energy Systems in Vehicular Applications," *Energy Procedia*, vol. 162, pp. 14-23, 2019/04/01/ 2019.
- [5] N. Marx, L. Boulon, F. Gustin, D. Hissel, and K. Agbossou, "A review of multi-stack and modular fuel cell systems: Interests, application areas and on-going research activities," *International Journal of Hydrogen Energy*, vol. 39, pp. 12101-12111, 2014.
- [6] P. Thounthong, B. Davat, S. Rael, and P. Sethakul, "Fuel cell high-power applications," *IEEE Industrial Electronics Magazine*, vol. 3, pp. 32-46, 2009.
- [7] B. Somaiah and V. Agarwal, "Distributed maximum power extraction from fuel cell stack arrays using dedicated power converters in series and parallel configuration," *IEEE Transactions on Energy Conversion*, vol. 31, pp. 1442-1451, 2016.
- [8] X. Han, F. Li, T. Zhang, T. Zhang, and K. Song, "Economic energy management strategy design and simulation for a dual-stack fuel cell electric vehicle," *International Journal of Hydrogen Energy*, vol. 42, pp. 11584-11595, 2017/04/20/ 2017.
- [9] N. Herr, J.-M. Nicod, C. Varnier, L. Jardin, A. Sorrentino, D. Hissel, *et al.*, "Decision process to manage useful life of multi-stacks fuel cell systems under service constraint," *Renewable Energy*, vol. 105, pp. 590-600, 2017/05/01/ 2017.
- [10] A. O. M. Fernandez, M. Kandidayeni, L. Boulon, and H. J. I. T. o. V. T. Chaoui, "An Adaptive State Machine Based Energy Management Strategy for a Multi-Stack Fuel Cell Hybrid Electric Vehicle," 2019.
- [11] Y. Yan, Q. Li, W. Chen, W. Huang, and J. Liu, "Hierarchical Management Control Based on Equivalent Fitting Circle and Equivalent Energy Consumption Method for Multiple Fuel Cells Hybrid Power System," *IEEE Transactions on Industrial Electronics*, vol. 67, pp. 2786-2797, 2019.
- [12] H. Zhang, X. Li, X. Liu, and J. Yan, "Enhancing fuel cell durability for fuel cell plug-in hybrid electric vehicles through strategic power management," *Applied Energy*, vol. 241, pp. 483-490, 2019/05/01/ 2019.
- [13] T. Wang, Q. Li, X. Wang, W. Chen, E. Breaz, and F. Gao, "A Power Allocation Method for Multistack PEMFC System Considering Fuel Cell Performance Consistency," *IEEE Transactions on Industry Applications*, vol. 56, pp. 5340-5351, 2020.
- [14] W. Greenwell and A. Vahidi, "Predictive Control of Voltage and Current in a Fuel Cell-Ultracapacitor Hybrid," *IEEE Transactions on Industrial Electronics*, vol. 57, pp. 1954-1963, 2010.
- [15] B. Geng, J. K. Mills, and D. Sun, "Two-Stage Energy Management Control of Fuel Cell Plug-In Hybrid Electric Vehicles Considering Fuel Cell Longevity," *IEEE Transactions on Vehicular Technology*, vol. 61, pp. 498-508, 2012.
- [16] Amin, R. T. Bambang, A. S. Rohman, C. J. Dronkers, R. Ortega, and A. Sasongko, "Energy Management of Fuel Cell/Battery/Supercapacitor Hybrid Power Sources Using Model Predictive Control," *IEEE Transactions on Industrial Informatics*, vol. 10, pp. 1992-2002, 2014.
- [17] X. Hu, C. Zou, X. Tang, T. Liu, and L. Hu, "Cost-Optimal Energy Management of Hybrid Electric Vehicles Using Fuel Cell/Battery Health-Aware Predictive Control," *IEEE Transactions on Power Electronics*, vol. 35, pp. 382-392, 2020.

- [18] H. He, S. Quan, F. Sun, and Y.-X. J. I. T. o. I. E. Wang, "Model Predictive Control with Lifetime Constraints Based Energy Management Strategy for Proton Exchange Membrane Fuel Cell Hybrid Power Systems," 2020.
- [19] J. Luna, E. Usai, A. Husar, and M. Serra, "Enhancing the efficiency and lifetime of a proton exchange membrane fuel cell using nonlinear model-predictive control with nonlinear observation," *IEEE transactions on Industrial Electronics*, vol. 64, pp. 6649-6659, 2017.
- [20] D. F. Pereira, F. D. C. Lopes, and E. H. Watanabe, "Nonlinear Model Predictive Control for the Energy Management of Fuel Cell Hybrid Electric Vehicles in Real-Time," *IEEE Transactions on Industrial Electronics*, pp. 1-1, 2020.
- [21] S. Liu, Y. Bin, Y. Li, and B. Scheppat, "Hierarchical MPC Control Scheme for Fuel Cell Hybrid Electric Vehicles," *IFAC-PapersOnLine*, vol. 51, pp. 646-652, 2018/01/01/ 2018.
- [22] H. Zheng, J. Wu, W. Wu, and Y. Wang, "Integrated Motion and Powertrain Predictive Control of Intelligent Fuel Cell/Battery Hybrid Vehicles," *IEEE Transactions on Industrial Informatics*, vol. 16, pp. 3397-3406, 2020.
- [23] Y. Zhou, A. Ravey, and M.-C. Péra, "Multi-mode predictive energy management for fuel cell hybrid electric vehicles using Markov driving pattern recognizer," *Applied Energy*, vol. 258, p. 114057, 2020/01/15/ 2020.
- [24] A. J. Conejo, E. Castillo, R. Minguez, and R. Garcia-Bertrand, *Decomposition techniques in mathematical programming: engineering and science applications*: Springer Science & Business Media, 2006.
- [25] R. Olfati-Saber, J. A. Fax, and R. M. Murray, "Consensus and Cooperation in Networked Multi-Agent Systems," *Proceedings of the IEEE*, vol. 95, pp. 215-233, 2007.
- [26] S. Boyd, N. Parikh, and E. Chu, *Distributed optimization and statistical learning via the alternating direction method of multipliers*: Now Publishers Inc, 2011.
- [27] A. Khalatbarisoltani, M. Kandidayeni, L. Boulon, and X. Hu, "Power Allocation Strategy based on Decentralized Convex Optimization in Modular Fuel Cell Systems for Vehicular Applications," *IEEE Transactions on Vehicular Technology*, pp. 1-1, 2020.
- [28] R. S. Sutton and A. G. Barto, *Reinforcement learning: An introduction*: MIT press, 2018.
- [29] W.-S. Lin and C.-H. Zheng, "Energy management of a fuel cell/ultracapacitor hybrid power system using an adaptive optimal-control method," *Journal of Power Sources*, vol. 196, pp. 3280-3289, 2011.
- [30] R. C. Hsu, S.-M. Chen, W.-Y. Chen, and C.-T. Liu, "A reinforcement learning based dynamic power management for fuel cell hybrid electric vehicle," in *2016 Joint 8th International Conference on Soft Computing and Intelligent Systems (SCIS) and 17th International Symposium on Advanced Intelligent Systems (ISIS)*, 2016, pp. 460-464.
- [31] N. P. Reddy, D. Padeloup, M. K. Zadeh, and R. Skjetne, "An intelligent power and energy management system for fuel cell/battery hybrid electric vehicle using reinforcement learning," in *2019 IEEE Transportation Electrification Conference and Expo (ITEC)*, 2019, pp. 1-6.
- [32] X. Lin, B. Zhou, and Y. Xia, "Online recursive power management strategy based on the reinforcement learning algorithm with cosine similarity and a forgetting factor," *IEEE Transactions on Industrial Electronics*, vol. 68, pp. 5013-5023, 2020.
- [33] J. Yuan, L. Yang, and Q. Chen, "Intelligent energy management strategy based on hierarchical approximate global optimization for plug-in fuel cell hybrid electric vehicles," *International Journal of Hydrogen Energy*, vol. 43, pp. 8063-8078, 2018.
- [34] H. Sun, Z. Fu, F. Tao, L. Zhu, and P. Si, "Data-driven reinforcement-learning-based hierarchical energy management strategy for fuel cell/battery/ultracapacitor hybrid electric vehicles," *Journal of Power Sources*, vol. 455, p. 227964, 2020.
- [35] G. Dulac-Arnold, D. Mankowitz, and T. Hester, "Challenges of real-world reinforcement learning," *arXiv preprint arXiv:1904.12901*, 2019.
- [36] H. Zhang, J. Peng, H. Tan, H. Dong, and F. Ding, "A Deep Reinforcement Learning Based Energy Management Framework with Lagrangian Relaxation for Plug-in Hybrid Electric Vehicle," *IEEE Transactions on Transportation Electrification*, 2020.
- [37] E. Behn, S. Gros, S. Moe, and T. A. Johansen, "Reinforcement Learning of the Prediction Horizon in Model Predictive Control," *arXiv preprint arXiv:2102.11122*, 2021.
- [38] T. Koller, F. Berkenkamp, M. Turchetta, and A. Krause, "Learning-based model predictive control for safe exploration," in *2018 IEEE conference on decision and control (CDC)*, 2018, pp. 6059-6066.
- [39] M. Zanon and S. Gros, "Safe reinforcement learning using robust MPC," *IEEE Transactions on Automatic Control*, 2020.
- [40] L. Wen, J. Duan, S. E. Li, S. Xu, and H. Peng, "Safe reinforcement learning for autonomous vehicles through parallel constrained policy optimization," in *2020 IEEE 23rd International Conference on Intelligent Transportation Systems (ITSC)*, 2020, pp. 1-7.
- [41] M. Alshiekh, R. Bloem, R. Ehlers, B. Könighofer, S. Niekum, and U. Topcu, "Safe reinforcement learning via shielding," in *Thirty-Second AAAI Conference on Artificial Intelligence*, 2018.
- [42] N. Jansen, B. Könighofer, S. Junges, A. Serban, and R. Bloem, "Safe reinforcement learning using probabilistic shields," 2020.
- [43] F. Berkenkamp, M. Turchetta, A. P. Schoellig, and A. Krause, "Safe model-based reinforcement learning with stability guarantees," *arXiv preprint arXiv:1705.08551*, 2017.
- [44] F. Martel, S. Kelouwani, Y. Dubé, and K. Agbossou, "Optimal economy-based battery degradation management dynamics for fuel-cell plug-in hybrid electric vehicles," *Journal of Power Sources*, vol. 274, pp. 367-381, 2015/01/15/ 2015.
- [45] S. Satyapal, "US Department of energy hydrogen and fuel cell technology overview," *Presented at The 14th International Hydrogen and Fuel Cell Expo (FC EXPO 2018)*, 2018.
- [46] T. Benjamin, R. Borup, N. Garland, C. Gittleman, B. Habibzadeh, and S. Hirano, "Fuel Cell Technical Team Roadmap," *Energy.gov (Office of Energy Efficiency & Renewable Energy)*, 2017.
- [47] H. Chen, P. Pei, and M. Song, "Lifetime prediction and the economic lifetime of Proton Exchange Membrane fuel cells," *Applied Energy*, vol. 142, pp. 154-163, 2015/03/15/ 2015.
- [48] K. Mongird, V. V. Viswanathan, P. J. Balducci, M. J. E. Alam, V. Fotedar, V. S. Koritarov, *et al.*, "Energy Storage Technology and Cost Characterization Report," Pacific Northwest National Lab.(PNNL), Richland, WA (United States)2019.
- [49] S. Boyd, N. Parikh, E. Chu, B. Peleato, and J. Eckstein, "Distributed optimization and statistical learning via the alternating direction method of multipliers," *Foundations and Trends® in Machine Learning*, vol. 3, pp. 1-122, 2011.
- [50] C. J. Watkins and P. Dayan, "Q-learning," *Machines learning*, vol. 8, pp. 279-292, 1992.
- [51] J. Solano, S. Jemei, L. Boulon, L. Silva, D. Hissel, and M.-C. Pera, "IEEE VTS Motor Vehicles Challenge 2020-Energy Management of a Fuel Cell/Ultracapacitor/Lead-Acid Battery Hybrid Electric Vehicle," in *2019 IEEE Vehicle Power and Propulsion Conference (VPPC)*, 2019, pp. 1-6.



## **Chapitre 5 - Conclusion and Future Directions**

### **5.1 Outline of the Research Achievements**

Contrary to traditional centralized EMSs, this Ph.D. thesis principally concentrated on the possibility of embedding a fully decentralized power-splitting scheme into the real-time multi-objective decision-making strategy to explore additional performance improvement concerning the modularity and flexibility (plug and play) by decomposing the optimization problem besides considering hydrogen economy, FCS, and battery unit lifetime prolongation.

First, the related research literature on the multi-stack FCV and centralized EMSs was thoroughly reviewed. Then, by analyzing the benefits and weaknesses of existing centralized approaches, a decentralized convex optimization scheme was introduced for real-time power allocation purposes because of its capacity to contribute modularity and flexibility (plug and play) for heterogeneous time-varying constrained optimization problems. After that, the following influential contributions were introduced via this dissertation to bridge the gaps versus existing research.

First, a decentralized optimization strategy for the power allocation decision-making problem was proposed to prove the concept. Numerical and experimental results have shown that the introduced decentralized approach outperformed the benchmark EMSs in computational time, achieving very close accuracy compared to the centralized ones.



After that, a comprehensive comparison of two decomposing-based power-splitting methods was conducted to explore further the benefits and the potential impacts of the decentralized optimization framework on EMS performance, such as parameter sensibility and robustness. This study established a solid basis for realizing an exemplary algorithm for the decentralized EMS framework.

Next, a look-ahead EMS based on decentralized convex optimization was devised to combine the predictive information with the introduced power allocation in the previous step. In addition, with the assistance of a multi-agent federated reinforcement learning algorithm, a learning-based tuning approach was established to optimally seek the best hyperparameters based on the SoC level and the future behaviors of the FCV over each decentralized rolling optimization horizon.

## **5.2 Outlook and Future Research Trends for Decentralized EMS**

As far as we have discussed in this thesis, it is clear that the upcoming future for fuel cell technologies is very bright but needs tremendous attention to push them to a higher standard. This thesis provides a more flexible (plug-and-play) and modular system with high reliabilities. Until now, the efforts made could be as light for future studies in this newly developed field to make it possible to be applicable in the next generation of FCVs. Notwithstanding the signs of development regarding the decentralized EMSs in this thesis, multiple forward-looking and revolutionary strategies should be developed to improve the proposed scheme's performance. To encourage more innovative ideas, future works on the decentralized approach would be possible to focus on the following perspectives:

### *5.2.1 Integrating Advanced Modeling Methods*

Accurate modeling methods of the modular powertrain components are crucial for enhancing the FCVs' EMS efficiency. Although simple modeling approaches are used in the thesis, they cannot fully reflect each powertrain module's complexity and nonlinearity characteristics. Using measured and recorded data, several advanced modeling techniques based on data-driven strategies should be introduced to improve power source modeling. Thus, considering these advanced modeling methods in the developed decentralized EMS needs further investigation.

Auxiliary systems, such as air conditioning and cooling systems, power conditioning systems, power steering, and electronic boards, consume energy during FCV operation conditions. In addition, the auxiliary components of the FCS, such as compressors, fans, and pumps, also consume some part of the generated power. However, in the modeling and designing process of the developed EMSs, these power consumptions and losses were ignored or treated as a constant. This ignorance can lead to inaccuracies, specifically for heavy-duty multi-stack FCV applications. From this perspective, taking these losses is an essential aspect for improving the established decentralized EMS performance.

Because keeping the decentralized strategy as simple as possible, all the models are considered fixed and valid during all examinations. However, the central fact is that these parameters are changing and are very sensitive to other factors such as temperature, humidity, the purity of the consumed hydrogen, etc. So one direction could be to include different advanced model updating approaches to push the developed decentralized strategies in this regard.

### *5.2.2 Including Fault Diagnosis and Fault-Tolerant Control*

As one of the growing trends in fuel cell application, the fault-tolerant control topic is explored in many research studies. Fault and failure modes in a FCS can result in performance decline and severe safety concerns. In this regard, fault-tolerant control is introduced to satisfy the performance desires and keep a safe operation in fault occurrence [99]. The essential missing point is that most developed methods are for a centralized system. The fault diagnosis and tolerant approaches based on the centralized structures are not preferred for interconnected and multi-fuel cell systems because such methods need sensing, processing, and communication of many variables measured from the different components of the powertrain system. A multi-stack with a decentralized control scheme may need decentralized fault detection, fault isolation, diagnosis tools, and a decision-making structure to manage the powertrain system and control an irregular operation system. It could be a network of several local fault detectors, which screens each FC module employing only the local measured information. Each under-control module could provide helpful information for neighbors to share and process for future decisions. Shifting into a decentralized fault-tolerant scheme may reduce the need for communication, simplify the fault control problem, and improve general performance. Therefore, developing a decentralized EMS enabled with a decentralized fault-tolerant control method could be one of the possible future works that could be done to reach a safer and more reliable modular powertrain configuration.

### *5.2.3 Co-optimization and integration of different objectives*

This thesis only considered hydrogen consumption and degradation (FC and battery) costs. However, other advanced goals that may enhance the general operating performance were not considered along with the decentralized EMSs. An exciting optimization point for

the future possible direction of the developed decentralized optimization schemes could be to advance the cooperation level of the modular system. Specific optimization techniques, such as cooperative game theory, can be combined and implemented in the developed method. For instance, encouraging the modules may be more beneficial as the decision-makers share their benefits to reduce the total team cost. Another more exciting direction could be including machine-learning methods with the game theory approach to solve this optimization problem more efficiently. A security-constrained control strategy seems to be necessary for a modular FCV powertrain to guarantee robustness and reliability under possible disturbances and malfunctions.

Because of the inadequate durability of FCS, the prognostic and health management approaches used to achieve a longer life have recently gained considerable attention. Prognostics and health management (PHM) techniques have been introduced to estimate the remaining useful life (RUL)'s health state [100, 101]. Substantial attention should be given to developing reliable health indicators and integrating the accurate degradation model into a well-designed decision-making strategy. The health management approach of a decentralized system could be more challenging and need to be implemented cautiously, which needs attention from researchers and professionals in this field.

One of the principal hypotheses in the thesis's optimization problem is that all the modules are selected to be the same size. As it is self-evident, the power-allocation problem cannot be optimally solved without including the size and dimension of the powertrain components because each of the FCV owners can have specific driving behaviors with its unique driving pattern. Therefore, the sizing and power-sharing decision-making problems need to be considered simultaneously.



A modular system by integrating the decentralized concept will offer more flexibility than a centralized one. To enhance the market penetration of the FCV in the new future, it may be more attractive to move forward into a customer-based production system. Each driver should select a customized FCV that is more suitable regarding the historical data and driving pattern. Thus, more investigation needs to be done to reach an economical and cost-optimal configuration from both short-term and long-term perspectives for the manufacturers and car owners.

Integrating uncertainty knowledge into the optimization problem is an exciting area of research that has mainly escaped the attention of researchers in the electrified vehicle domain. In the coming years, because of the increasing trend toward green hydrogen production and including sustainable energy sources (wind turbines and solar panels), constant hydrogen production will be more challenging, and more hydrogen cost fluctuation will be observed. Stochastic optimization approaches can be applied to address this issue, and one of the fascinating techniques is chance-constrained optimization. Investigating how to model this trajectory and integrating it into the proposed optimization method would be exciting for the scientific research sectors.

This thesis solves the EMS optimization problem relatively quickly under a single driving profile in a single FCV. However, considering a trip ahead and facilities (refueling stations and parking places) is necessary for a more general scheduling problem. This concept could be included by shifting from a decentralized short time-scale EMS with a single FCV into a longer time-scale with multi FCVs for further work.

One of the future research trends of the modular and decentralized EMS lies in integrating advanced AI and machine learning methods, like NN, SVM, Bayesian inference, RL, deep

NN, and deep reinforcement learning (DRL), into the control strategy. Among these approaches, the RL and DRL methods are essential subjects that catch much attention from academic researchers [102]. Therefore, applying these algorithms and integrating these approaches into the decentralized and modular EMSs should be further addressed in future works.

From an energy perspective, the central concept of eco-driving is to seek the best and optimal way to reduce energy consumption by optimizing velocity trajectory [103]. However, the current literature on eco-driving generally focuses on the HEVs and EVs and rarely considers the EMS of FCVs. Therefore, the eco-driving concept is an important subject to consider for integrating the developed decentralized EMS in the future. Based on this idea, an eco-driving hierarchical controller could be designed to assist the decentralized scheme to follow the best trajectory and improve operational performance.

#### *5.2.4 Improving the implementation capabilities of the proposed decentralized method*

Other missing aspects of the newly developed decentralized methods are how implementable these techniques are in the current prototypes or future FCVs and whether the control units can run these algorithms. An essential step to solving this deficiency of the proposed method in the thesis is to design a cheaper and easier decentralized algorithm for the available processors. One of the straightforward solutions is to simplify the control strategy without losing its operation efficiency. Another option could be to allocate some part of the analysis in a cloud-based and use the information to control the modules. Another forward-looking step could include different communication technologies using cables or wireless communication. When shifting to wireless communication, the flexibility of the modular system will be improved, and the system can be easily fitted with any developed

chassis reconfiguration. It can be easily reconfigured whenever necessary for the new structure; however, several important points must be considered at this stage. For instance, it is very likely that either command signals or measured variables be damaged by noise and affect the management process of the FCVs. Another implementation point that needs to be considered is how the CAN bus can be involved in the modular powertrain project to have a more robust communication channel.

## References

- [1] N. Marx, L. Boulon, F. Gustin, D. Hissel, and K. Agbossou, "A review of multi-stack and modular fuel cell systems: Interests, application areas and on-going research activities," *International Journal of Hydrogen Energy*, vol. 39, no. 23, pp. 12101-12111, 2014.
- [2] J. Garnier *et al.*, "Study of a PEFC power generator modular architecture based on a multi-stack association," *Journal of Power Sources*, vol. 156, no. 1, pp. 108-113, 2006/05/19/ 2006, doi: <https://doi.org/10.1016/j.jpowsour.2005.08.031>.
- [3] D. Candusso *et al.*, "Fuel cell operation under degraded working modes and study of diode by-pass circuit dedicated to multi-stack association," *Energy Conversion and Management*, vol. 49, no. 4, pp. 880-895, 2008/04/01/ 2008, doi: <https://doi.org/10.1016/j.enconman.2007.10.007>.
- [4] A. De Bernardinis, M.-C. Péra, J. Garnier, D. Hissel, G. Coquery, and J.-M. Kauffmann, "Fuel cells multi-stack power architectures and experimental validation of 1kW parallel twin stack PEFC generator based on high frequency magnetic coupling dedicated to on board power unit," *Energy Conversion and Management*, vol. 49, no. 8, pp. 2367-2383, 2008/08/01/ 2008, doi: <https://doi.org/10.1016/j.enconman.2008.01.022>.
- [5] P. Thounthong, B. Davat, S. Rael, and P. Sethakul, "Fuel cell high-power applications," *IEEE Industrial Electronics Magazine*, vol. 3, no. 1, pp. 32-46, 2009, doi: 10.1109/MIE.2008.930365.
- [6] L. Palma and P. N. Enjeti, "A Modular Fuel Cell, Modular DC-DC Converter Concept for High Performance and Enhanced Reliability," *IEEE Transactions on Power Electronics*, vol. 24, no. 6, pp. 1437-1443, 2009, doi: 10.1109/TPEL.2009.2012498.
- [7] L. Boulon, A. Bouscayrol, D. Hissel, O. Pape, and M. Pera, "Inversion-Based Control of a Highly Redundant Military HEV," *IEEE Transactions on Vehicular Technology*, vol. 62, no. 2, pp. 500-510, 2013, doi: 10.1109/TVT.2012.2226219.
- [8] J. Cardozo, N. Marx, L. Boulon, and D. Hissel, "Comparison of Multi-Stack Fuel Cell System Architectures for Residential Power Generation Applications Including Electrical Vehicle Charging," in *2015 IEEE Vehicle Power and Propulsion Conference (VPPC)*, 19-22 Oct. 2015 2015, pp. 1-6, doi: 10.1109/VPPC.2015.7352912.
- [9] N. Marx, D. C. T. Cárdenas, L. Boulon, F. Gustin, and D. Hissel, "Degraded mode operation of multi-stack fuel cell systems," *IET Electrical Systems in Transportation*, vol. 6, no. 1, pp. 3-11, 2016, doi: 10.1049/iet-est.2015.0012.
- [10] M. Becherif, F. Claude, T. Hervier, and L. Boulon, "Multi-stack Fuel Cells Powering a Vehicle," *Energy Procedia*, vol. 74, pp. 308-319, 2015/08/01/ 2015, doi: <https://doi.org/10.1016/j.egypro.2015.07.613>.
- [11] L. Palma and P. Enjeti, "A Modular Fuel Cell, Modular DC-DC Converter Concept



- for High Performance and Enhanced Reliability," in *2007 IEEE Power Electronics Specialists Conference*, 17-21 June 2007 2007, pp. 2633-2638, doi: 10.1109/PESC.2007.4342432.
- [12] J. Liu and E. Zio, "Prognostics of a multistack PEMFC system with multiagent modeling," *Energy Science & Engineering*, vol. 7, no. 1, pp. 76-87, 2019, doi: 10.1002/ese3.254.
- [13] A. K. Soltani, M. Kandidayeni, L. Boulon, and D. L. St-Pierre, "Modular Energy Systems in Vehicular Applications," *Energy Procedia*, vol. 162, pp. 14-23, 2019/04/01/ 2019, doi: <https://doi.org/10.1016/j.egypro.2019.04.003>.
- [14] N. Ghaviha, J. Campillo, M. Bohlin, and E. Dahlquist, "Review of Application of Energy Storage Devices in Railway Transportation," *Energy Procedia*, vol. 105, pp. 4561-4568, 2017/05/01/ 2017, doi: <https://doi.org/10.1016/j.egypro.2017.03.980>.
- [15] Y. Han, Q. Li, T. Wang, W. Chen, and L. Ma, "Multisource Coordination Energy Management Strategy Based on SOC Consensus for a PEMFC, Battery & Supercapacitor Hybrid Tramway," *IEEE Transactions on Vehicular Technology*, vol. 67, no. 1, pp. 296-305, 2018, doi: 10.1109/TVT.2017.2747135.
- [16] "New fuel cell bus will be in service in Hamburg next year  
." <http://media.daimler.com/marsMediaSite/en/instance/ko/New-fuel-cell-bus-will-be-in-service-in-Hamburg-next-year.xhtml?oid=9908536> (accessed).
- [17] J. Mulot *et al.*, "Fuel cell system integration into a heavy-duty hybrid vehicle: preliminary experimental results," in *2010 IEEE Vehicle Power and Propulsion Conference*, 1-3 Sept. 2010 2010, pp. 1-5, doi: 10.1109/VPPC.2010.5729076.
- [18] L. Xu, J. Li, J. Hua, X. Li, and M. Ouyang, "Adaptive supervisory control strategy of a fuel cell/battery-powered city bus," *Journal of Power Sources*, vol. 194, no. 1, pp. 360-368, 2009/10/20/ 2009, doi: <https://doi.org/10.1016/j.jpowsour.2009.04.074>.
- [19] E. Ovrum. "Shipping industry eyeing hydrogen fuel cells as possible pathway to emissions reduction; work by Germanischer Lloyd and DNV  
." <http://www.greencarcongress.com/2012/09/h2shipping-20120907.html> (accessed).
- [20] L. Luckose, H. L. Hess, and B. K. Johnson, "Fuel cell propulsion system for marine applications," in *2009 IEEE Electric Ship Technologies Symposium*, 20-22 April 2009 2009, pp. 574-580, doi: 10.1109/ESTS.2009.4906569.
- [21] M. Shin, D.-H. Choi, and J. Kim, "Cooperative management for PV/ESS-enabled electric vehicle charging stations: A multiagent deep reinforcement learning approach," *IEEE Transactions on Industrial Informatics*, vol. 16, no. 5, pp. 3493-3503, 2019.
- [22] J. J. de-Troya, C. Álvarez, C. Fernández-Garrido, and L. Carral, "Analysing the possibilities of using fuel cells in ships," *International Journal of Hydrogen Energy*, vol. 41, no. 4, pp. 2853-2866, 2016/01/30/ 2016, doi: <https://doi.org/10.1016/j.ijhydene.2015.11.145>.
- [23] P. Aguiar, D. J. L. Brett, and N. P. Brandon, "Solid oxide fuel cell/gas turbine hybrid system analysis for high-altitude long-endurance unmanned aerial vehicles," *International Journal of Hydrogen Energy*, vol. 33, no. 23, pp. 7214-7223, 2008/12/01/ 2008, doi: <https://doi.org/10.1016/j.ijhydene.2008.09.012>.
- [24] J. Kallo, "DLR leads HY4 project for four-seater fuel cell aircraft," *Fuel Cells Bulletin*, vol. 2015, no. 11, p. 13, 2015/11/01/ 2015, doi: [https://doi.org/10.1016/S1464-2859\(15\)30362-X](https://doi.org/10.1016/S1464-2859(15)30362-X).
- [25] F. Martel, S. Kelouwani, Y. Dubé, and K. Agbossou, "Optimal economy-based battery

- degradation management dynamics for fuel-cell plug-in hybrid electric vehicles," *Journal of Power Sources*, vol. 274, pp. 367-381, 2015/01/15/ 2015, doi: <https://doi.org/10.1016/j.jpowsour.2014.10.011>.
- [26] C. H. Choi *et al.*, "Development and demonstration of PEM fuel-cell-battery hybrid system for propulsion of tourist boat," *International Journal of Hydrogen Energy*, vol. 41, no. 5, pp. 3591-3599, 2016/02/09/ 2016, doi: <https://doi.org/10.1016/j.ijhydene.2015.12.186>.
- [27] X. Han, F. Li, T. Zhang, T. Zhang, and K. Song, "Economic energy management strategy design and simulation for a dual-stack fuel cell electric vehicle," *International Journal of Hydrogen Energy*, vol. 42, no. 16, pp. 11584-11595, 2017/04/20/ 2017, doi: <https://doi.org/10.1016/j.ijhydene.2017.01.085>.
- [28] B. Somaiah and V. Agarwal, "Distributed maximum power extraction from fuel cell stack arrays using dedicated power converters in series and parallel configuration," *IEEE Transactions on Energy Conversion*, vol. 31, no. 4, pp. 1442-1451, 2016.
- [29] H. S. M. Ramadan, Q. de Bortoli, M. Becherif, and F. Claude, "Multi-stack fuel cell efficiency enhancement based on thermal management," *IET Electrical Systems in Transportation*, vol. 7, no. 1, pp. 65-73, 2016.
- [30] N. Herr *et al.*, "Decision process to manage useful life of multi-stacks fuel cell systems under service constraint," *Renewable Energy*, vol. 105, pp. 590-600, 2017/05/01/ 2017, doi: <https://doi.org/10.1016/j.renene.2017.01.001>.
- [31] N. Marx, D. Hissel, F. Gustin, L. Boulon, and K. Agbossou, "On the sizing and energy management of an hybrid multistack fuel cell – Battery system for automotive applications," *International Journal of Hydrogen Energy*, vol. 42, no. 2, pp. 1518-1526, 2017/01/12/ 2017, doi: <https://doi.org/10.1016/j.ijhydene.2016.06.111>.
- [32] A. O. M. Fernandez, M. Kandidayeni, L. Boulon, and H. J. I. T. o. V. T. Chaoui, "An Adaptive State Machine Based Energy Management Strategy for a Multi-Stack Fuel Cell Hybrid Electric Vehicle," 2019.
- [33] T. Wang, Q. Li, L. Yin, and W. Chen, "Hydrogen consumption minimization method based on the online identification for multi-stack PEMFCs system," *International Journal of Hydrogen Energy*, vol. 44, no. 11, pp. 5074-5081, 2019/02/26/ 2019, doi: <https://doi.org/10.1016/j.ijhydene.2018.09.181>.
- [34] Y. Yan, Q. Li, W. Chen, W. Huang, and J. Liu, "Hierarchical Management Control Based on Equivalent Fitting Circle and Equivalent Energy Consumption Method for Multiple Fuel Cells Hybrid Power System," *IEEE Transactions on Industrial Electronics*, vol. 67, no. 4, pp. 2786-2797, 2019.
- [35] H. Zhang, X. Li, X. Liu, and J. Yan, "Enhancing fuel cell durability for fuel cell plug-in hybrid electric vehicles through strategic power management," *Applied Energy*, vol. 241, pp. 483-490, 2019/05/01/ 2019, doi: <https://doi.org/10.1016/j.apenergy.2019.02.040>.
- [36] L. Bakule, "Decentralized control: An overview," *Annual Reviews in Control*, vol. 32, no. 1, pp. 87-98, 2008/04/01/ 2008, doi: <https://doi.org/10.1016/j.arcontrol.2008.03.004>.
- [37] Z. Cheng, J. Duan, and M. Chow, "To Centralize or to Distribute: That Is the Question: A Comparison of Advanced Microgrid Management Systems," *IEEE Industrial Electronics Magazine*, vol. 12, no. 1, pp. 6-24, 2018, doi: 10.1109/MIE.2018.2789926.
- [38] H. Yin, C. Zhao, and C. Ma, "Decentralized Real-Time Energy Management for a



- Reconfigurable Multiple-Source Energy System," *IEEE Transactions on Industrial Informatics*, vol. 14, no. 9, pp. 4128-4137, 9/1/2018 2018, doi: 10.1109/tii.2018.2827466.
- [39] H. Yin, C. Zhao, M. Li, C. Ma, and M.-Y. Chow, "A Game Theory Approach to Energy Management of An Engine-Generator/Battery/Ultracapacitor Hybrid Energy System," *IEEE Transactions on Industrial Electronics*, vol. 63, no. 7, pp. 4266-4277, 7/1/2016 2016, doi: 10.1109/TIE.2016.2539245.
- [40] Q. Li, T. Wang, C. Dai, W. Chen, and L. Ma, "Power Management Strategy Based on Adaptive Droop Control for a Fuel Cell-Battery-Supercapacitor Hybrid Tramway," *IEEE Transactions on Vehicular Technology*, vol. 67, no. 7, pp. 5658-5670, 2018, doi: 10.1109/TVT.2017.2715178.
- [41] D. K. Molzahn *et al.*, "A Survey of Distributed Optimization and Control Algorithms for Electric Power Systems," *IEEE Transactions on Smart Grid*, vol. 8, no. 6, pp. 2941-2962, 2017, doi: 10.1109/TSG.2017.2720471.
- [42] A. Kargarian *et al.*, "Toward Distributed/Decentralized DC Optimal Power Flow Implementation in Future Electric Power Systems," *IEEE Transactions on Smart Grid*, vol. 9, no. 4, pp. 2574-2594, 2018, doi: 10.1109/TSG.2016.2614904.
- [43] D. P. Bertsekas and A. Scientific, *Convex optimization algorithms*. Athena Scientific Belmont, 2015.
- [44] A. J. Conejo and J. A. Aguado, "Multi-area coordinated decentralized DC optimal power flow," *IEEE transactions on power systems*, vol. 13, no. 4, pp. 1272-1278, 1998.
- [45] G. Cohen, "Auxiliary problem principle and decomposition of optimization problems," *Journal of optimization Theory and Applications*, vol. 32, no. 3, pp. 277-305, 1980.
- [46] Z. Zhang and M.-Y. Chow, "Convergence analysis of the incremental cost consensus algorithm under different communication network topologies in a smart grid," *IEEE Transactions on Power Systems*, vol. 27, no. 4, pp. 1761-1768, 2012.
- [47] F. J. Nogales, F. J. Prieto, and A. J. Conejo, "A decomposition methodology applied to the multi-area optimal power flow problem," *Annals of operations research*, vol. 120, no. 1, pp. 99-116, 2003.
- [48] D. Gabay and B. Mercier, "A dual algorithm for the solution of nonlinear variational problems via finite element approximation," *Computers & mathematics with applications*, vol. 2, no. 1, pp. 17-40, 1976.
- [49] S. Boyd, N. Parikh, E. Chu, B. Peleato, and J. Eckstein, "Distributed optimization and statistical learning via the alternating direction method of multipliers," *Foundations and Trends® in Machine learning*, vol. 3, no. 1, pp. 1-122, 2011.
- [50] W. Deng, M.-J. Lai, Z. Peng, and W. Yin, "Parallel multi-block ADMM with  $O(1/k)$  convergence," *Journal of Scientific Computing*, vol. 71, no. 2, pp. 712-736, 2017.
- [51] L. Liu and Z. Han, "Multi-block ADMM for big data optimization in smart grid," in *2015 International Conference on Computing, Networking and Communications (ICNC)*, 2015: IEEE, pp. 556-561.
- [52] S. East and M. Cannon, "Fast Optimal Energy Management With Engine On/Off Decisions for Plug-in Hybrid Electric Vehicles," presented at the IEEE Control Systems Letters, 10/1/2019, 2019. [Online]. Available: <https://academic.microsoft.com/paper/2947922664>.
- [53] S. East and M. Cannon, "Energy Management in Plug-In Hybrid Electric Vehicles:

- Convex Optimization Algorithms for Model Predictive Control," *IEEE Transactions on Control Systems and Technology*, pp. 1-13, 1/1/2019 2019, doi: 10.1109/tcst.2019.2933793.
- [54] Z. Zhang and M. Chow, "Convergence Analysis of the Incremental Cost Consensus Algorithm Under Different Communication Network Topologies in a Smart Grid," *IEEE Transactions on Power Systems*, vol. 27, no. 4, pp. 1761-1768, 2012, doi: 10.1109/TPWRS.2012.2188912.
- [55] Y. Wang, L. Wu, and S. Wang, "A Fully-Decentralized Consensus-Based ADMM Approach for DC-OPF With Demand Response," *IEEE Transactions on Smart Grid*, vol. 8, no. 6, pp. 2637-2647, 2017, doi: 10.1109/TSG.2016.2532467.
- [56] H. Koptez, "Real-time systems: design principles for distributed embedded applications," ed: Kluwer Academic Publisher, 1997.
- [57] A. Khalatbarisoltani, M. Kandidayeni, L. Boulon, and X. Hu, "Power Allocation Strategy Based on Decentralized Convex Optimization in Modular Fuel Cell Systems for Vehicular Applications," *IEEE Transactions on Vehicular Technology*, vol. 69, no. 12, pp. 14563-14574, 2020, doi: 10.1109/TVT.2020.3028089.
- [58] J. Garcia and F. Fernández, "A comprehensive survey on safe reinforcement learning," *Journal of Machine Learning Research*, vol. 16, no. 1, pp. 1437-1480, 2015.
- [59] Z. P. Cano *et al.*, "Batteries and fuel cells for emerging electric vehicle markets," *Nature Energy*, vol. 3, no. 4, pp. 279-289, 2018/04/01 2018, doi: 10.1038/s41560-018-0108-1.
- [60] N. Sulaiman, M. A. Hannan, A. Mohamed, E. H. Majlan, and W. R. Wan Daud, "A review on energy management system for fuel cell hybrid electric vehicle: Issues and challenges," *Renewable and Sustainable Energy Reviews*, vol. 52, pp. 802-814, 2015/12/01/ 2015, doi: <https://doi.org/10.1016/j.rser.2015.07.132>.
- [61] H. S. Das, C. W. Tan, and A. H. M. Yatim, "Fuel cell hybrid electric vehicles: A review on power conditioning units and topologies," *Renewable and Sustainable Energy Reviews*, vol. 76, pp. 268-291, 2017/09/01/ 2017, doi: <https://doi.org/10.1016/j.rser.2017.03.056>.
- [62] T. Wang, Q. Li, X. Wang, W. Chen, E. Breaz, and F. Gao, "A Power Allocation Method for Multistack PEMFC System Considering Fuel Cell Performance Consistency," *IEEE Transactions on Industry Applications*, vol. 56, no. 5, pp. 5340-5351, 2020, doi: 10.1109/TIA.2020.3001254.
- [63] W. Greenwell and A. Vahidi, "Predictive Control of Voltage and Current in a Fuel Cell-Ultracapacitor Hybrid," *IEEE Transactions on Industrial Electronics*, vol. 57, no. 6, pp. 1954-1963, 2010, doi: 10.1109/TIE.2009.2031663.
- [64] B. Geng, J. K. Mills, and D. Sun, "Two-Stage Energy Management Control of Fuel Cell Plug-In Hybrid Electric Vehicles Considering Fuel Cell Longevity," *IEEE Transactions on Vehicular Technology*, vol. 61, no. 2, pp. 498-508, 2012, doi: 10.1109/TVT.2011.2177483.
- [65] Amin, R. T. Bambang, A. S. Rohman, C. J. Dronkers, R. Ortega, and A. Sasongko, "Energy Management of Fuel Cell/Battery/Supercapacitor Hybrid Power Sources Using Model Predictive Control," *IEEE Transactions on Industrial Informatics*, vol. 10, no. 4, pp. 1992-2002, 2014, doi: 10.1109/TII.2014.2333873.
- [66] X. Hu, C. Zou, X. Tang, T. Liu, and L. Hu, "Cost-Optimal Energy Management of Hybrid Electric Vehicles Using Fuel Cell/Battery Health-Aware Predictive Control,"



- IEEE Transactions on Power Electronics*, vol. 35, no. 1, pp. 382-392, 2020, doi: 10.1109/TPEL.2019.2915675.
- [67] H. He, S. Quan, F. Sun, and Y.-X. J. I. T. o. I. E. Wang, "Model Predictive Control with Lifetime Constraints Based Energy Management Strategy for Proton Exchange Membrane Fuel Cell Hybrid Power Systems," 2020.
- [68] J. Luna, E. Usai, A. Husar, and M. Serra, "Enhancing the efficiency and lifetime of a proton exchange membrane fuel cell using nonlinear model-predictive control with nonlinear observation," *IEEE transactions on Industrial Electronics*, vol. 64, no. 8, pp. 6649-6659, 2017.
- [69] D. F. Pereira, F. D. C. Lopes, and E. H. Watanabe, "Nonlinear Model Predictive Control for the Energy Management of Fuel Cell Hybrid Electric Vehicles in Real-Time," *IEEE Transactions on Industrial Electronics*, pp. 1-1, 2020, doi: 10.1109/TIE.2020.2979528.
- [70] S. Liu, Y. Bin, Y. Li, and B. Scheppat, "Hierarchical MPC Control Scheme for Fuel Cell Hybrid Electric Vehicles," *IFAC-PapersOnLine*, vol. 51, no. 31, pp. 646-652, 2018/01/01/ 2018, doi: <https://doi.org/10.1016/j.ifacol.2018.10.151>.
- [71] H. Zheng, J. Wu, W. Wu, and Y. Wang, "Integrated Motion and Powertrain Predictive Control of Intelligent Fuel Cell/Battery Hybrid Vehicles," *IEEE Transactions on Industrial Informatics*, vol. 16, no. 5, pp. 3397-3406, 2020, doi: 10.1109/TII.2019.2956209.
- [72] Y. Zhou, A. Ravey, and M.-C. Péra, "Multi-mode predictive energy management for fuel cell hybrid electric vehicles using Markov driving pattern recognizer," *Applied Energy*, vol. 258, p. 114057, 2020/01/15/ 2020, doi: <https://doi.org/10.1016/j.apenergy.2019.114057>.
- [73] A. J. Conejo, E. Castillo, R. Minguez, and R. Garcia-Bertrand, *Decomposition techniques in mathematical programming: engineering and science applications*. Springer Science & Business Media, 2006.
- [74] R. Olfati-Saber, J. A. Fax, and R. M. Murray, "Consensus and Cooperation in Networked Multi-Agent Systems," *Proceedings of the IEEE*, vol. 95, no. 1, pp. 215-233, 2007, doi: 10.1109/JPROC.2006.887293.
- [75] S. Boyd, N. Parikh, and E. Chu, *Distributed optimization and statistical learning via the alternating direction method of multipliers*. Now Publishers Inc, 2011.
- [76] A. Khalatbarisoltani, M. Kandidayeni, L. Boulon, and X. Hu, "Power Allocation Strategy based on Decentralized Convex Optimization in Modular Fuel Cell Systems for Vehicular Applications," *IEEE Transactions on Vehicular Technology*, pp. 1-1, 2020, doi: 10.1109/TVT.2020.3028089.
- [77] R. S. Sutton and A. G. Barto, *Reinforcement learning: An introduction*. MIT press, 2018.
- [78] W.-S. Lin and C.-H. Zheng, "Energy management of a fuel cell/ultracapacitor hybrid power system using an adaptive optimal-control method," *Journal of Power Sources*, vol. 196, no. 6, pp. 3280-3289, 2011.
- [79] R. C. Hsu, S.-M. Chen, W.-Y. Chen, and C.-T. Liu, "A reinforcement learning based dynamic power management for fuel cell hybrid electric vehicle," in *2016 Joint 8th International Conference on Soft Computing and Intelligent Systems (SCIS) and 17th International Symposium on Advanced Intelligent Systems (ISIS)*, 2016: IEEE, pp. 460-464.
- [80] N. P. Reddy, D. Padeloup, M. K. Zadeh, and R. Skjetne, "An intelligent power and

- energy management system for fuel cell/battery hybrid electric vehicle using reinforcement learning," in *2019 IEEE Transportation Electrification Conference and Expo (ITEC)*, 2019: IEEE, pp. 1-6.
- [81] X. Lin, B. Zhou, and Y. Xia, "Online recursive power management strategy based on the reinforcement learning algorithm with cosine similarity and a forgetting factor," *IEEE Transactions on Industrial Electronics*, vol. 68, no. 6, pp. 5013-5023, 2020.
- [82] J. Yuan, L. Yang, and Q. Chen, "Intelligent energy management strategy based on hierarchical approximate global optimization for plug-in fuel cell hybrid electric vehicles," *International Journal of Hydrogen Energy*, vol. 43, no. 16, pp. 8063-8078, 2018.
- [83] H. Sun, Z. Fu, F. Tao, L. Zhu, and P. Si, "Data-driven reinforcement-learning-based hierarchical energy management strategy for fuel cell/battery/ultracapacitor hybrid electric vehicles," *Journal of Power Sources*, vol. 455, p. 227964, 2020.
- [84] G. Dulac-Arnold, D. Mankowitz, and T. Hester, "Challenges of real-world reinforcement learning," *arXiv preprint arXiv:1904.12901*, 2019.
- [85] H. Zhang, J. Peng, H. Tan, H. Dong, and F. Ding, "A Deep Reinforcement Learning Based Energy Management Framework with Lagrangian Relaxation for Plug-in Hybrid Electric Vehicle," *IEEE Transactions on Transportation Electrification*, 2020.
- [86] E. Bøhn, S. Gros, S. Moe, and T. A. Johansen, "Reinforcement Learning of the Prediction Horizon in Model Predictive Control," *arXiv preprint arXiv:2102.11122*, 2021.
- [87] T. Koller, F. Berkenkamp, M. Turchetta, and A. Krause, "Learning-based model predictive control for safe exploration," in *2018 IEEE conference on decision and control (CDC)*, 2018: IEEE, pp. 6059-6066.
- [88] M. Zanon and S. Gros, "Safe reinforcement learning using robust MPC," *IEEE Transactions on Automatic Control*, 2020.
- [89] L. Wen, J. Duan, S. E. Li, S. Xu, and H. Peng, "Safe reinforcement learning for autonomous vehicles through parallel constrained policy optimization," in *2020 IEEE 23rd International Conference on Intelligent Transportation Systems (ITSC)*, 2020: IEEE, pp. 1-7.
- [90] M. Alshiekh, R. Bloem, R. Ehlers, B. Könighofer, S. Niekum, and U. Topcu, "Safe reinforcement learning via shielding," in *Thirty-Second AAAI Conference on Artificial Intelligence*, 2018.
- [91] N. Jansen, B. Könighofer, S. Junges, A. Serban, and R. Bloem, "Safe reinforcement learning using probabilistic shields," 2020.
- [92] F. Berkenkamp, M. Turchetta, A. P. Schoellig, and A. Krause, "Safe model-based reinforcement learning with stability guarantees," *arXiv preprint arXiv:1705.08551*, 2017.
- [93] S. Satyapal, "US Department of energy hydrogen and fuel cell technology overview," *Presented at The 14th International Hydrogen and Fuel Cell Expo (FC EXPO 2018)*, 2018.
- [94] T. Benjamin, R. Borup, N. Garland, C. Gittleman, B. Habibzadeh, and S. Hirano, "Fuel Cell Technical Team Roadmap," *Energy.gov (Office of Energy Efficiency & Renewable Energy)*, 2017.
- [95] H. Chen, P. Pei, and M. Song, "Lifetime prediction and the economic lifetime of Proton Exchange Membrane fuel cells," *Applied Energy*, vol. 142, pp. 154-163, 2015/03/15/ 2015, doi: <https://doi.org/10.1016/j.apenergy.2014.12.062>.

- [96] K. Mongird *et al.*, "Energy Storage Technology and Cost Characterization Report," Pacific Northwest National Lab.(PNNL), Richland, WA (United States), 2019.
- [97] C. J. Watkins and P. Dayan, "Q-learning," *Machine learning*, vol. 8, no. 3-4, pp. 279-292, 1992.
- [98] J. Solano, S. Jemei, L. Boulon, L. Silva, D. Hissel, and M.-C. Pera, "IEEE VTS Motor Vehicles Challenge 2020-Energy Management of a Fuel Cell/Ultracapacitor/Lead-Acid Battery Hybrid Electric Vehicle," in *2019 IEEE Vehicle Power and Propulsion Conference (VPPC)*, 2019: IEEE, pp. 1-6.
- [99] Z. Donghua and X. Ding, "Theory and applications of fault tolerant control," *Acta Automatica Sinica*, vol. 26, no. 6, pp. 788-797, 2000.
- [100] K. Goebel, B. Saha, A. Saxena, J. R. Celaya, and J. P. Christophersen, "Prognostics in battery health management," *IEEE instrumentation & measurement magazine*, vol. 11, no. 4, pp. 33-40, 2008.
- [101] M. Jouin, R. Gouriveau, D. Hissel, M.-C. Péra, and N. Zerhouni, "Prognostics and Health Management of PEMFC—State of the art and remaining challenges," *International Journal of Hydrogen Energy*, vol. 38, no. 35, pp. 15307-15317, 2013.
- [102] X. Hu, T. Liu, X. Qi, and M. J. I. I. E. M. Barth, "Reinforcement Learning for Hybrid and Plug-In Hybrid Electric Vehicle Energy Management: Recent Advances and Prospects," vol. 13, no. 3, pp. 16-25, 2019.
- [103] L. Guo, H. Chen, Q. Liu, B. J. I. T. o. S. Gao, Man,, and C. Systems, "A computationally efficient and hierarchical control strategy for velocity optimization of on-road vehicles," vol. 49, no. 1, pp. 31-41, 2018.



## Publication and conference papers

### Peer-reviewed Journals:

1- **Arash Khalatbarisoltani**, Mohsen Kandidayeni, Loïc Boulon, and Xiaosong Hu, “**An Adjustable Look-Ahead Decentralized Control for a Multi Fuel Cells/Battery Powertrain Using Convex Optimization and Reinforcement Learning**”, IEEE Transactions on Mechatronics, (under review).

2- **Arash Khalatbarisoltani**, Mohsen Kandidayeni, Loïc Boulon, and Xiaosong Hu, “**A Decentralized Multi-Agent Power Allocation Strategy based on Reinforcement Learning for a Modular Fuel Cell Vehicle**”, SAE International Journal of Electrified Vehicles, (Accepted).

3- Haitao Zhou, **Arash Khalatbarisoltani**, Mohsen Kandidayeni, Xiaolin Tang, Loïc Boulon, and Xiaosong Hu, “**Fuel Cell Vehicles Energy Management Strategies: A Comprehensive Review of the Latest Development, Related Issues, and Outlook for Future Prospects**”, IEEE Intelligent Transportation Systems Transactions, (under review).

4- **Arash Khalatbarisoltani**, Mohsen Kandidayeni, Loïc Boulon, and Xiaosong Hu, “**A Comparison of Decentralized ADMM Optimization Algorithms for Power Allocation in Modular Fuel Cell Vehicles**”, IEEE Transactions on Mechatronics, (Minor Revision)

5- **Arash Khalatbarisoltani**, Mohsen Kandidayeni, Loïc Boulon, and Xiaosong Hu, “**Power Allocation Strategy based on Decentralized Convex Optimization in**



**Modular Fuel Cell Systems for Vehicular Applications**”, IEEE Transactions on Vehicular Technology, Dec 2020.

6- Juan Carlos Oviedo Cepeda, **Arash Khalatbarisoltani**, Loic Boulon, German Alfonso Osma Pinto, Cesar Antonio Duarte Gualdron, and Javier Enrique Solano Martinez, **“Design of an Incentive-based Demand Side Management Strategy for Stand-Alone Microgrids Planning”**, International Journal of Sustainable Energy Planning and Management, Jun 2020.

7- Mohsen Kandidayeni, Alvaro Omar Macias Fernandez, **Arash Khalatbarisoltani**, Loïc Boulon, Sousso Kelouwani, and Hicham Chaoui, **“An online energy management strategy for a fuel cell/battery vehicle considering the driving pattern and performance drift impacts”**, IEEE Transactions on Vehicular Technology, August 2019.

8- M. Kandidayeni, A. Macias, **A. Khalatbarisoltani**, L. Boulon, and S. Kelouwani, **“Benchmark of proton exchange membrane fuel cell parameters extraction with metaheuristic optimization algorithms”**, Energy, September 2019.

9- **Arash Khalatbarisoltani**, Mohsen Kandidayeni, Loïc Boulon, and David Lupien St-Pierre, **“Modular Energy Systems in Vehicular Applications”**, Energy Procedia, April 2019.

#### **Conferences:**

1- **Khalatbarisoltani A.**, Boulon L., Hu X. Fully Decentralized Energy Management Strategy Based on Model Predictive Control in a Modular Fuel Cell Vehicle, **IEEE Transportation Electrification Conference and Expo**, CHICAGO, JUNE 23-25, 2021.

2- **Arash Khalatbarisoltani**, Loic Boulon, David Lupien St-Pierre, and Xiaosong Hu, “Decentralized Implementation of an Optimal Energy Management Strategy in Interconnected Modular Fuel Cell Systems”, **2019 IEEE Vehicle Power and Propulsion Conference (VPPC)**, Vietnam, October 2019.

3- **Arash Khalatbarisoltani**, Loïc Boulon, and David Lupien St-Pierre, “A New Decentralized Energy Management Strategy for a Modular Fuel Cell System” **8th International Conference on Fundamentals & Development of Fuel Cells FDFC2019**, France, February 2019.

4- **Arash Khalatbarisoltani**, Juan Carlos Oviedo Cepeda, Loïc Boulon, David Lupien St-Pierre, Javier Solano, and Cesar Duarte, “A New Real-Time Centralized Energy Management Strategy for Modular Electric Vehicles”, **IEEE Vehicle Power and Propulsion Conference (VPPC)**, USA, August 2018.

## Appendix A – Résumé

Pour atténuer les dépendances aux carburants fossiles, des alternatives prometteuses impliquant des véhicules électriques (VE), des véhicules électriques hybrides (VEH) et des véhicules électriques hybrides rechargeables (PHEV) ont été étudiées pour assurer l'avenir vert au domaine des transports. Considérant la croissance significative des technologies de pile à combustible (FC), les systèmes à hydrogène deviennent une alternative compétitive à leurs homologues de l'industrie automobile. Cela est dû notamment à leur rendement élevé, leur faible bruit, leur faible temps de ravitaillement ainsi que leur absence d'émissions locales au véhicule. Ces caractéristiques ont propulsé les véhicules à pile à combustible (FCV) au cœur de la recherche industrielle et académiques. Les FCV se composent de deux sources d'énergie, FCS comme source principale et une unité batterie/supercondensateur comme source secondaire. Le développement d'une stratégie de gestion énergétique (SME) efficace doit être étudié attentivement pour coordonner efficacement les multiples sources d'énergie. Bien que de nombreux efforts soient déployés pour améliorer les FCVS intégrant une unique pile à combustible, certains problèmes persistent notamment en termes d'efficacité, de disponibilité, de flexibilité (plug & play), de robustesse, de durabilité et de coût. Ces défis incitent la technologie FCV actuelle à évoluer vers des systèmes énergétiques modulaires (MES). La modularité matérielle a déjà été étudiée dans les FCV multi-piles pour fournir un avantage technologique et une meilleure rentabilité comparé à un système de conversion d'énergie à pile à combustible unique. Néanmoins, le point de vue de la modularité du logiciel, en particulier de l'unité EMS, a échappé à l'attention. À cet égard, par rapport aux études existantes, cette thèse se concentrera fondamentalement sur les EMS décentralisés

émergentes pour les FCV multi-piles afin d'examiner les améliorations inhérentes à la modularité et à la robustesse imposées en étudiant l'intégration des techniques de décomposition. La structure principale de cette thèse est définie comme suit. Le chapitre 1 présente l'introduction de la thèse, incluant les systèmes énergétiques modulaires et la revue de littérature sur les algorithmes d'optimisation décentralisés. Les techniques actuelles sont classées et examinées en termes de vitesse de convergence, de communication, d'exactitude et d'applicabilité en temps réel. Le chapitre 2 propose une méthode de décomposition lagrangienne au cadre décisionnel de puissance, dont les performances sont validées par des études numériques et expérimentales. Ensuite, le chapitre 3 présente une comparaison détaillée entre deux techniques de décomposition avancées pour identifier les principales caractéristiques du cadre EMS modulaire proposé, qui établit une base solide pour la réalisation des EMS. Considérant les techniques établies, le chapitre 4 propose l'intégration d'une EMS basée sur la prévision avec la méthode de décomposition, conduisant à la conception d'un principe innovant de EMS décentralisée et anticipée. De plus, pour améliorer l'approche suggérée, une technique basée sur l'apprentissage intelligent permettant le réglage paramétrique de l'EMS conçue est proposée. Enfin, en conclusion, le chapitre 5 décrit les travaux de recherche effectués tout au long de ce doctorat, avec une mise en évidence des principaux résultats significatifs et une ouverture sur les futures orientations de recherche autour des EMS décentralisées.